Internal Note No. 68-FM-269

NATIONAL AERONAUTICS AND SPACE ADMINISTRATION

MSC INTERNAL NOTE NO. 68-FM-269

October 28, 1968

APOLLO MISSION F SPACECRAFT REFERENCE TRAJECTORY

VOLUME I

REFERENCE TRAJECTORY PROFILE (LAUNCHED AUGUST 14, 1969)

(NASA-TM-X-69977) APOLLO MISSION F SPACECRAFT REFERENCE TRAJECTORY. VOLUME 1: REFERENCE TRAJECTORY PROFILE (LAUNCHED 14 AUGUST 1969) (NASA) 103 p

N74-71962

Unclas
00/99 16734

Lunar Mission Analysis Branch

and

Orbital Mission Analysis Branch

MISSION PLANNING AND ANALYSIS DIVISION

MANNED SPACECRAFT CENTER
HOUSTON, TEXAS

MSC INTERNAL NOTE NO. 68-FM-269

PROJECT APOLLO

APOLLO MISSION F SPACECRAFT REFERENCE TRAJECTORY
VOLUME I - REFERENCE TRAJECTORY PROFILE
(LAUNCHED AUGUST 14, 1969)

By Lunar Mission Analysis Branch and
Orbital Mission Analysis Branch

October 28, 1968

MISSION PLANNING AND ANALYSIS DIVISION
NATIONAL AERONAUTICS AND SPACE ADMINISTRATION
MANNED SPACECRAFT CENTER
HOUSTON, TEXAS

Approved: Ronald L. Berry
Ronald L. Berry, Chief
Lunar Mission Analysis Branch

Approved: Edgar C. Lineberry
Edgar C. Lineberry, Chief
Orbital Mission Analysis Branch

Approved: David H. Owen for
John P. Mayer, Chief
Mission Planning and Analysis Division

CONTENTS

TABLES

FIGURES

Figure		Page

APOLLO MISSION F SPACECRAFT REFERENCE TRAJECTORY

VOLUME I - REFERENCE TRAJECTORY PROFILE

(LAUNCHED AUGUST 14, 1969)

By Lunar Mission Analysis Branch and
Orbital Mission Analysis Branch

1.0 SUMMARY

This volume, Volume I, in combination with Volumes I and II of the Mission G reference trajectory and Volume II of the Mission F reference trajectory, is a detailed reference mission profile for one typical lunar orbit mission launched on August 14, 1969. The launch azimuth is 72° and translunar injection occurs over the Atlantic Ocean during the second revolution of the earth parking orbit.

The mission phases from launch through descent orbit insertion in lunar orbit are essentially the same as those in the Mission G reference trajectory and, therefore, are not described in this document. The primary emphasis of this document is on the lunar orbit operations which include a LM-active rendezvous and a CSM-active rendezvous, since these are the phases which differ most significantly from Mission G. The lunar orbit operations are related to the same lunar site, II-P-2, as the Mission G reference trajectory (Volumes I and II).

Since there is no lunar orbit plane-change maneuver by the CSM while separated from the LM, as there is for Mission G, the transearth injection and transearth coast phases differ slightly from Mission G. For this reason data are shown for these phases for the August 14, 1969, 72° launch azimuth mission, and for the other launch days and launch azimuths being considered for the third quarter of 1969.

This reference trajectory satisfies all of the mission-related test objectives for Mission F.

2.0 INTRODUCTION

This volume presents the Mission F profile for the first launch opportunity, 72° launch azimuth, first injection opportunity on August 14, 1969, and transearth phase scan data for the other launch opportunities being considered for the third quarter of 1969.

Since Mission F differs from Mission G only in the lunar orbit operations and transearth injection, the tables and figures of this volume present data only for these mission phases. A complete trajectory listing is presented in Volume II on the Apollo Mission F reference trajectory (ref. 1).

The ground rules and guidelines used in the design of the reference trajectory are defined in reference 2. The spacecraft weight configuration and vehicle performance data are the same as used in the G mission reference trajectory (refs. 3 and 4) with the exception that, for the LM maneuvers, the LM ascent propellant tanks are half loaded.

3.0 DATA USED IN THE GENERATION OF THE F MISSION REFERENCE TRAJECTORY

The primary input used in the computation of the Mission F reference trajectories can be obtained from the following sources:

Input	Reference no.
Mission objectives.	5
Mission constraints and ground rules. .	6, 7
Nominal LPO timeline.	8
RCS and consumables budget.	9
Vehicle characteristics:	
CSM weights	10
CSM performance properties.	11
LM weights.	10
LM performance properties	12
Ground support facility positions and capabilities.	13, 14
Lunar landing site positions.	15, 16
Standards and constants	17

4.0 REFERENCE MISSION PROFILE DESCRIPTION

This section provides a brief summary of each phase of the reference mission from LM-active rendezvous through transearth coast. The other mission phases are identical to those found in the Mission G reference trajectory (refs. 3 and 4).

4.1 LM-active Rendezvous

Since several significant changes have been made to this phase since this volume was generated, the data in this document should be considered as only roughly representative of the most recent profile. See reference 18 for a description of these recent changes.

Figures 1 through 7 present a description of the (manned) LM-active phase of Mission F. In brief, the phase occurs in lunar orbit and consists of a nominal Hohmann descent sequence and a nominal in-orbit ascent-to-rendezvous sequence, the two sequences separated by a phasing period.

One of the primary objectives of Mission F is to demonstrate all phases of Mission G except those directly involving the LM powered descent and powered ascent. Relative to the LM-active phase, this objective is accomplished by incorporating between the Hohmann descent and the in-orbit ascent approximately one revolution, during which the required adjustment in CSM lead angle is made. This phase angle adjustment is at least approximately 22.5°, since the CSM trails the LM at the end of Hohmann descent by approximately 7° and must lead the LM at nominal LM insertion by approximately 15.5°.

As in Mission G, the LM-active phase begins with the CSM/LM docked configuration in a 60-n. mi. circular lunar orbit. The LM activities (including LM/CSM separation) prior to the Hohmann descent are performed as in Mission G. The descent orbit insertion (DOI) is performed by a descent propulsion system (DPS) burn (71.6 fps, horizontal, retrograde) 195° prior to the landing site so that the resulting pericynthion (50 000-ft altitude) occurs 15° prior to the landing site, the position at which the powered descent is initiated in Mission G. For Mission F, however, a second LM maneuver is performed approximately 7.2 minutes (23.5°) past pericynthion, or approximately 2.5 minutes (8.5°) past the landing site. This second LM maneuver is a DPS burn of 172.4 fps (horizontal, posigrade) designed to establish at the resulting LM pericynthion a CSM lead angle equivalent to that which occurs at nominal powered ascent cutoff in Mission G. This second maneuver is referred to in this document as phasing. Since phasing is performed approximately 23.5° past the original pericynthion, the resulting pericynthion occurs about 16° past the original pericynthion (or approximately 1° past the landing site). The apocynthion altitude of the phasing orbit is 195.2 n. mi., which affords the required CSM catch-up time between phasing and the resulting pericynthion. The CSM lead angle is approximately -9° at phasing and 15.5° at the resulting pericynthion. The resulting pericynthion altitude is approximately 60 000 ft, which is the nominal altitude at powered ascent cutoff for Mission G. Just prior to this resulting pericynthion, the LM descent stage is jettisoned. Then at pericynthion an ascent propulsion system (APS) maneuver of 207.6 fps (horizontal, retrograde) is performed to establish the equivalent of the standard LM insertion orbit (30- by 9.9-n. mi.) of Mission G. This maneuver is referred to as insertion. At completion of insertion, the conditions are equivalent to those at powered ascent cutoff for Mission G, except that the LM ascent stage is considerably heavier since only a relatively small amount of APS propellant has been utilized.

Following insertion, the nominal LM in-orbit ascent profile (essentially the same as presented for Mission G) is followed. Table I presents information for each of the maneuvers during the LM-active phase.

In table I, the Δt's in column 2 are the elapsed times between the impulsive times of the burns. An ullage of approximately 2 fps from the pressurized RCS is required for each of the listed LM maneuvers (column 3) which utilizes a propulsion system other than the pressurized RCS. (The pressurized RCS utilizes propellant from the pressurized RCS tanks.) The notation "DPS (FT)" indicates that the DPS goes to full thrust after 26 seconds at 10 percent thrust. The notation "RCS (intc.)" indicates RCS thrusting utilizing APS propellant through the interconnect. The ΔV (column 4) for TPF is the theoretical value for the impulsive velocity match, and the other values (burn duration and Δt's) relative to the terminal phase finalization are based on a theoretical impulsive TPF. The burn durations in column 5 for the DPS and APS burns are the burn durations for the main propulsion system; i.e., the RCS ullage times are not included. However, for the RCS (intc.) burns the ullage times are included in the listed burn durations. The burn durations are based on a LM loading at earth launch equivalent to that for Mission G (total LM = 33 053 lb, LM ascent stage = 10 729 lb). The burn attitude (column 6) is measured counterclockwise from the local horizontal in the direction of motion to the direction of the impulsive ΔV vector. Where the RCS is not the main propulsion system, the indicated RCS thruster usage (column 7) refers to ullage.

Additional profile information is presented in the figures. It is noted that the segments of the curves from insertion to TPF are essentially the same (except for time reference) as the insertion-to-TPF curves in reference 3.

Figure 1 is a relative motion profile (curvilinear, CSM-centered) from DOI to TPF. The darkness periods (for CSM) and 10-minute time ticks relative to DOI are indicated.

Figures 2 through 7 present time histories of various relative parameters time-referenced from DOI. In each of the figures, the maneuvers and darkness periods are indicated.

Figures 2 and 3 are time histories of the LM-to-CSM elevation angle and the CSM-to-LM elevation angle, respectively. Figure 4 provides the same information for the CSM-LM-sun angle. Elevation angle is defined as the angle (measured counterclockwise) from a vehicle's local horizontal in the direction of motion to its line of sight to the applicable object (the other vehicle or the sun).

Time histories of vehicle-to-vehicle range, range rate, and central phase angle (CSM lead angle) are shown in figures 5, 6, and 7, respectively. From figure 5 it can be seen that throughout the total profile the range (between the CSM and LM) does not exceed the rendezvous radar limit of 400 n. mi.

A 10° sun elevation angle at the time of the first (separated-LM) pass over the landing site was assumed for the mission profile. This sun elevation is the mid-point value of the current limits on sun elevation at landing for Mission G (3° to 17°). Although a 10° sun elevation at landing was also assumed for the Mission G profile, TPI is performed 5 minutes prior to darkness for Mission F so that the Δt from insertion to TPI is 12 minutes longer than the corresponding Δt for Mission G.

All of the LM maneuvers prior to the rendezvous terminal phase are nominally horizontal burns. In addition to the economical factor (which applies for all the horizontal maneuvers), the horizontal thrusting is incorporated for phasing, insertion, and CSI due to safe-pericynthion considerations.

A major consideration in designing the Δt from DOI to phasing was to incorporate a value which would result in approximately a 60 000-ft pericynthion altitude for insertion. For example, if phasing were to occur approximately 3 minutes later than the time specified, the resulting pericynthion altitude would be approximately 2 n. mi. above the desired value. In addition to yielding the 60 000-ft pericynthion altitude, the incorporated DOI-to-phasing Δt affords a free-flight look at the landing site area prior to phasing.

4.2 CSM-active Rendezvous Phase

There have been several significant profile changes for the CSM-active rendezvous phase since the data for this volume were generated. For the most recent profile see reference 19.

The presented rendezvous profile is essentially applicable for any simulated landing site or for any translunar time, or both. Since the ground elapsed time (g.e.t.) for initiation of the profile would vary for the different landing sites or different translunar times, or both, the profile's maneuvers are referenced to ground elapsed time only for a specific trajectory. The phasing maneuver (the initial separation maneuver following the undocking) occurs about 13 hours after docking at completion of the LM-active rendezvous. The time references shown for each maneuver in table II are the Δt from the phasing maneuver and the Δt from the previous maneuver.

Prior to the CSM-active rendezvous the docked configuration (CSM/LM ascent stage) is in the nominal 60-n. mi. circular orbit. The profile begins after the crew has set the LM in the selected attitude mode, unmanned the LM, and undocked. The selected attitude mode has not yet been determined.

The NCC/NSR sequence was selected instead of the CSI/CDH sequence for two related reasons. The phasing and coelliptic maneuvers necessarily have to be ground-computed for either sequence since there is no onboard (CMC) solution capability; however, the NCC/NSR sequence requires only two maneuvers (NCC and NSR) prior to terminal phase, whereas the CSI/CDH sequence would require three maneuvers prior to terminal phase, since CSI could not be used as the separation maneuver.

The phasing maneuver (NCC) is targeted to establish 90 minutes later an offset [h = 10 n. mi. (CSM above) and $\Delta\theta$ (LM central lead angle = -2.89°] at which the coelliptic maneuver (NSR) is to occur. The phasing maneuver is a near-radial-down SPS burn of 71.2 fps and 4.0-seconds burn duration. As a result of the total selection of parameters, this maneuver occurs about 54° east of the landing site. The perigee altitude of the orbit between the phasing and coelliptic maneuvers is 42 n. mi. The profile's maximum relative range of about 67 n. mi. also occurs during this phase. The coelliptic maneuver is an SPS burn of 36.1 fps and 2.0-seconds burn duration; the ΔV-vector is about 15° below the positive horizontal; and the maneuver occurs about 27° east of the landing site. The Δt between the coelliptic maneuver and TPI is approximately 38 minutes. TPI is a near-line-of-sight-thrusting SM RCS burn of 15.6 fps and 43.4-seconds burn duration. The TPI elevation angle utilized is 206.6° (or -26.6°). TPI occurs approximately at the mid-point of darkness about 2° east of the landing site. A 130° terminal phasing is incorporated, and the CSM approaches from above. The theoretical values for TPF are 23.7 fps and 66.9-seconds burn duration.

The extent of the final braking depends on the real-time situation (that is, SM RCS and LM electrical power margins). Should the CSM close to station-keeping conditions, the station keeping would probably be terminated by a small separation maneuver to avoid recontact problems prior to TEI.

The total Δt between the phasing maneuver and the end of braking is slightly more than 3 hours. The RCS propellant usage is approximately that which would be required in any actual rescue situation. The SPS propellant usage is slightly less than that required for the normal four-impulse rescue sequence, but is substantially less than that required if five-impulse and six-impulse rescue sequences were used.

Table II is a sequence of maneuvers for the CSM-active rendezvous phase and includes various pertinent data associated with each maneuver. The Δt's in the second and third columns are from maneuver initiation to maneuver initiation. The RCS thruster usage refers to ullage when the SPS is the main propulsion system. The SPS burn durations do not include ullage. The burn attitude is the direction of thrust at burn initiation; it is measured (starting upward) from the direction-of-motion local horizontal to the direction of thrust. All values relative to TPF are based on a theoretical (impulsive) TPF.

Presented in figure 8 is the relative motion profile (curvilinear, LM-centered). The darkness periods (for the LM) and 10-minute time ticks (relative to the phasing maneuver) are indicated.

Figures 9 through 14 present time histories of various relative parameters, time referenced from the phasing maneuver (NCC). For each of the figures, the occurrence of the maneuvers and the designated darkness periods are shown.

Figures 9 and 10 are time histories of LM-to-CSM and CSM-to-LM elevation angles, and figure 11 is a time history of the LM-CSM-sun angle. CSM-to-LM visibility problems exist if the vehicles are in daylight and the CSM-to-LM elevation angle is within approximately 15° of the CSM-to-sun elevation angle. Visibility problems also exist when the CSM-to-LM elevation angle is between approximately 200° and 340° (i.e., a lunar surface background exists) and the lunar surface is lit by the sun, or, in some cases, by earth-reflected light. The LM tracking light is visible to the CSM if the LM +Z-axis points within approximately 35° of the LM-to-CSM elevation angle.

Elevation angle is defined as the angle (measured counterclockwise) from a vehicle's local horizontal in the direction of motion to its line of sight to the applicable object (the other vehicle or the sun).

Time histories of vehicle-to-vehicle range, range rate, and central phase angle (LM lead angle) are shown in figures 12, 13, and 14, respectively.

4.3 Transearth Phase

Since there is no CSM lunar orbit plane change in Mission F as there is in Mission G, the transearth injection and coast phase is slightly different than in the Mission G reference trajectory.

Tables III and IV show the radar and shadow timelines from CSM-LM final docking following the CSM-active rendezvous through transearth coast.

Figure 15 shows the time history of significant parameters during the transearth injection maneuver for the August 14, 1969, 72° launch azimuth, first opportunity mission. These data were generated with a precision integrated powered-flight simulation.

Figures 16 through 27 show scans of selected TEI and transearth coast trajectory parameters for the other launch opportunities being considered for the third quarter of 1969. These data were generated using patch-conic computer programs. The 1969 launch dates included in the scans were July 15, 16, 18, 22; August 14, 15, 17, 21; and September 13, 14, 16, 19. These dates are identical to the Mission G launch dates considered and result from targeting the F mission to the same lunar sites as the G mission.

5.0 REFERENCE TRAJECTORY EVALUATION

All of the comments in the reference trajectory evaluation section of the Mission G reference trajectory, Volume I (ref. 3) apply also to the Mission F reference trajectory. It should be pointed out again that this reference trajectory does not reflect the recent changes to the LM-active and CSM-active rendezvous phases as documented in references 18 and 19. Therefore, the profiles described should be considered as only roughly representative of the most recent mission planning.

TABLE I.- SEQUENCE OF MANEUVERS FOR LM-ACTIVE RENDEZVOUS PHASE

Maneuver	Δt from previous maneuver, min	Main propulsion system	ΔV, fps	Burn duration, sec	Burn attitude, deg	RCS thruster usage	Resultant LM orbit, h_a/h_p, n. mi.
DOI		DPS(FT)	71.6	30.2	180.0	+X, 2-jet	60.0/8.2
Phasing	64.5	DPS(FT)	172.4	15.5	0.0	+X, 2-jet	195.2/9.9
Insertion	124.7	APS	207.6	15.0	180.0	+X, 2-jet	31.9/9.9
CSI	30.0	RCS(intc.)	28.8	18.0	0.0	+X, 4-jet	45.7/17.0
CDH	42.5	RCS(intc.)	38.9	24.2	0.0	+X, 4-jet	45.7/45.0
TPI	43.5	RCS(intc.)	25.8	32.0	37.3	+X, 4-jet	61.2/44.4
TPF	46.2	RCS	29.8	36.9	297.3	-Z, 2-jet	60.0/60.0

[a]The LM descent stage is jettisoned just prior to insertion.

TABLE II.- SEQUENCE OF MANEUVERS FOR CSM-ACTIVE RENDEZVOUS PHASE

Maneuver	Δt from phasing (NCC), min	Δt from previous maneuver, min	Main propulsion system	RCS thruster usage	ΔV, fps	Burn duration, sec	Burn attitude, deg	Resultant CSM orbit, h_a/h_p (conic), n. mi.[a]
Phasing (NCC)			SPS		71.2	4.0	277.1	68.6/42.0
Coelliptic (NSR)	90.0	90.0	SPS		36.1	2.0	344.86	68.5/68.3
TPI	130.0	40.0	RCS	+X, 4-jet	15.6	43.4	190.06	67.9/57.5
TPF	172.4	42.4	RCS	-X, 4-jet	23.5	66.4	117.4	60.2/59.7

[a]Altitude measured with respect to the landing site radius.

TABLE III.- MISSION RADAR TIMELINE

Station	Acquisition				Termination			
	g.e.t., hr:min:sec	Azimuth, deg	Elevation, deg	Range, n. mi.	g.e.t., hr:min:sec	Azimuth, deg	Elevation, deg	Range, n. mi.
(a) Docking to TEI initiation								
Merritt Island	121:08:09	-114.06	8.02	205 040.28	121:46:28	-109.72	.56	206 736.42
Grand Bahama	121:08:09	-112.59	6.82	205 111.99	121:42:31	-109.02	-.00	206 574.93
Carnarvon	121:08:09	107.13	.74	205 482.36	121:46:09	103.83	8.64	206 243.60
Guam	121:08:09	112.85	18.57	204 428.23	121:46:03	116.73	26.38	205 227.23
Hawaii	121:08:09	166.01	49.98	202 899.22	121:46:14	179.58	50.78	204 107.20
Guaymas	121:08:09	-134.01	30.57	203 775.35	121:46:25	-127.22	24.33	205 353.22
Corpus	121:08:09	-123.86	21.51	204 261.35	121:46:26	-118.49	14.51	205 907.29
Canberra	121:08:09	86.75	32.32	203 692.64	121:46:12	81.26	39.74	204 571.34
Goldstone	121:08:09	-142.43	28.55	203 878.92	121:46:22	-134.63	23.46	205 396.44
Guam	122:32:45	122.98	36.47	204 661.88	123:44:19	137.50	48.87	203 986.78
Carnarvon	122:32:51	99.34	19.13	205 572.46	123:44:19	93.68	34.55	204 624.06
Canberra	122:32:54	72.07	49.13	204 106.64	123:44:29	53.58	61.86	203 561.10
Hawaii	122:32:57	-162.71	49.22	204 095.07	123:44:35	-142.22	41.37	204 312.80
Goldstone	122:33:05	-125.39	16.10	205 726.50	123:44:42	-114.66	3.83	206 351.68
Guaymas	122:33:06	-119.42	15.62	205 754.32	123:44:45	-110.83	1.83	206 475.11
Corpus	122:33:06	-112.09	5.09	206 374.68	122:58:24	-109.34	-.00	205 477.20
Guam	124:30:57	152.57	55.61	203 684.49	125:42:42	-177.54	58.81	203 452.80
Carnarvon	124:30:57	88.84	45.29	204 077.06	125:42:40	80.57	60.89	203 392.49
Canberra	124:31:09	31.04	68.40	203 322.48	125:42:50	-16.69	70.78	203 160.80
Hawaii	124:31:14	-131.43	33.87	204 581.16	125:42:55	-120.55	20.80	205 167.72
(b) Transearth Phase[a] [TEI initiation - 125:58:01.6 g.e.t.; TEI cutoff - 126:00:16.6 g.e.t.]								
Carnarvon	126:16:31	72.69	68.60	203 898.59	134:06:18	-108.33	-.00	197 841.29
Guam	126:16:32	-161.85	57.41	204 195.70	131:13:42	-107.73	-.00	201 260.37
Canberra	126:16:40	-38.27	67.32	203 925.59	132:02:44	-110.32	-.00	200 305.28
Hawaii	126:16:41	-115.92	13.78	206 256.40	127:19:50	-108.88	-.00	205 985.26
Ascension	130:04:59	107.01	.00	202 648.55	142:16:58	-107.21	.00	187 469.51
Madrid	130:35:51	113.47	.00	202 033.77	140:23:37	-113.73	-.00	189 954.41
Grand Canary	130:57:40	109.85	.00	201 573.19	141:34:05	-110.06	-.00	188 414.89
Antigua Isle	133:46:14	108.14	.00	198 218.56	144:55:16	-108.44	.00	183 856.72
Bermuda	134:21:33	110.93	.00	197 527.05	144:42:35	-111.30	.00	184 148.39
Grand Bahama	135:05:60	109.65	.00	196 621.34	145:46:35	-110.01	-.01	182 645.39
Merritt Island	135:18:40	110.05	.00	196 350.88	145:52:59	-110.41	-.00	182 493.74
Corpus	136:24:35	109.87	.00	195 024.33	147:02:00	-110.28	-.00	180 849.77
Guaymas	137:18:56	109.99	.00	193 862.39	147:54:59	-110.40	-.00	179 577.32
Goldstone	137:57:24	111.94	.00	192 973.84	148:06:07	-112.33	-.01	179 295.79
Hawaii	140:26:02	108.98	-.00	189 903.65	151:20:45	-109.45	-.00	174 419.02

[a]Entry interface is at $206^h40^m28.8^s$ g.e.t.

TABLE III.- MISSION RADAR TIMELINE - Concluded

Station	Acquisition				Termination			
	g.e.t., hr:min:sec	Azimuth, deg	Elevation, deg	Range, n. mi.	g.e.t., hr:min:sec	Azimuth, deg	Elevation, deg	Range, n. mi.
(b) Transearth Phase[a] - Continued [TEI initiation - 125:58:01.6 g.e.t.; TEI cutoff - 126:00:16.6 g.e.t.]								
Canberra	142:32:44	110.51	.00	187 113.07	156:09:18	-111.10	-.00	166 715.09
Guam	143:57:06	108.00	-.00	185 192.64	155:16:52	-108.49	-.00	168 155.62
Carnarvon	145:11:48	108.60	-.00	183 467.60	158:13:13	-109.15	.00	163 213.45
Ascension	154:09:49	107.65	.01	169 976.96	166:25:48	-108.28	.00	148 033.58
Madrid	154:44:24	114.60	-.00	169 037.50	164:26:35	-115.42	-.00	151 899.06
Grand Canary	155:04:45	110.73	-.00	168 485.16	165:39:14	-111.46	.00	149 557.68
Antigua Isle	157:54:11	109.06	-.00	163 754.33	169:02:37	-109.79	-.00	142 726.96
Bermuda	158:31:25	112.10	-.00	162 682.90	168:47:53	-112.93	-.01	143.23
Grand Bahama	159:15:34	110.75	-.01	161 401.39	169:52:57	-111.57	-.00	140 969.64
Merritt Island	159:28:33	111.20	-.00	161 049.11	169:59:09	-112.01	-.00	140 751.52
Corpus	160:35:04	111.06	-.01	159 051.33	171:08:36	-111.91	.00	138 279.39
Guaymas	161:29:37	111.20	-.00	157 408.22	172:01:48	-112.07	-.00	136 349.36
Goldstone	162:08:52	113.29	.00	156 209.54	172:11:40	-114.24	-.00	135 987.33
Hawaii	164:37:52	110.25	-.01	151 541.08	175:29:33	-111.17	-.00	128 494.08
Canberra	166:40:06	111.70	.00	147 563.25	180:28:09	-112.76	.00	116 214.87
Guam	168:09:40	109.27	-.01	144 546.49	179:28:38	-110.25	-.00	118 760.62
Carnarvon	169:21:20	109.77	.00	142 082.27	182:31:57	-110.80	.00	110 724.48
Ascension	178:25:52	109.14	.00	121 396.86	190:50:22	-110.54	.00	85 610.92
Madrid	179:09:04	117.24	-.00	119 584.25	188:36:51	-119.21	-.00	92 881.80
Grand Canary	179:26:40	112.84	-.00	118 842.05	189:55:01	-114.61	-.00	88 679.94
Antigua Isle	182:16:49	111.06	-.00	111 404.03	193:25:35	-113.01	-.00	76 503.69
Bermuda	182:57:58	114.67	-.00	109 530.78	193:05:20	-116.97	-.01	77 734.07
Grand Bahama	183:41:40	113.16	-.00	107 511.92	194:14:08	-115.47	-.01	73 488.57
Merritt Island	183:55:12	113.68	-.00	106 879.16	194:19:45	-116.07	-.00	73 134.54
Corpus	185:03:05	113.63	-.00	103 655.54	195:32:53	-116.39	-.00	68 879.61
Guaymas	185:59:00	113.88	-.00	100 931.68	196:26:09	-116.69	-.00	64 818.42
Goldstone	186:41:28	116.44	-.00	98 819.20	196:32:28	-119.62	-.00	64 382.57
Hawaii	189:11:05	113.07	-.00	91 061.45	200:07:11	-116.85	-.00	48 256.54
Canberra	191:05:28	113.95	.01	84 761.33	206:34:06	-19.85	-.00	2 158.48
Guam	192:48:43	112.27	-.00	78 736.59	205:11:24	-120.00	.00	16 837.45
Carnarvon	193:55:02	112.22	.00	74 692.08	206:34:15	54.47	.00	2 125.29
Carnarvon[b]	202:33:33	-91.69	71.11	31 999.99	206:34:15	54.49	.00	2 125.30
Guam	206:01:22	-123.68	.00	8 933.14	206:39:02	115.79	.00	9 948.88

[a]Entry interface is at $206^h40^m28.8^s$ g.e.t.

[b]C-band station; acquisition on range

TABLE IV.- MISSION SHADOW TIMELINE

Lighting	g.e.t. of entrance, hr:min:sec
(a) Docking to TEI initiation	
Sunlight	121:08:01
Lunar penumbra	121:10:47
Lunar umbra	121:10:11
Lunar penumbra	121:56:18
Sunlight	121:56:27
Lunar penumbra	123:08:29
Lunar umbra	123:08:44
Sunlight	123:54:57
Lunar penumbra	125:07:06
Lunar umbra	125:07:09
Lunar penumbra	125:53:27
Sunlight	125:53:29
(b) Transearth phase[a] [TEI initiation - $125^h58^m01.6^s$ g.e.t., TEI cutoff - $126^h00^m16.6^s$ g.e.t.]	
Earth penumbra	206:16:54
Earth umbra	206:17:07

[a]Entry interface occurs at $206^h40^m28.8^s$ g.e.t.

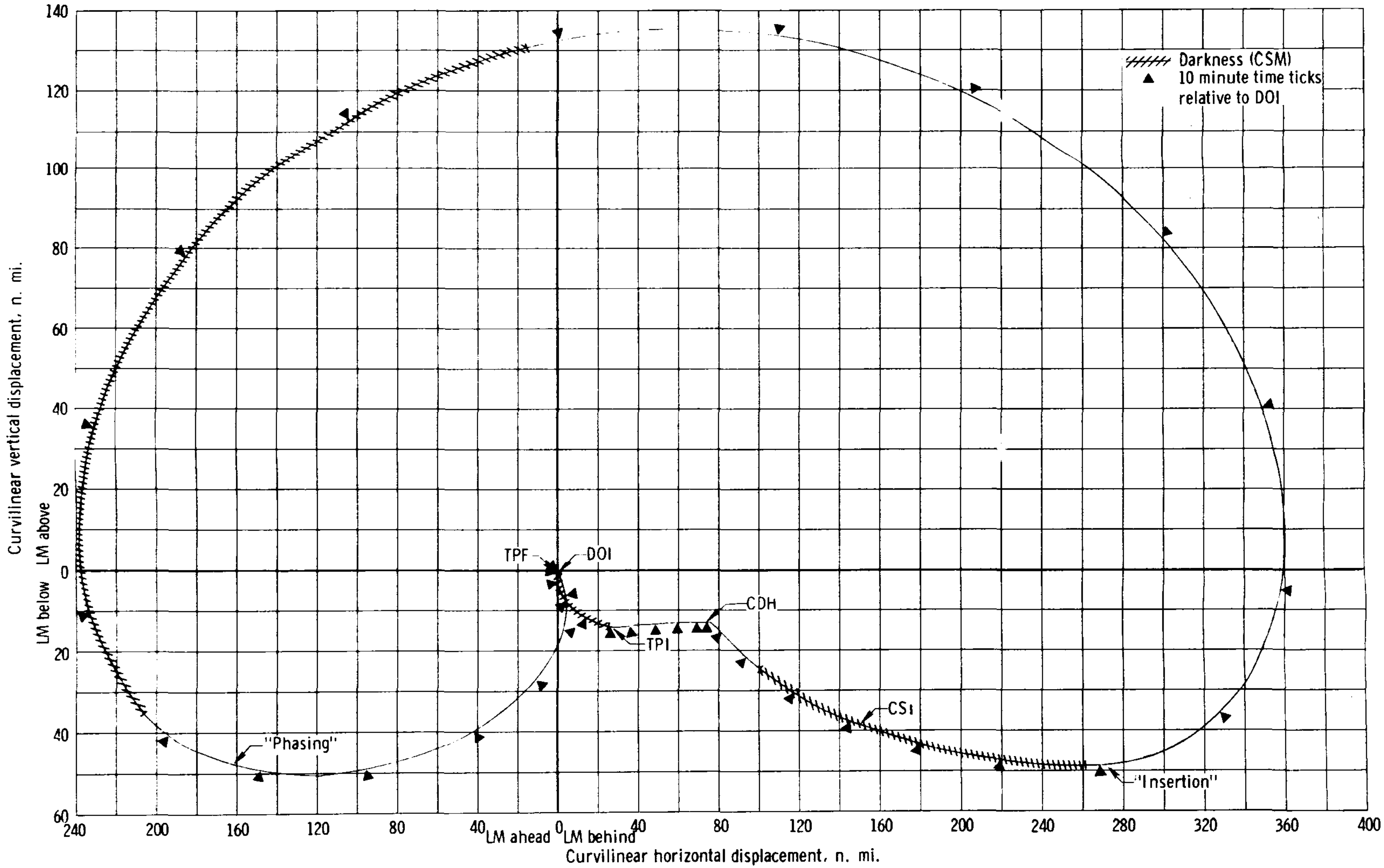

Figure 1. - Relative motion (curvilinear, CSM-centered) for LM-active phase of Mission F.

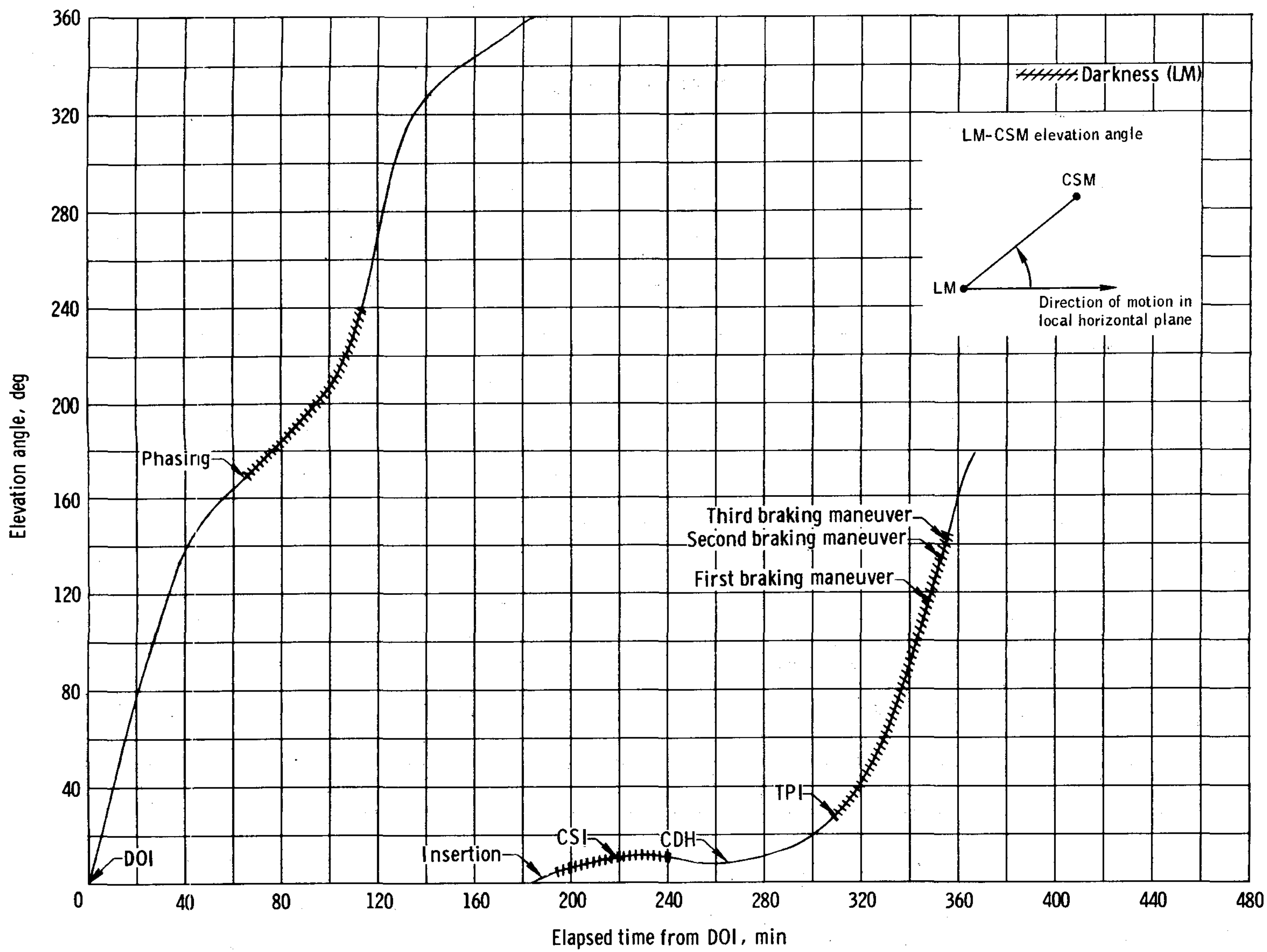

Figure 2. - Time history of LM-to-CSM elevation angle for LM-active phase of Mission F.

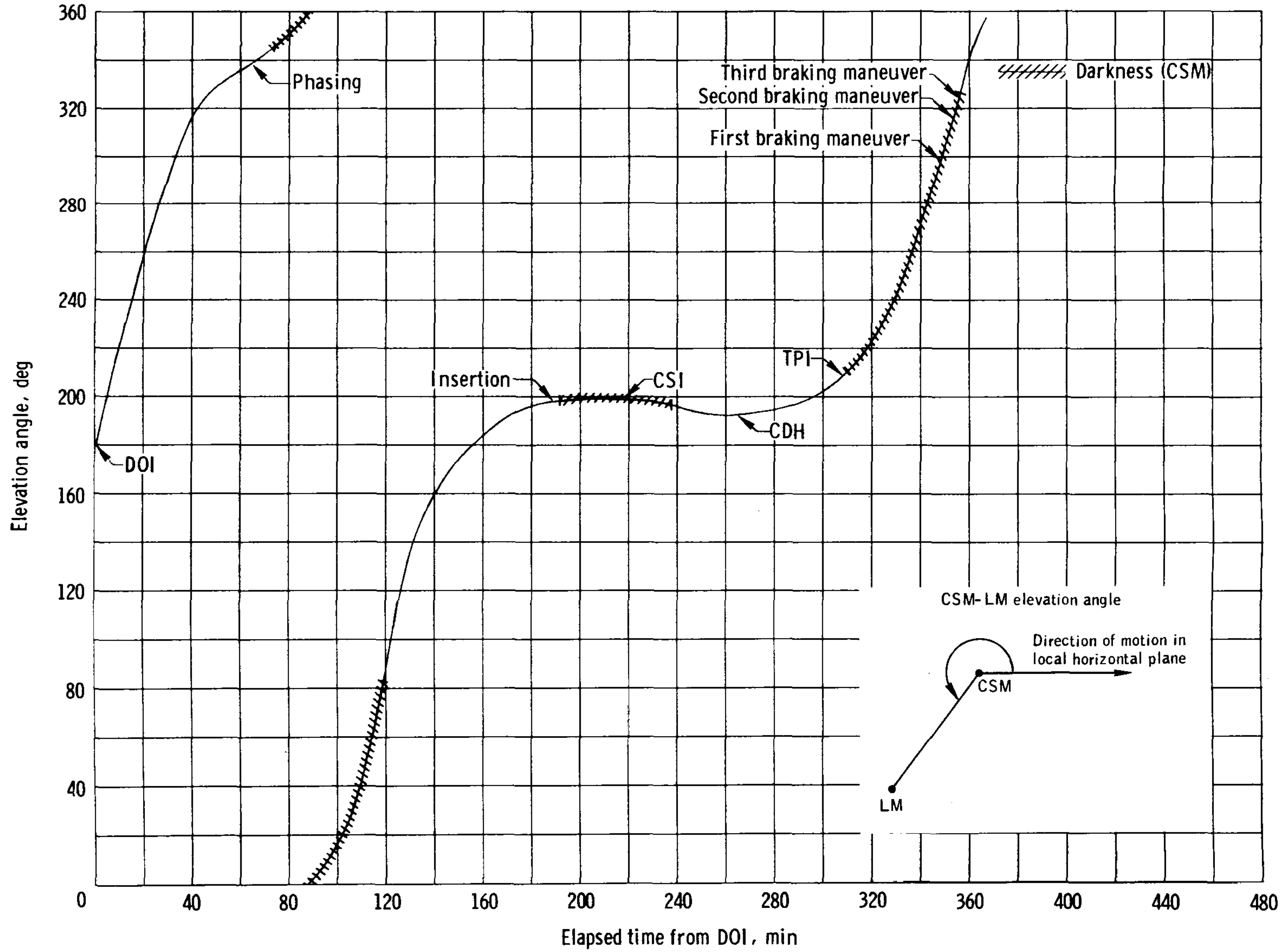

Figure 3. - Time history of CSM-to-LM elevation angle for LM-active phase of Mission F.

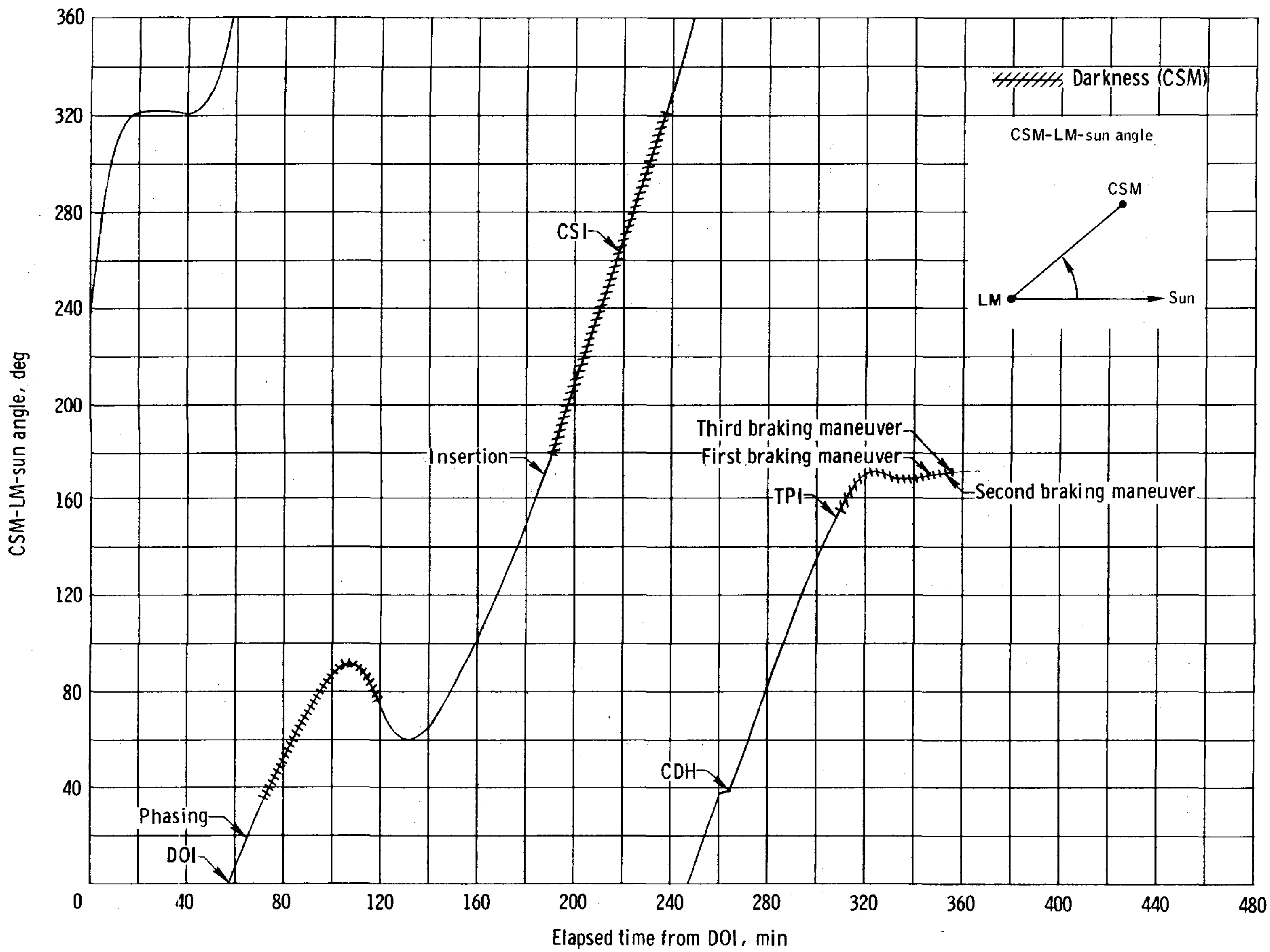

Figure 4. - Time history of CSM-LM-sun angle for LM-active phase of Mission F.

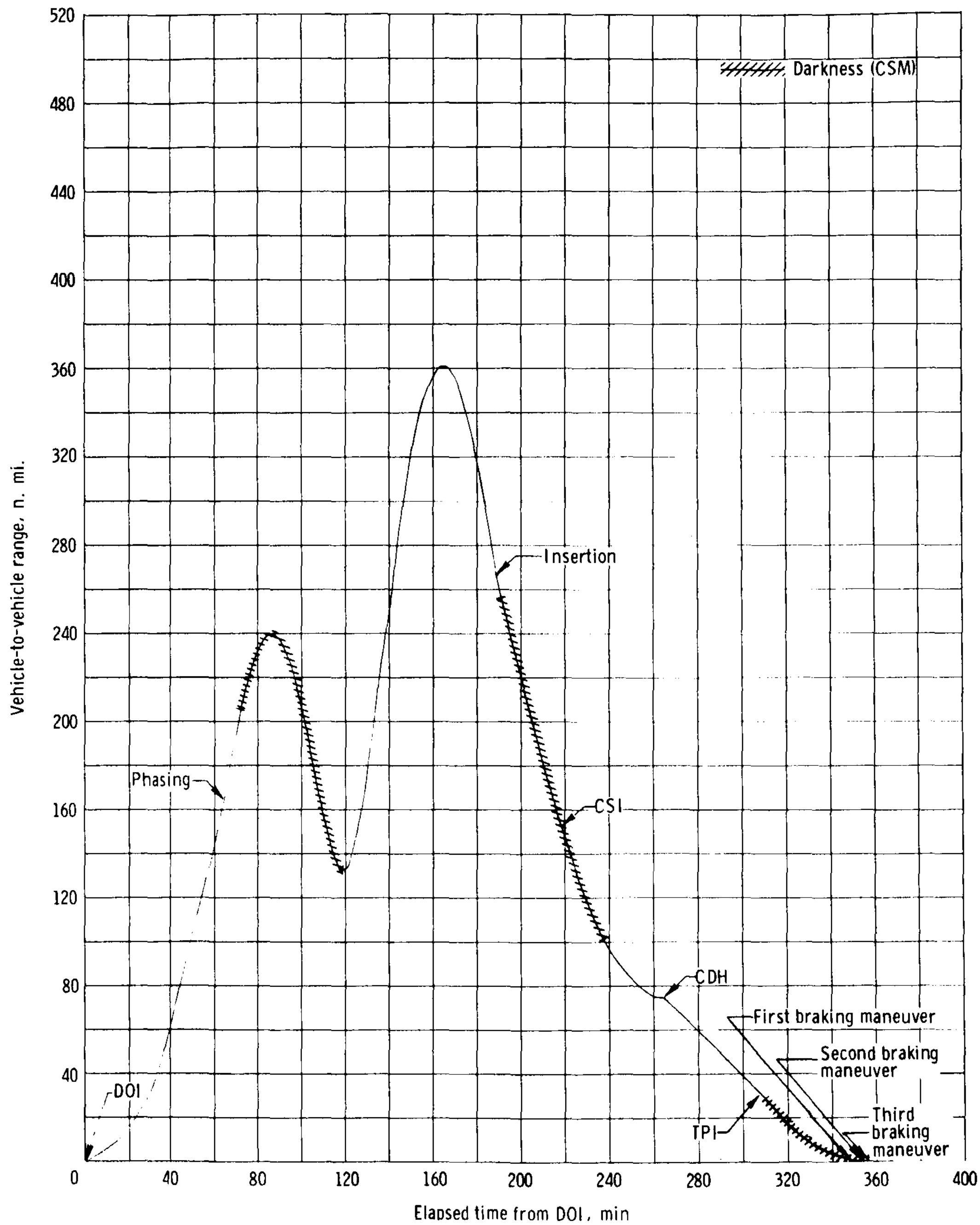

Figure 5. - Time history of vehicle-to-vehicle range for LM-active phase of Mission F.

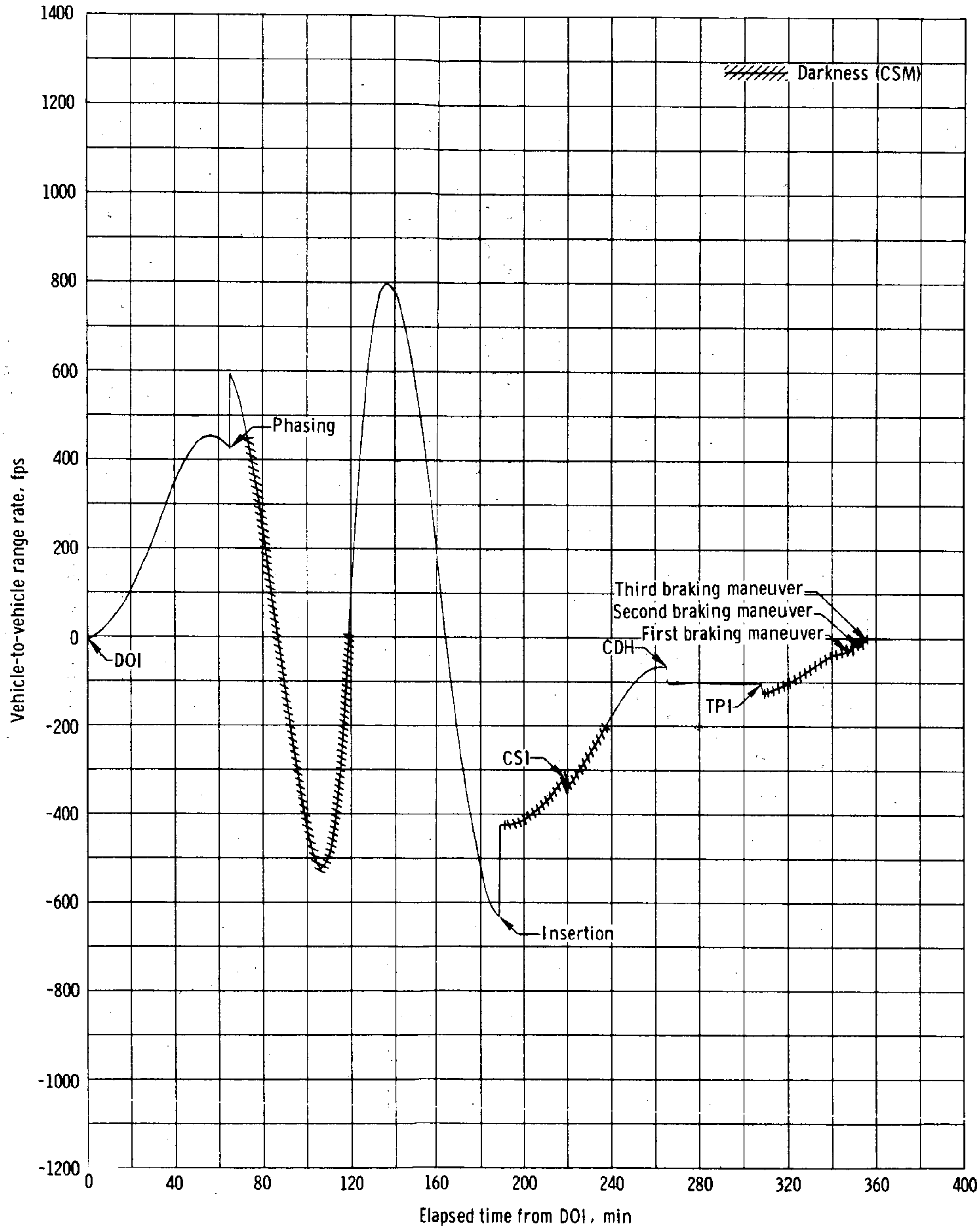

Figure 6. - Time history of vehicle-to-vehicle range rate for LM-active phase of Mission F.

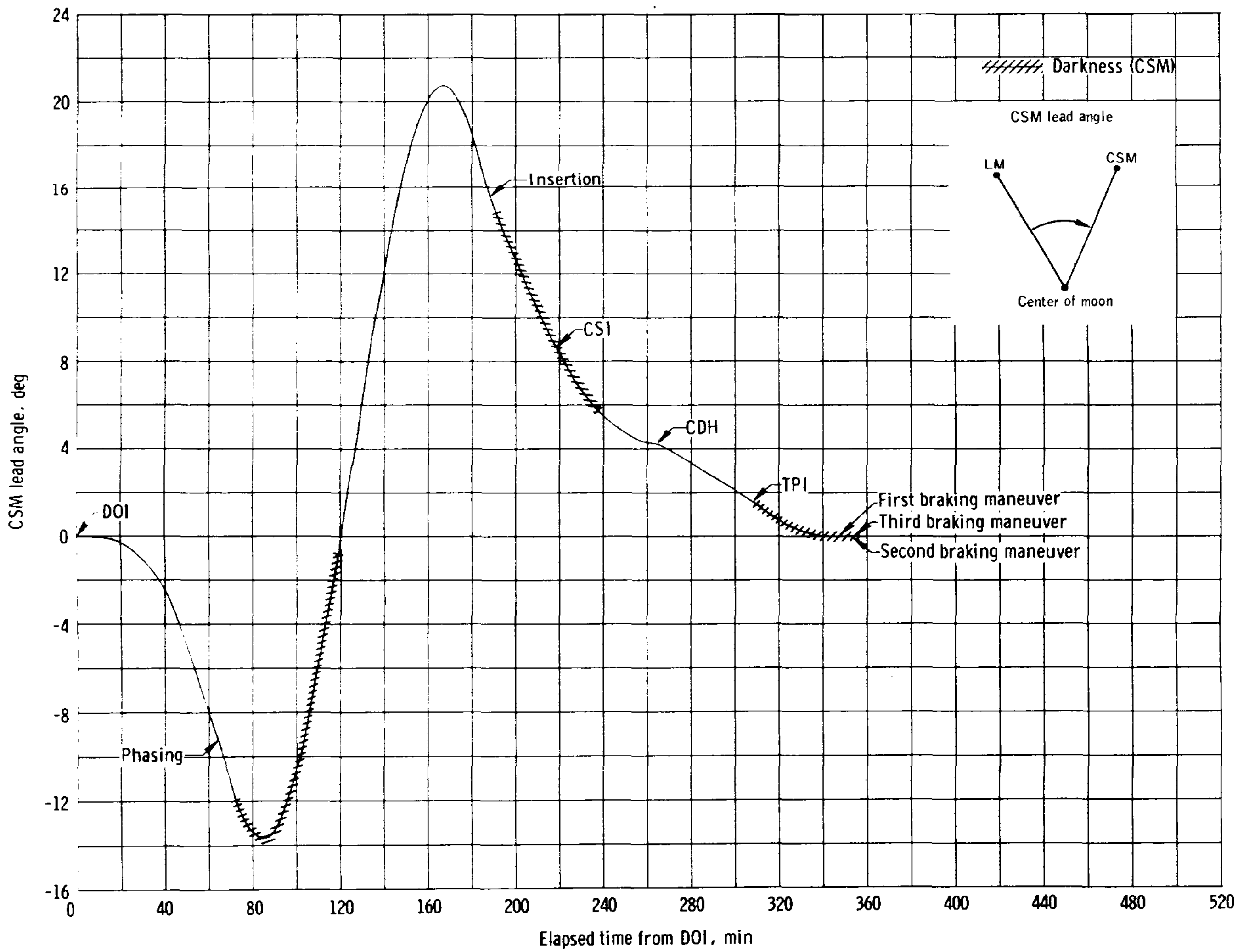

Figure 7.- Time history of CSM lead angle for LM-active phase of Mission F.

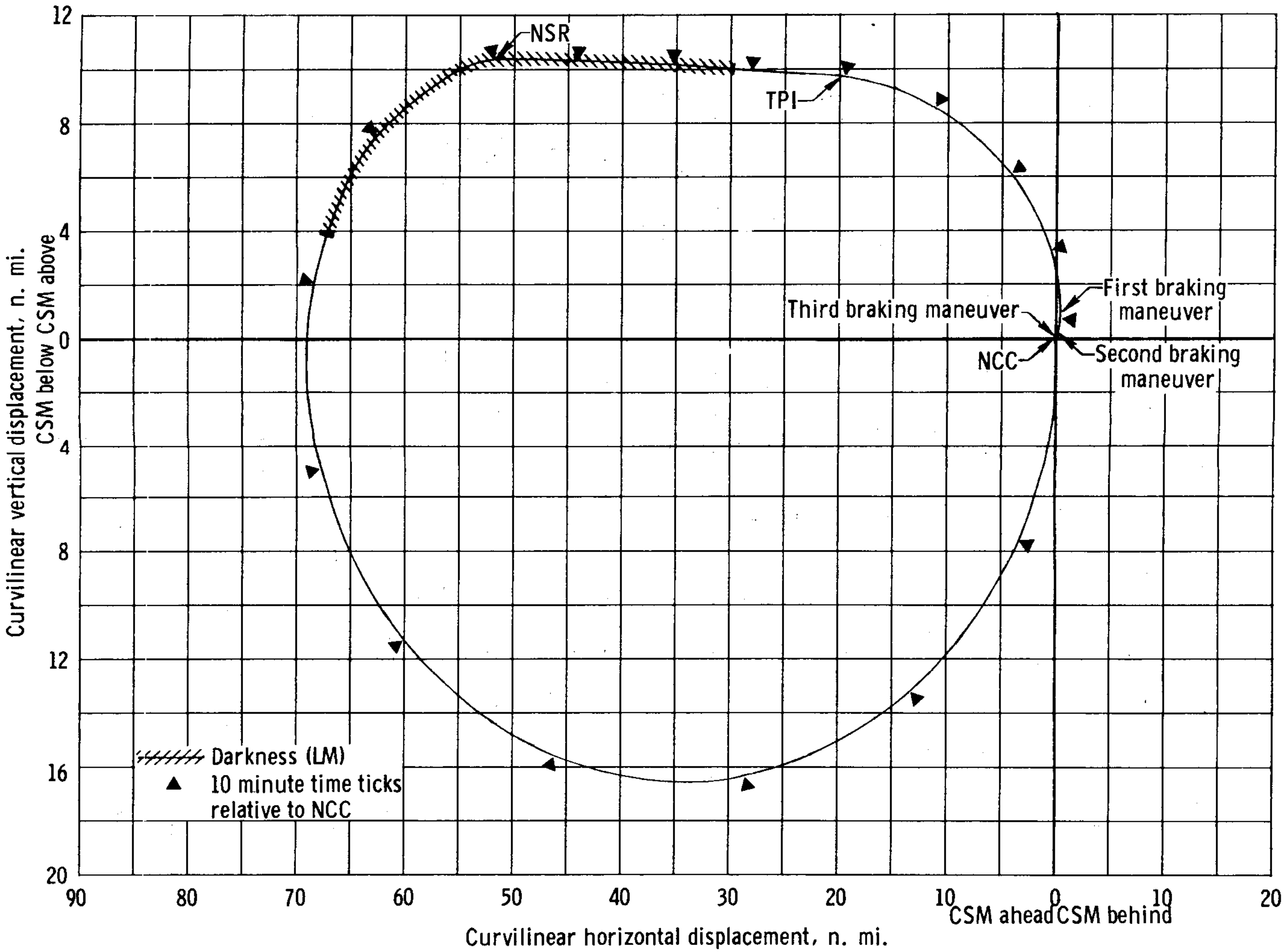

Figure 8. - Relative motion (curvilinear, LM-centered) for CSM-active phase of Mission F.

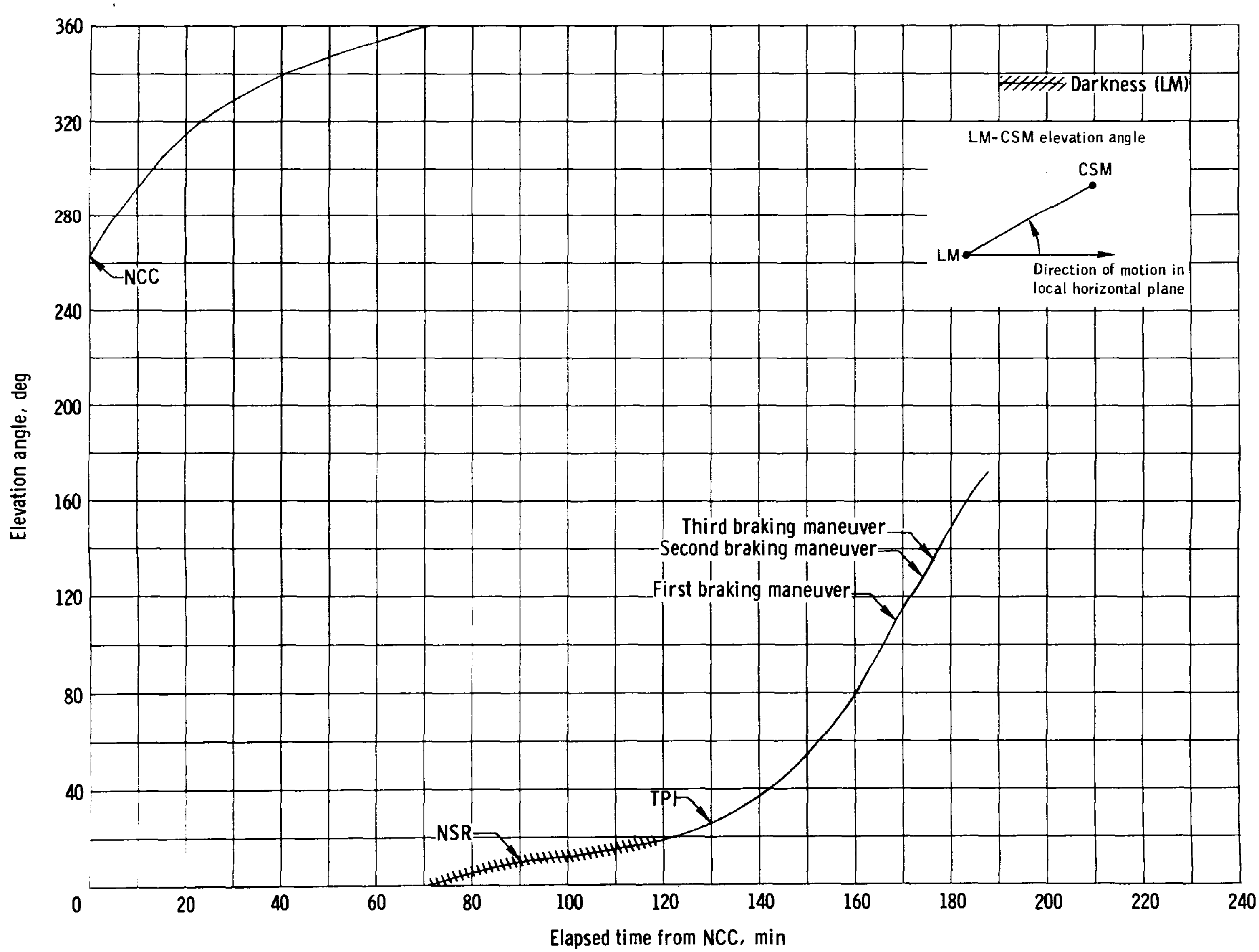

Figure 9. - Time history of LM-to-CSM elevation angle for CSM-active phase of Mission F.

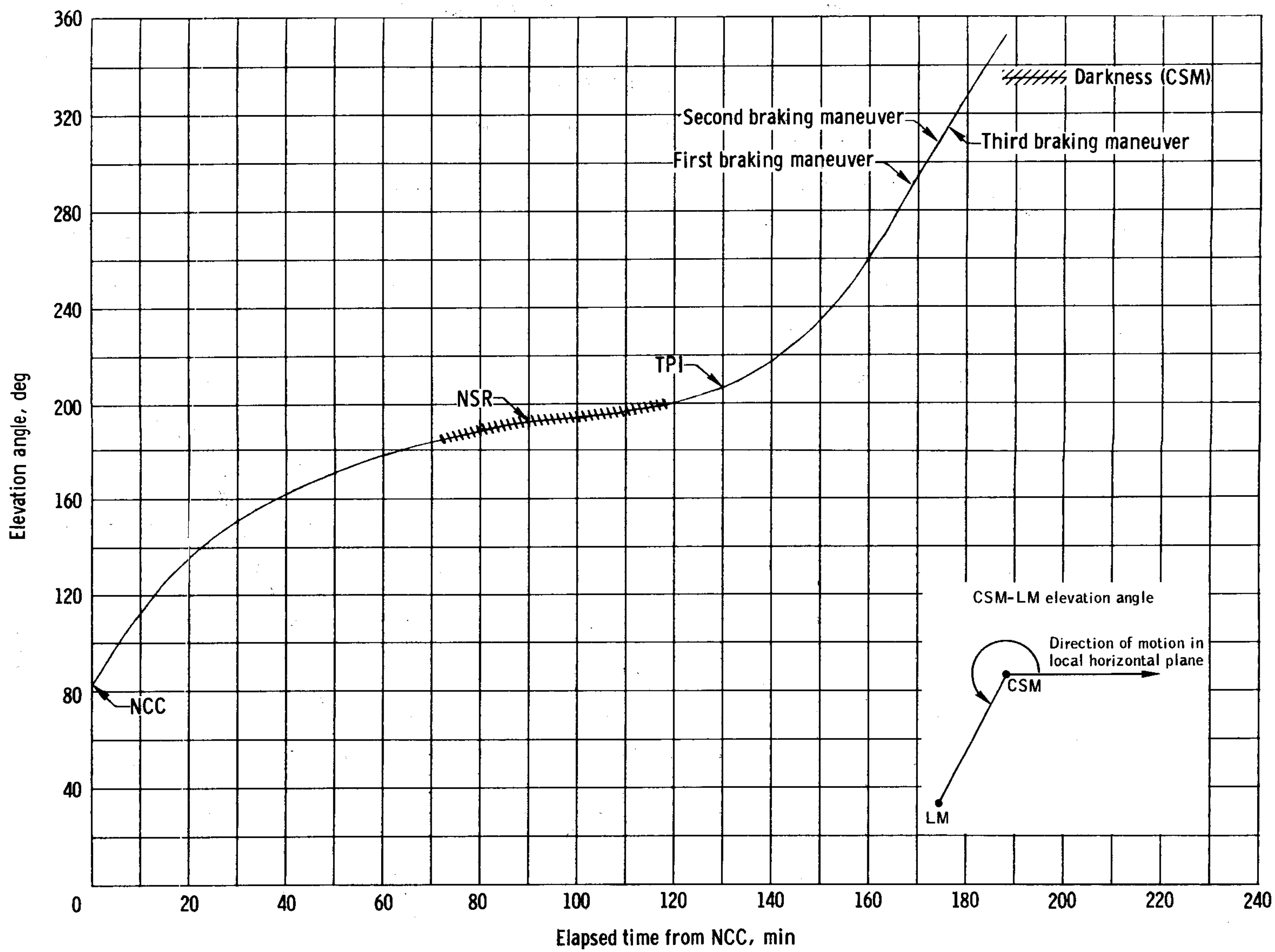

Figure 10.- Time history of CSM-to-LM elevation angle for CSM-active phase of Mission F.

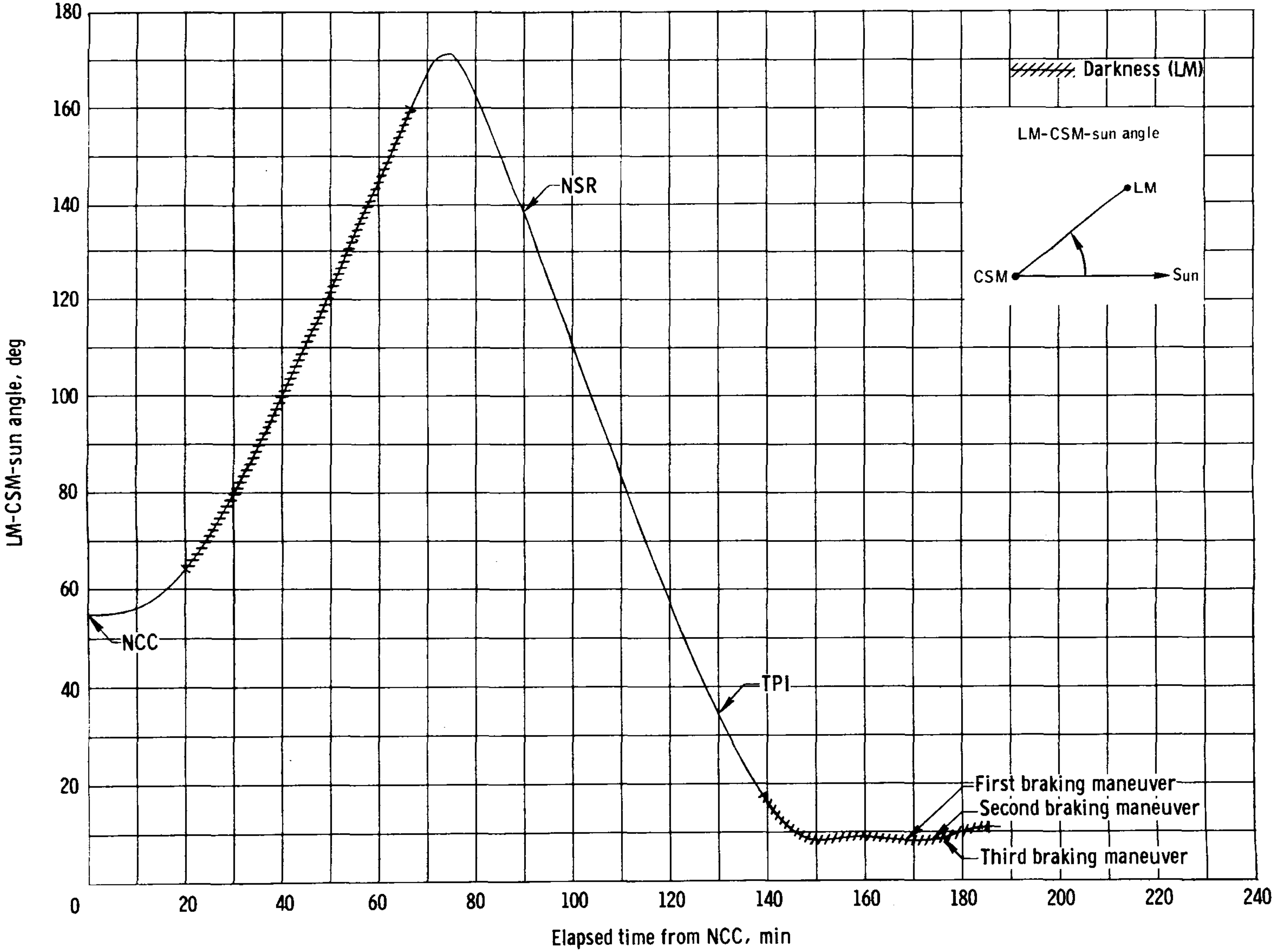

Figure 11. - Time history of LM-CSM-sun angle for CSM-active phase of Mission F.

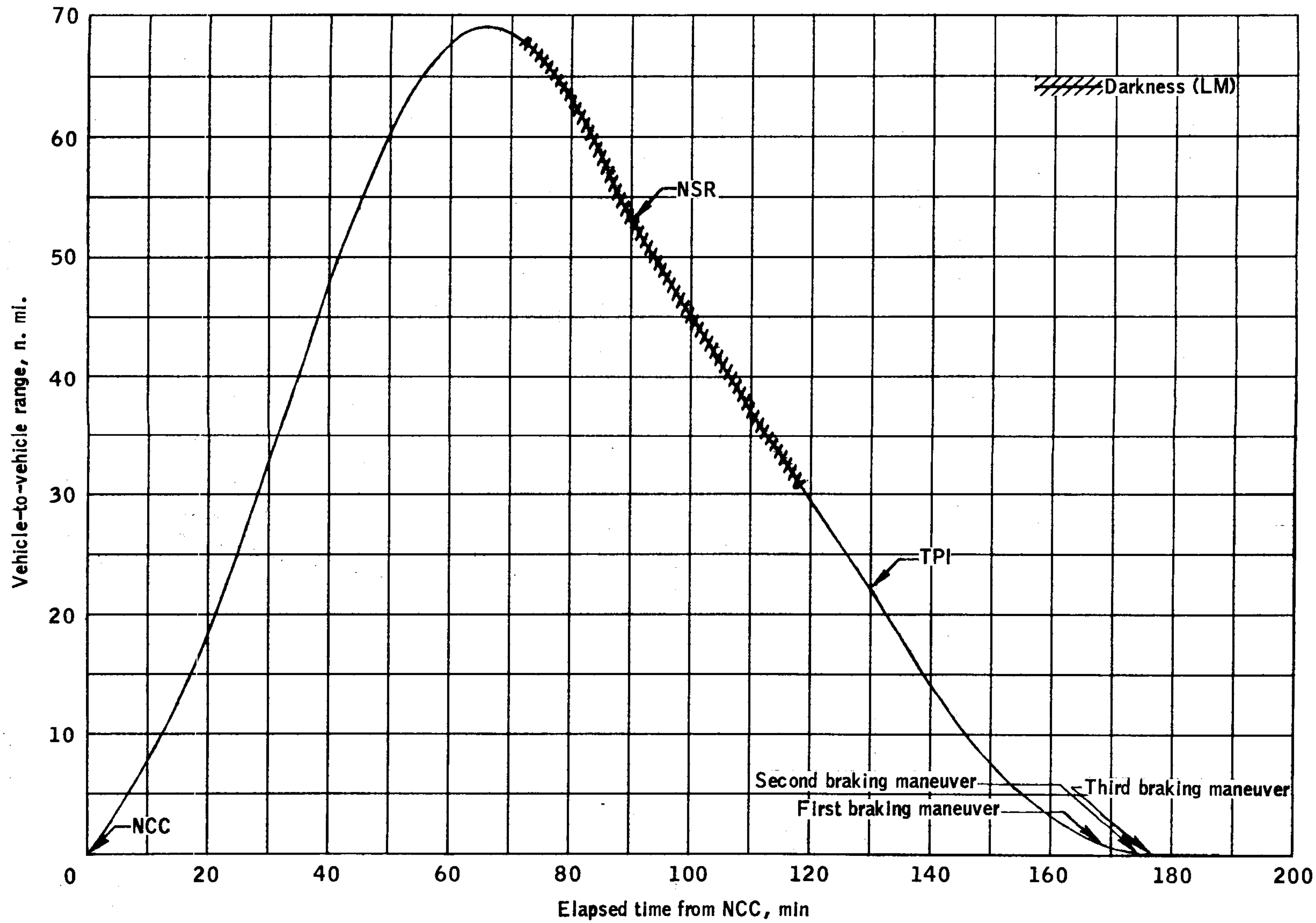

Figure 12. - Time history of vehicle-to-vehicle range for CSM-active phase of Mission F.

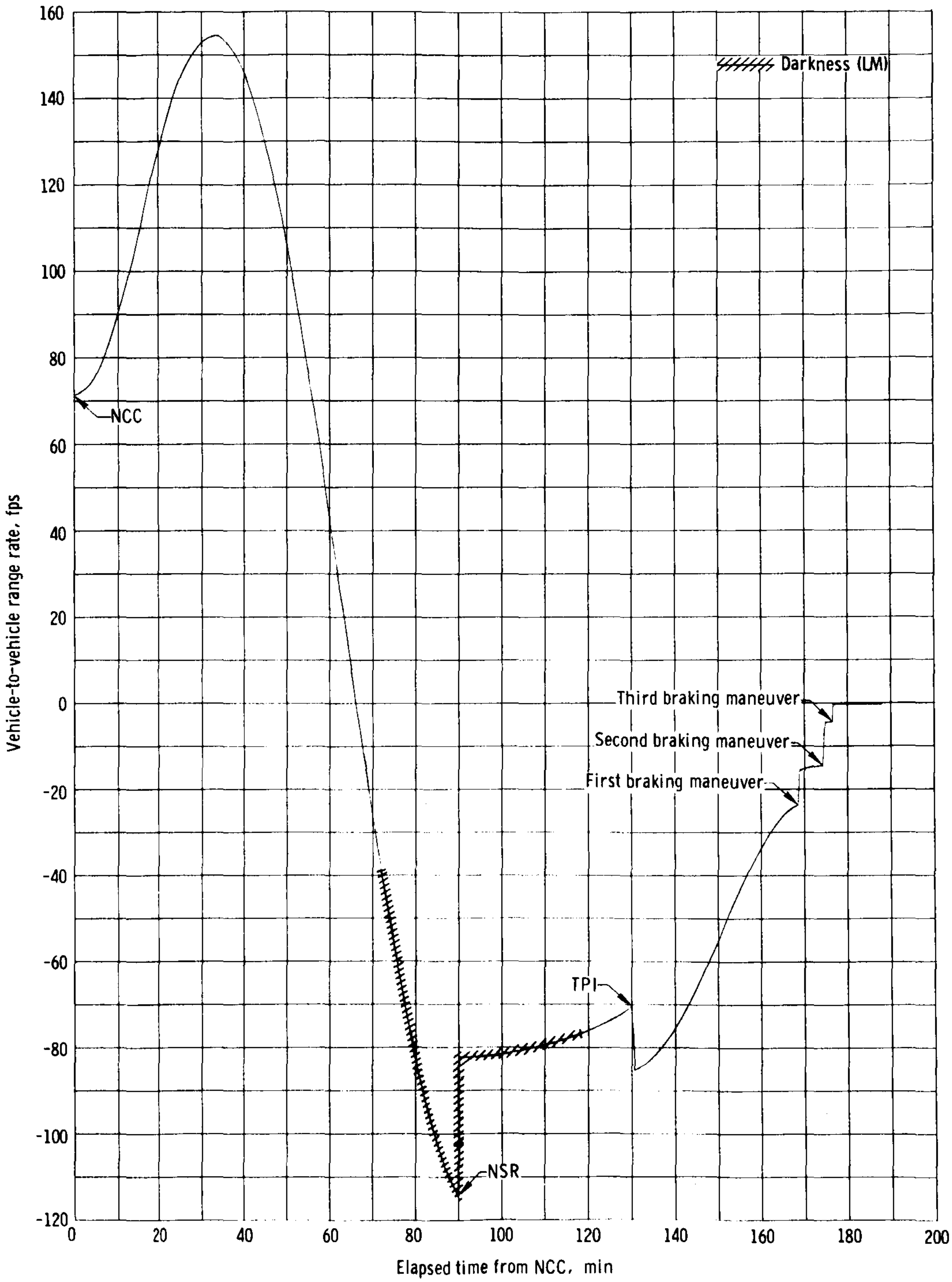

Figure 13. - Time history of vehicle-to-vehicle range rate for CSM-active phase of Misssion F.

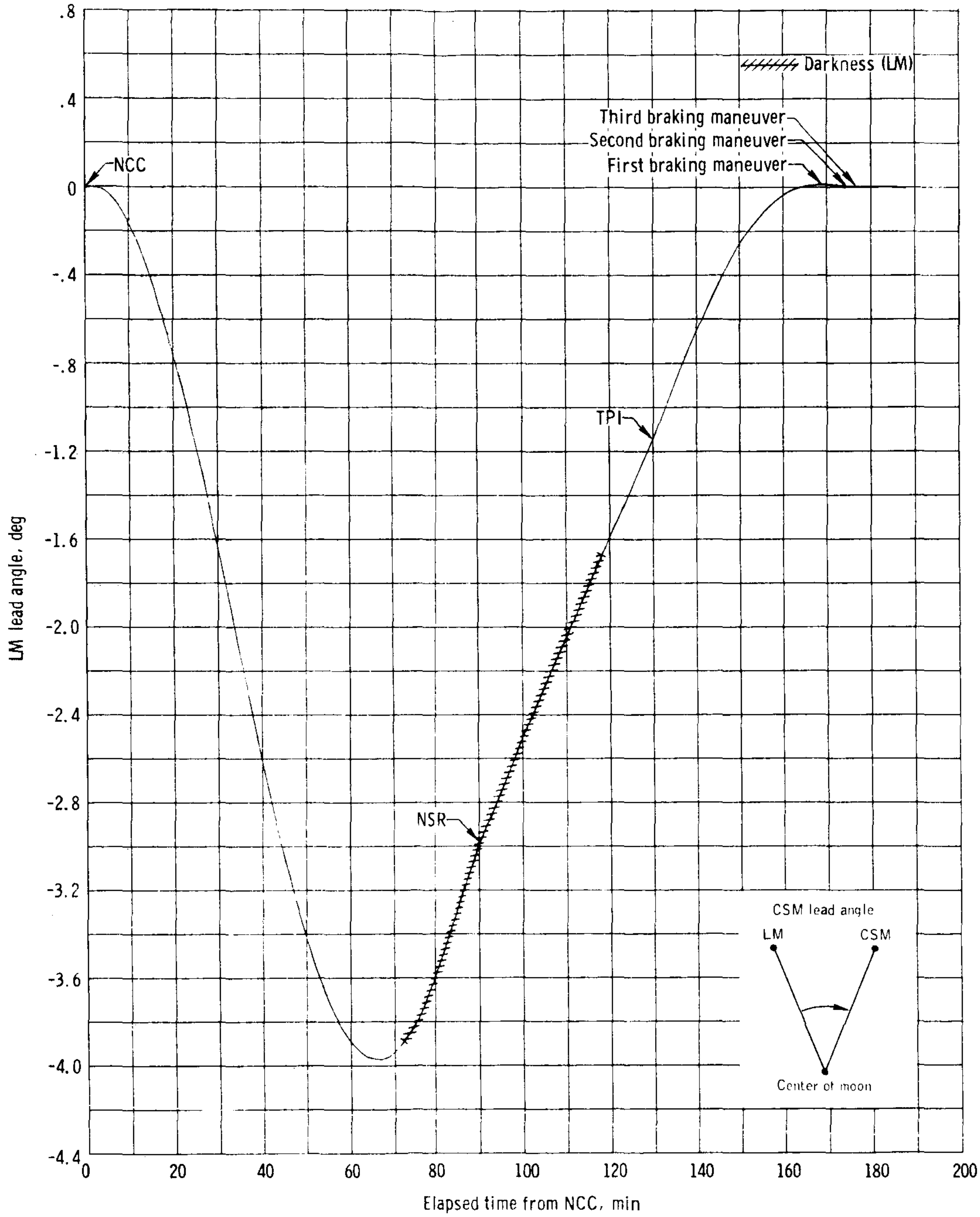

Figure 14. - Time history of LM lead angle for CSM-active phase of Mission F.

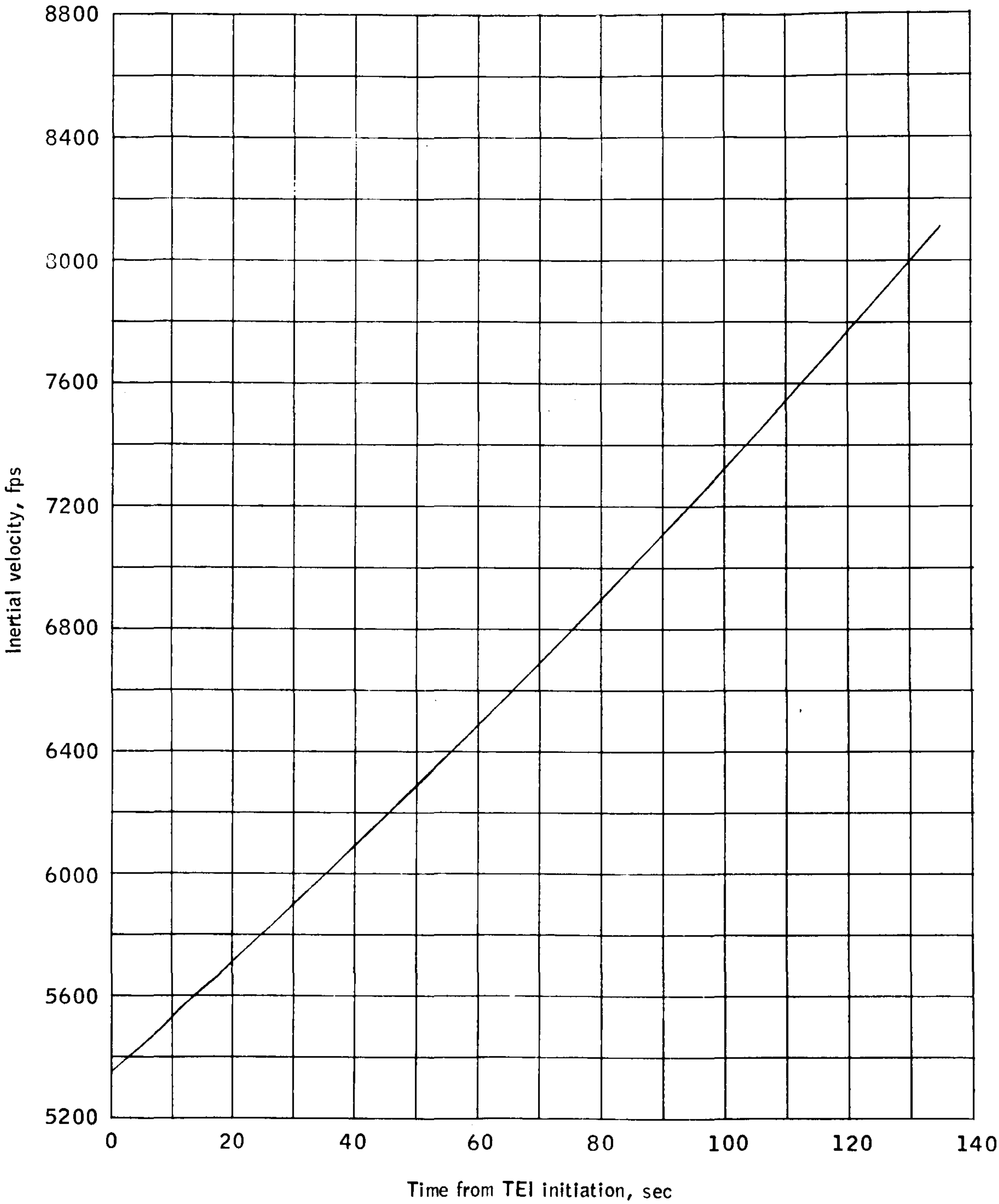

(a) Inertial velocity versus time from TEI initiation.

Figure 15.- Time histories of trajectory parameters for the transearth injection phase.

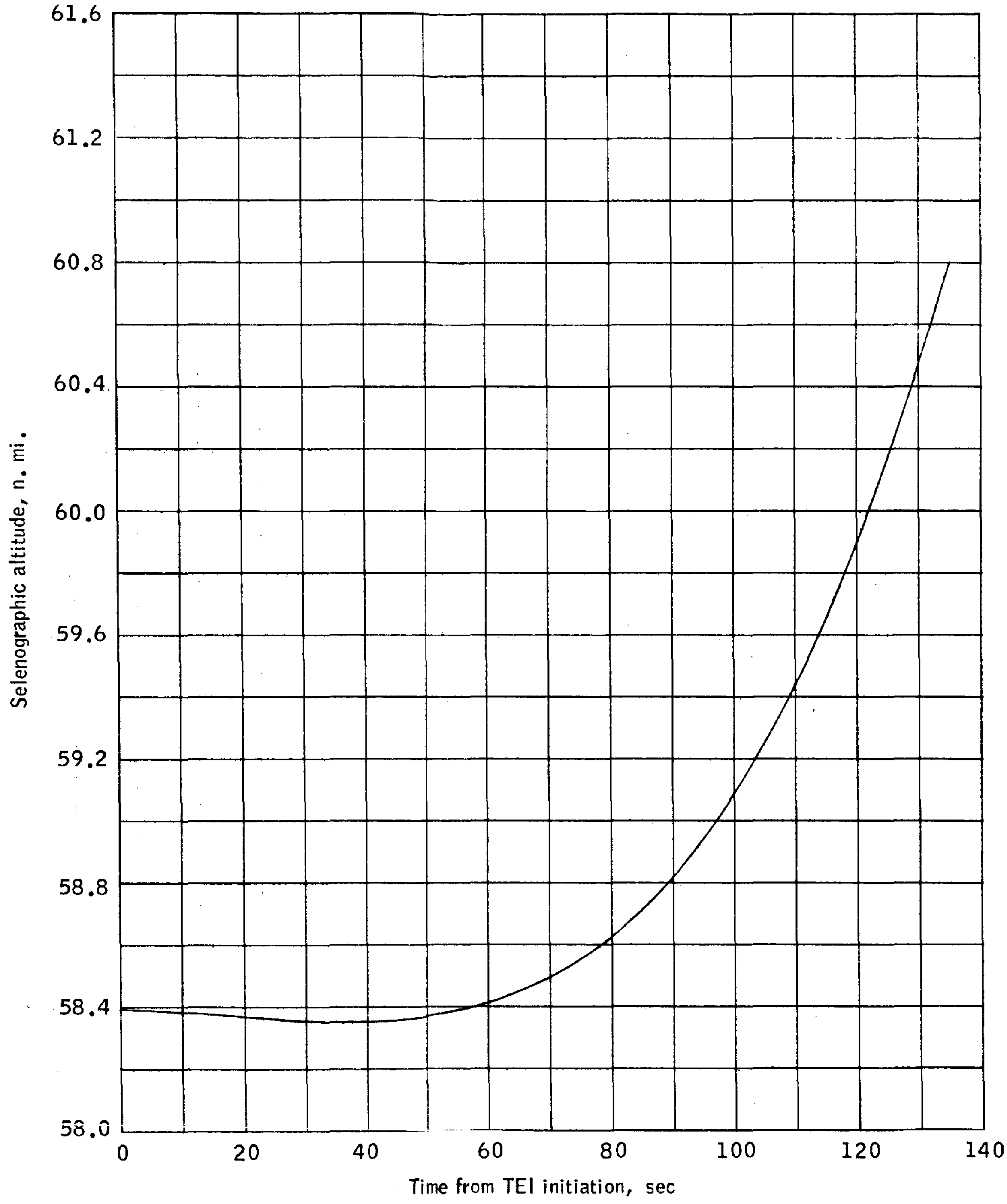

(b) Selenographic altitude versus time from TEI initiation.

Figure 15.- Continued.

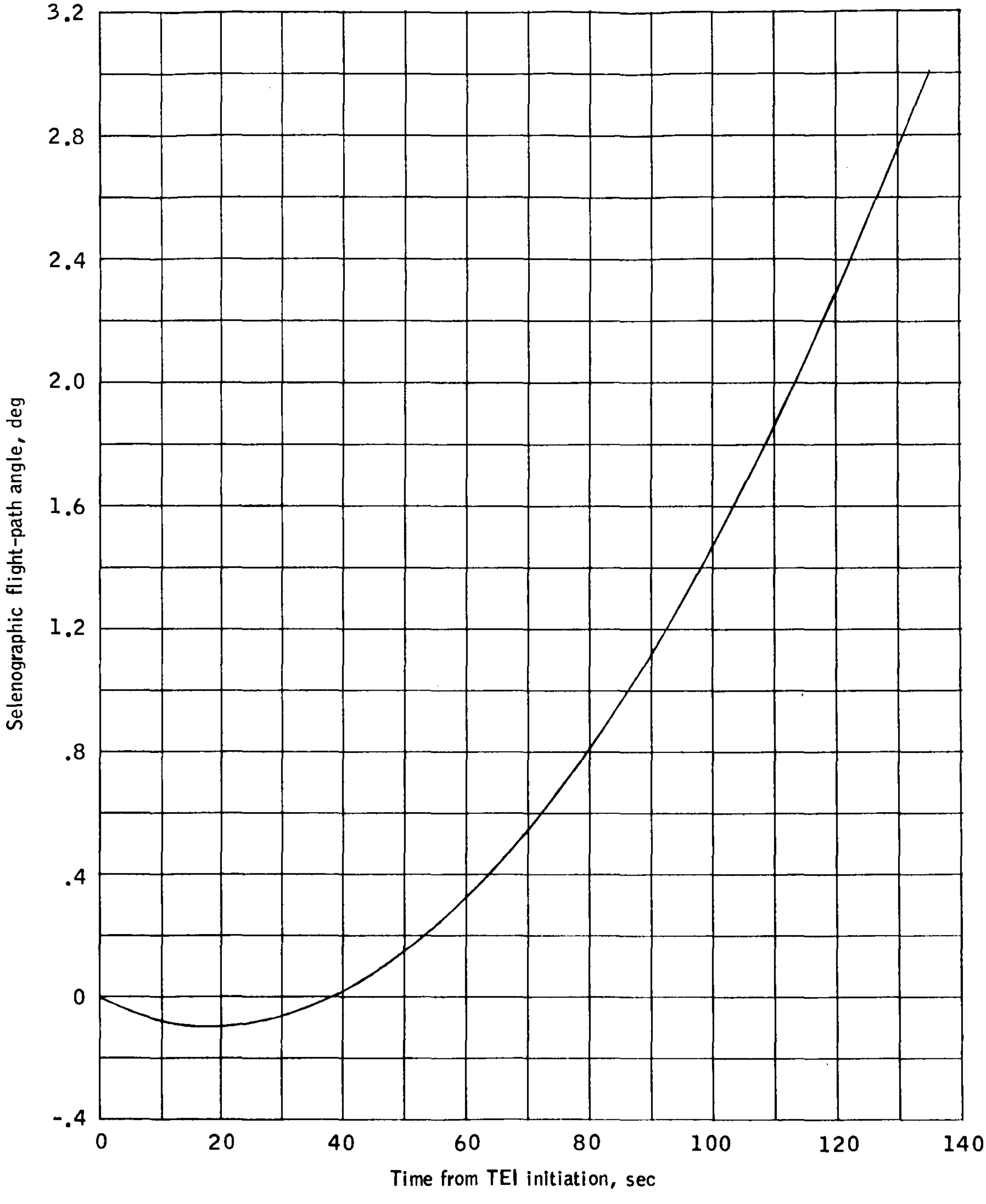

(c) Selenographic flight-path angle versus time from TEI initiation.

Figure 15.- Continued.

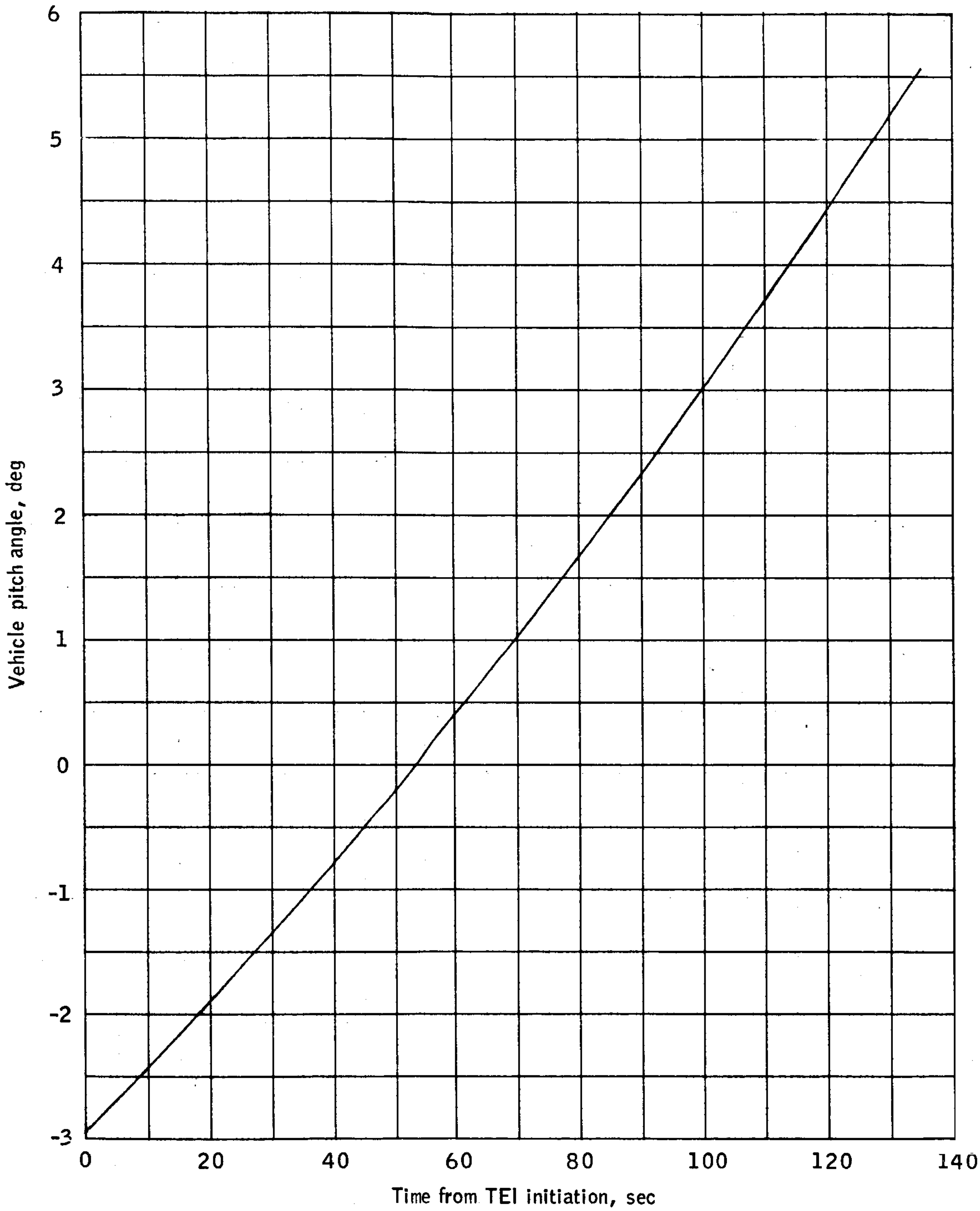

(d) Vehicle pitch angle (local horizontal coordinate system) versus time from TEI initiation.

Figure 15.- Continued.

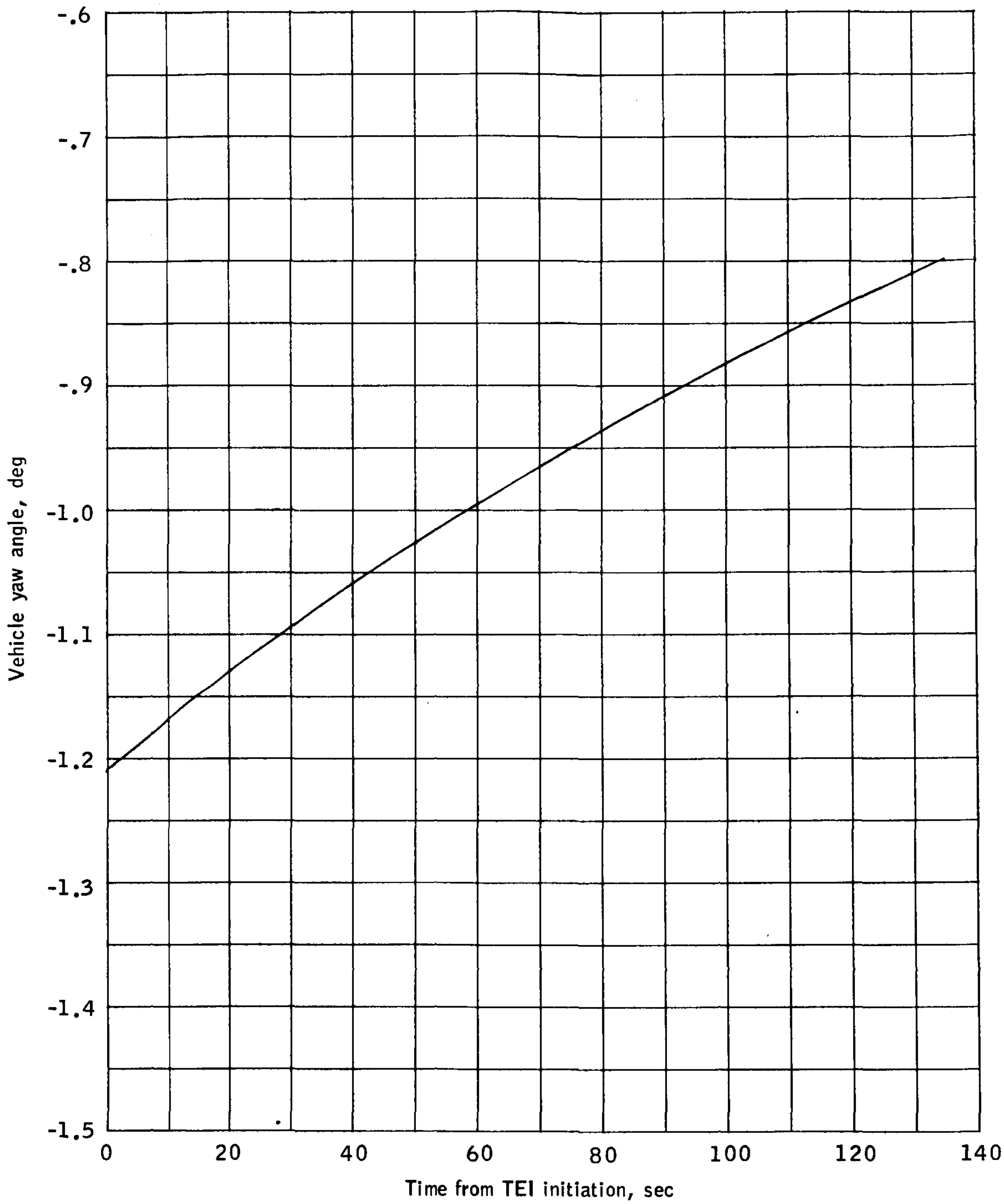

(e) Vehicle yaw angle (local horizontal coordinate system) versus time from TEI initiation.

Figure 15.- Continued.

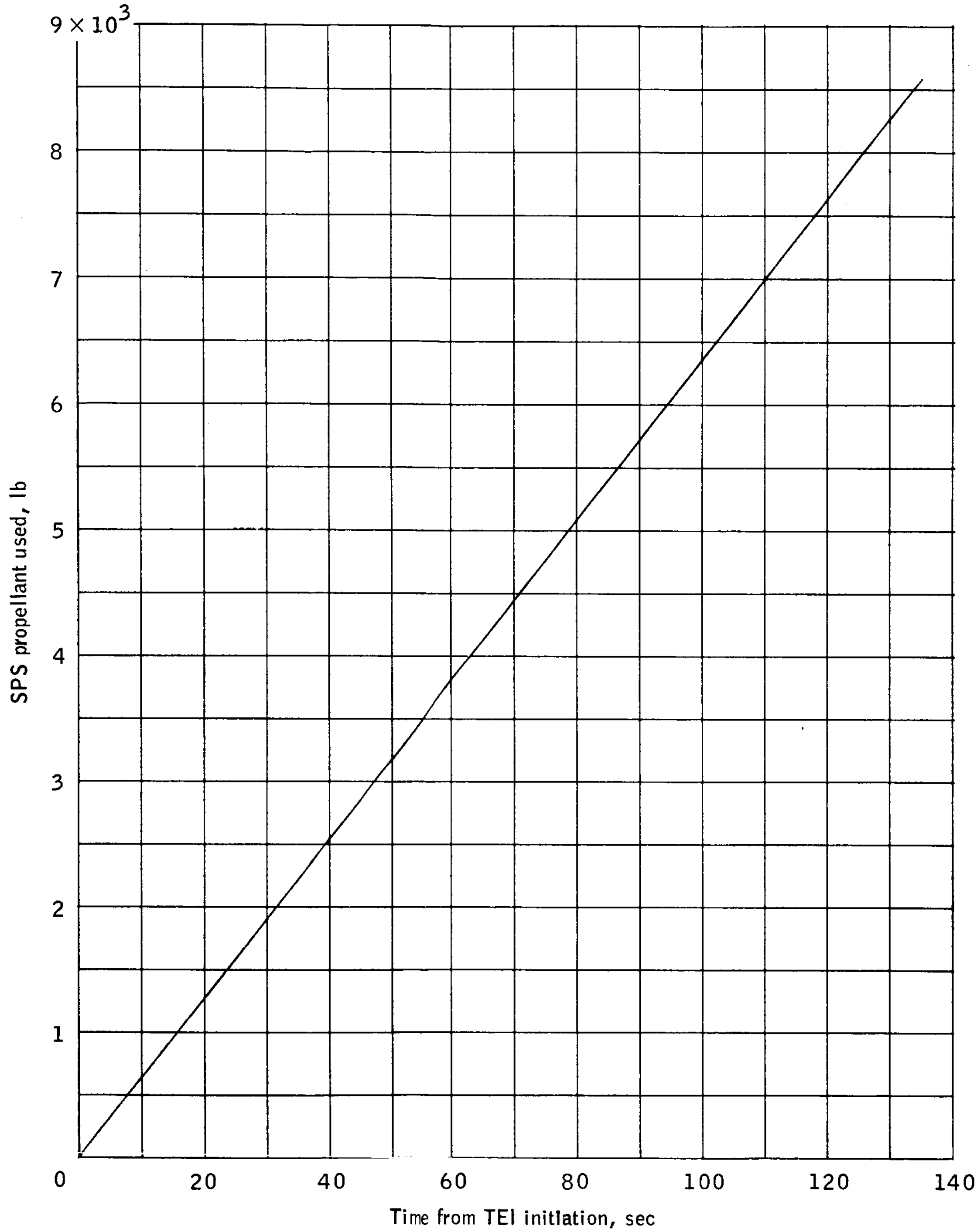

(f) SPS propellant used versus time from TEI initiation.

Figure 15.- Concluded.

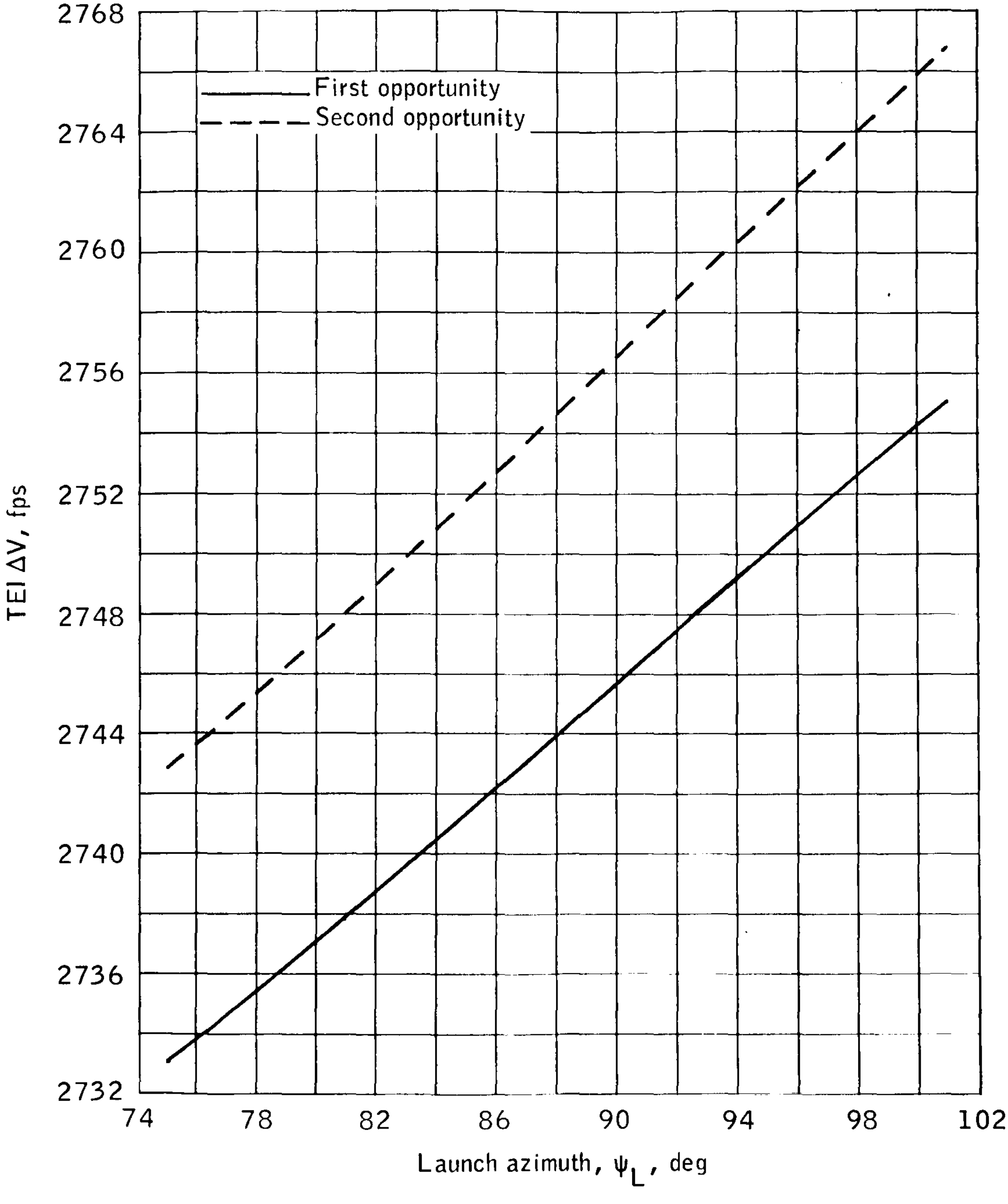

(a) TEI ΔV.

Figure 16.- Trajectory parameters as a function of launch azimuth for lift-off on July 15, 1969.

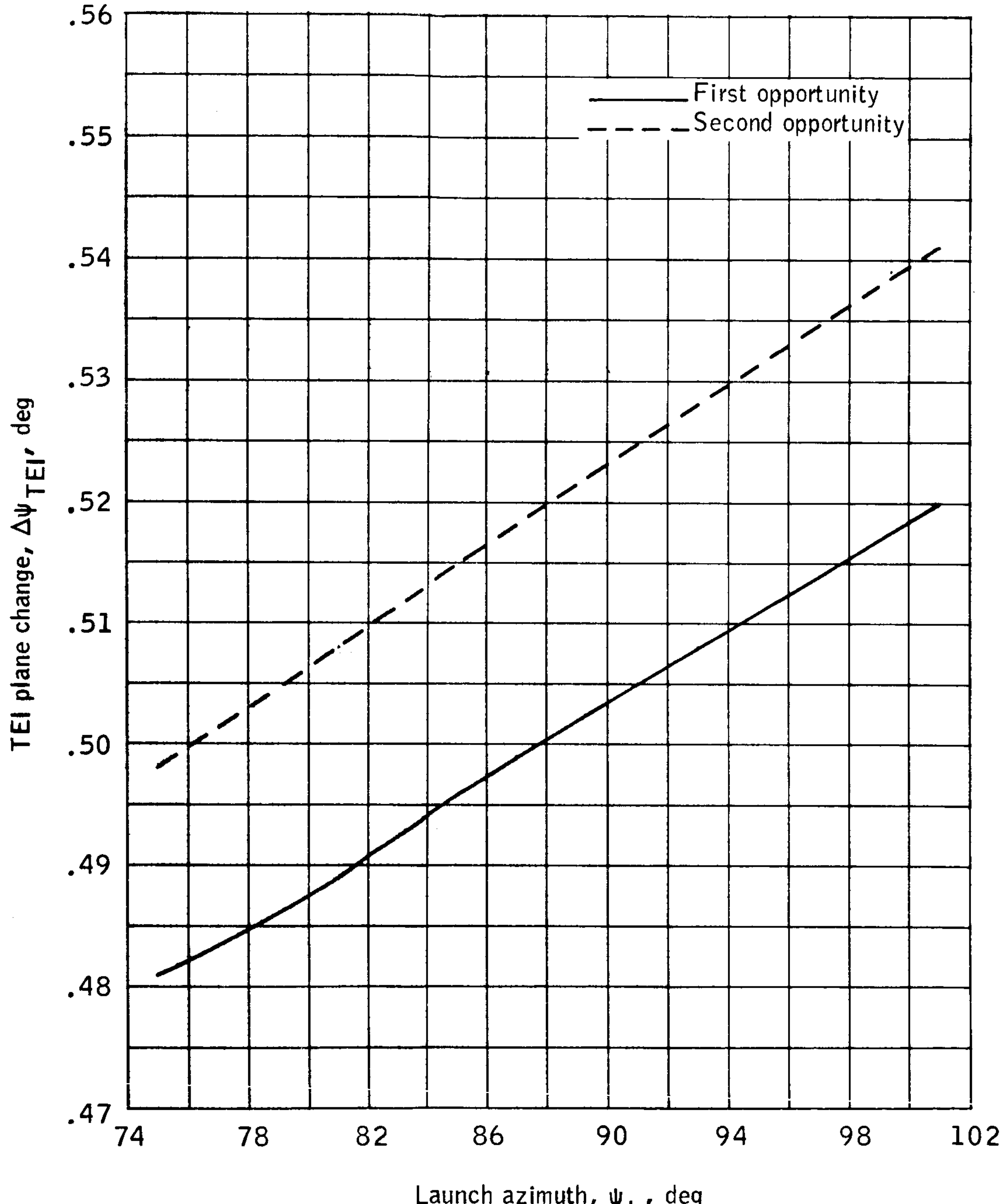

(b) TEI plane change.

Figure 16.- Continued.

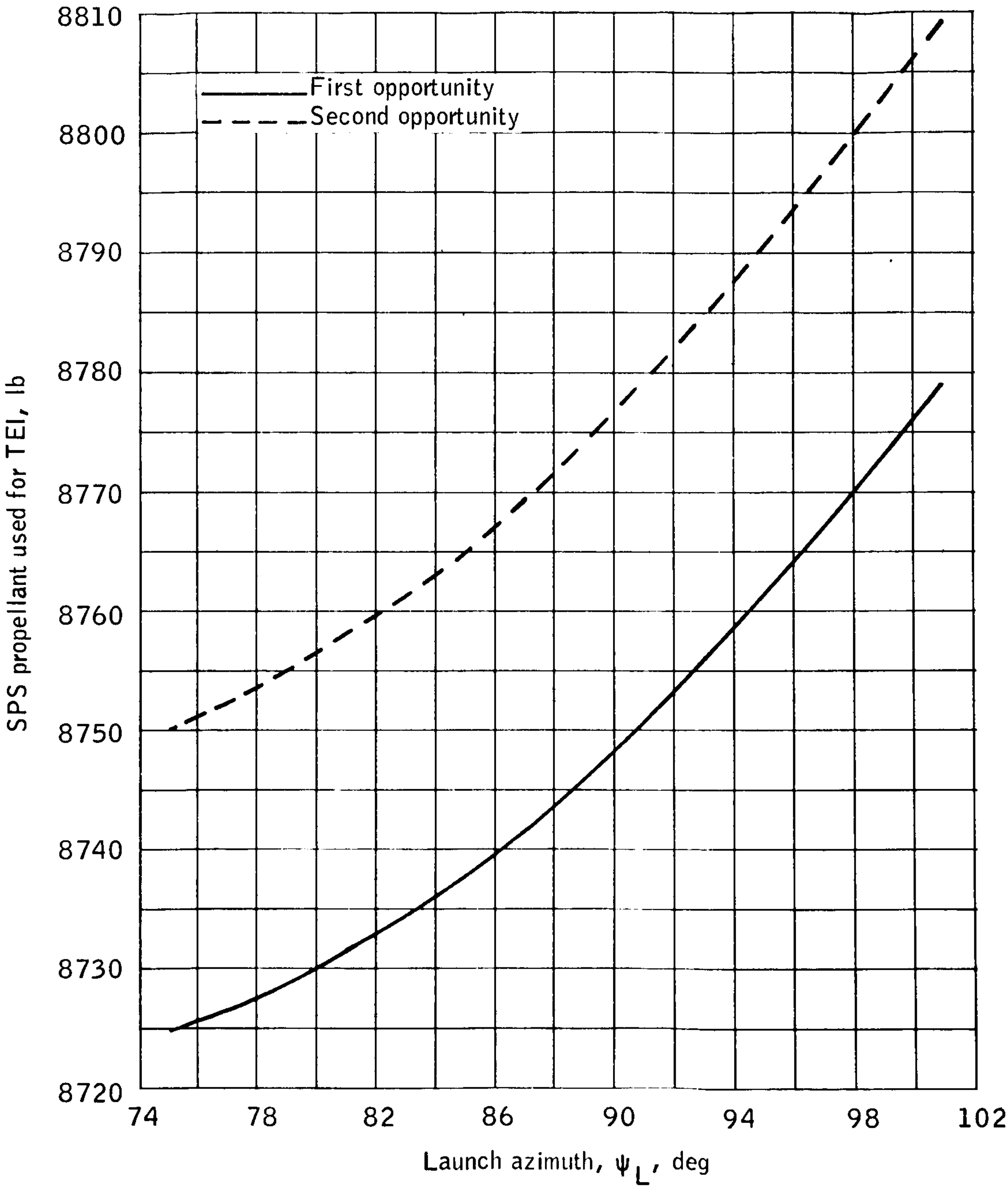

(c) SPS propellant used for TEI.

Figure 16.- Continued.

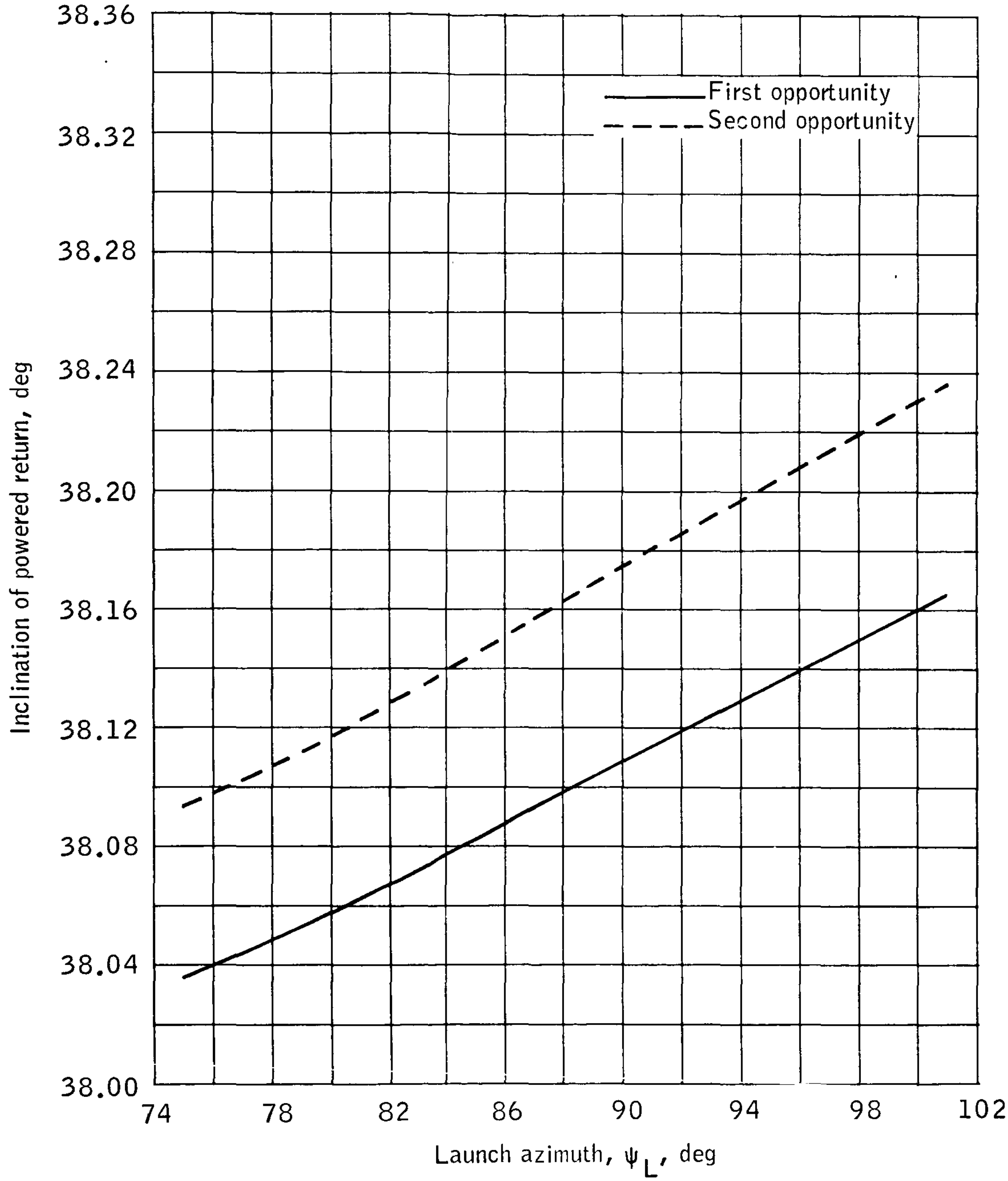

(d) Inclination of powered return.

Figure 16.- Continued.

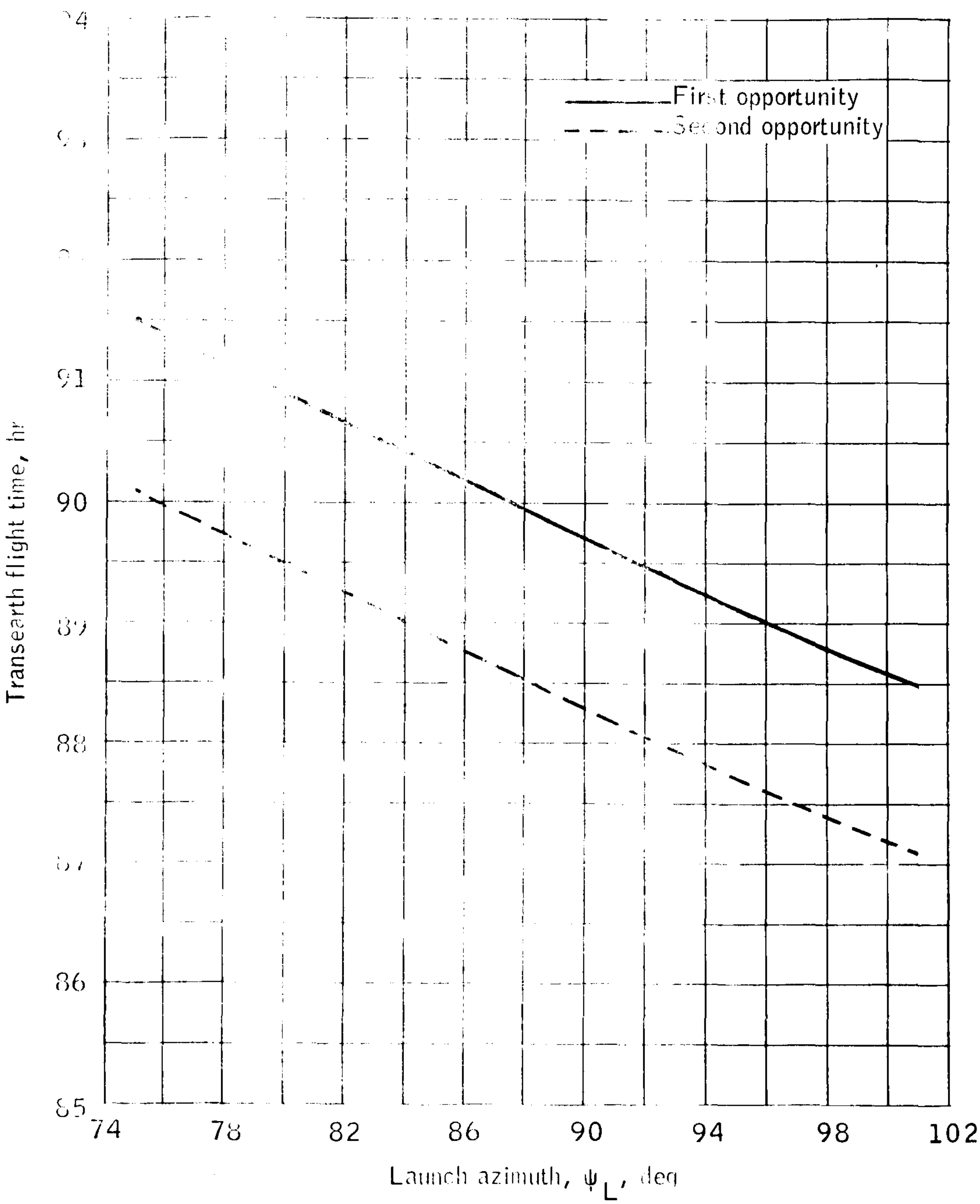

(c) Transearth flight time.

Figure 16.- Concluded.

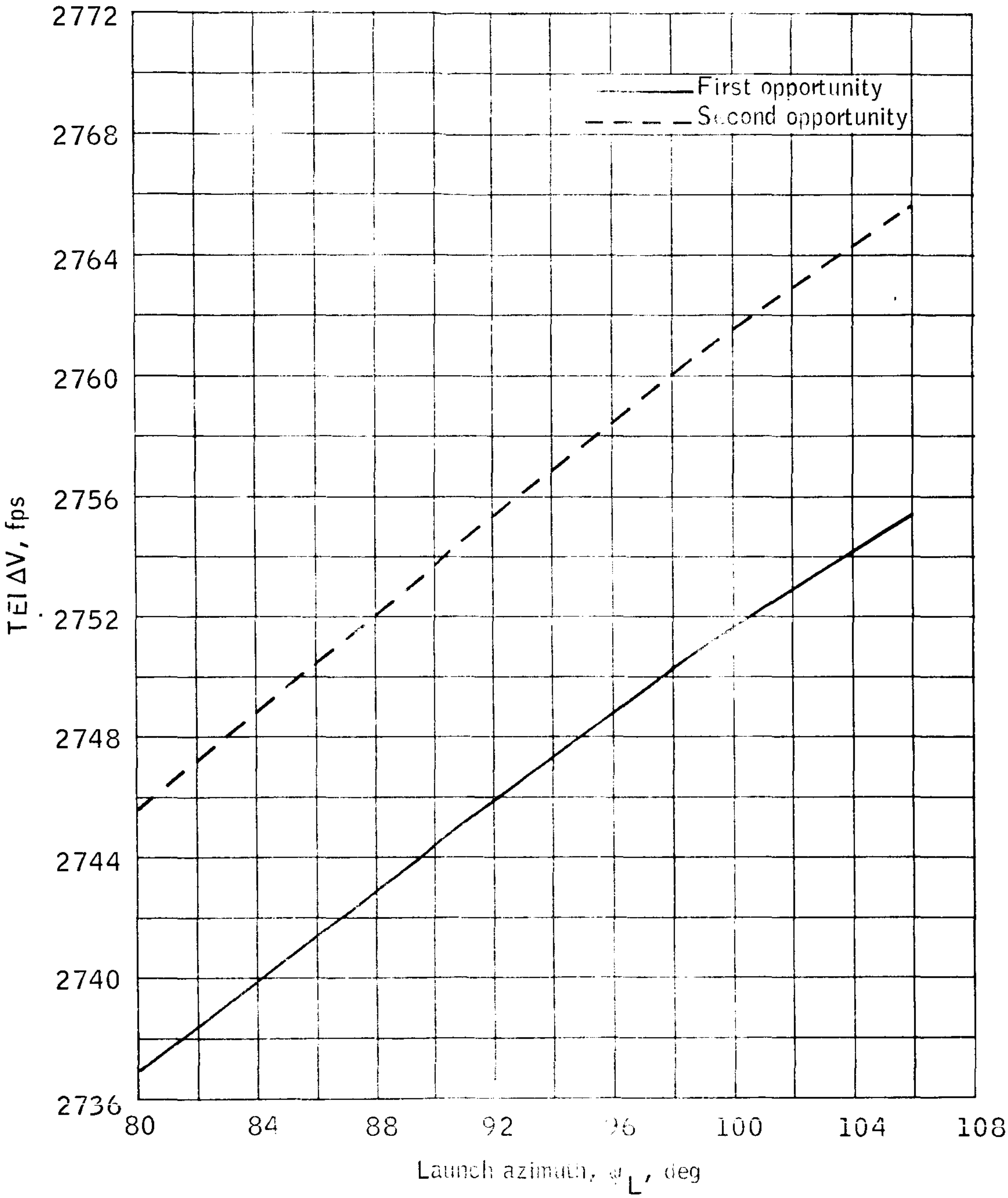

(a) TEI ΔV.

Figure 17.- Trajectory parameters as a function of launch azimuth for lift-off on July 16, 1969.

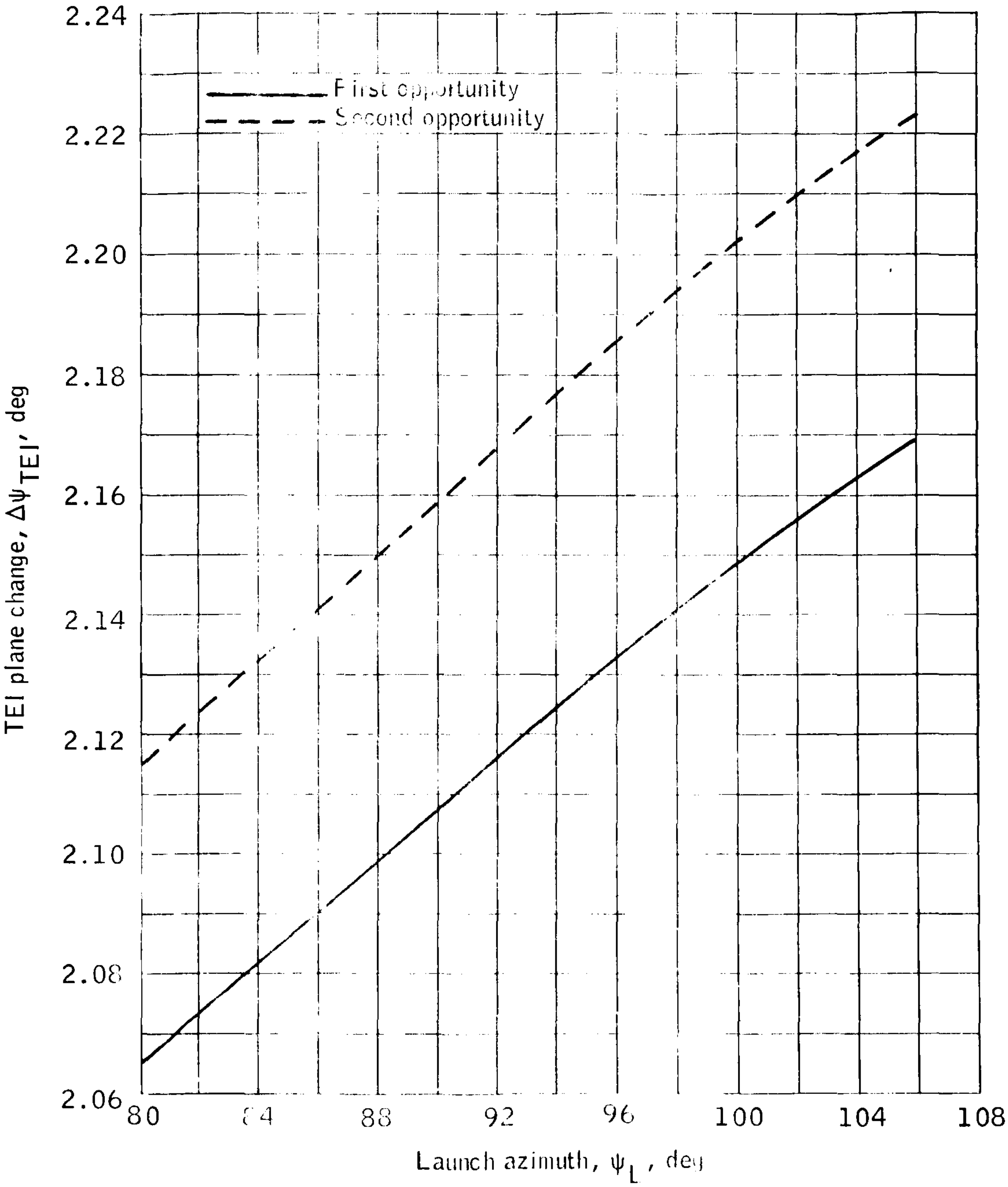

(b) TEI plane change.

Figure 17.- Continued.

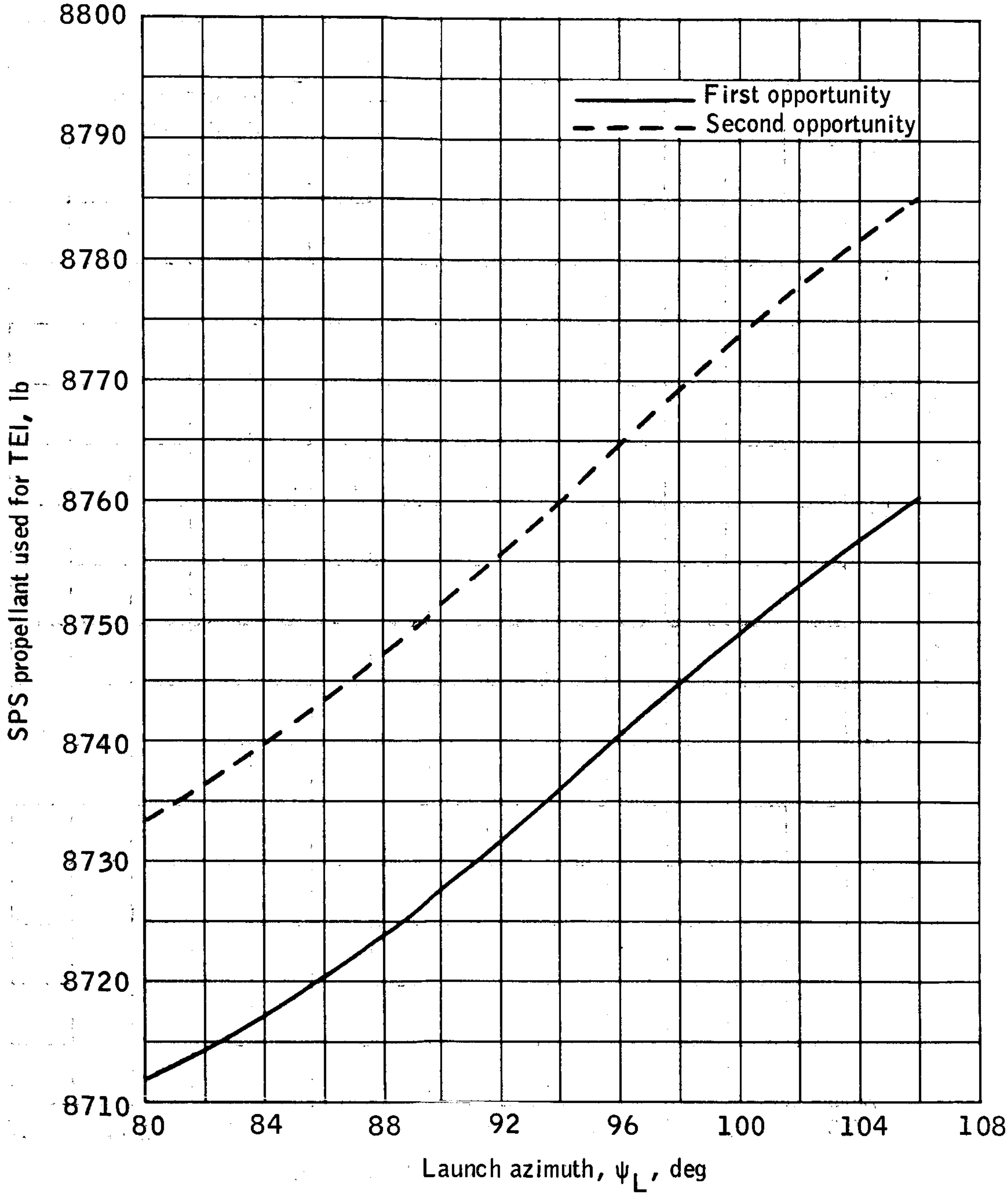

(c) SPS propellant used for TEI.

Figure 17.- Continued.

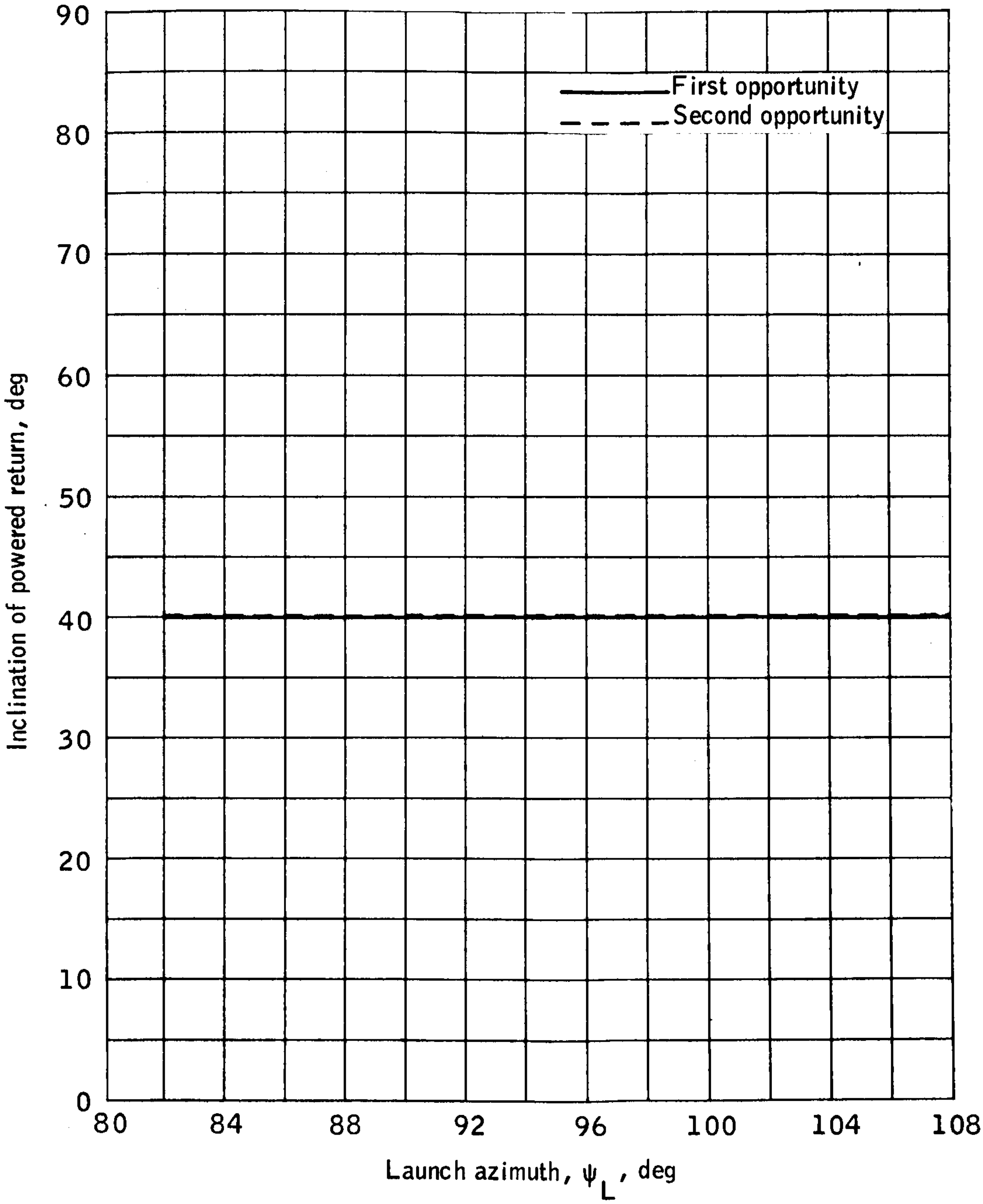

(d) Inclination of powered return.

Figure 17.- Continued.

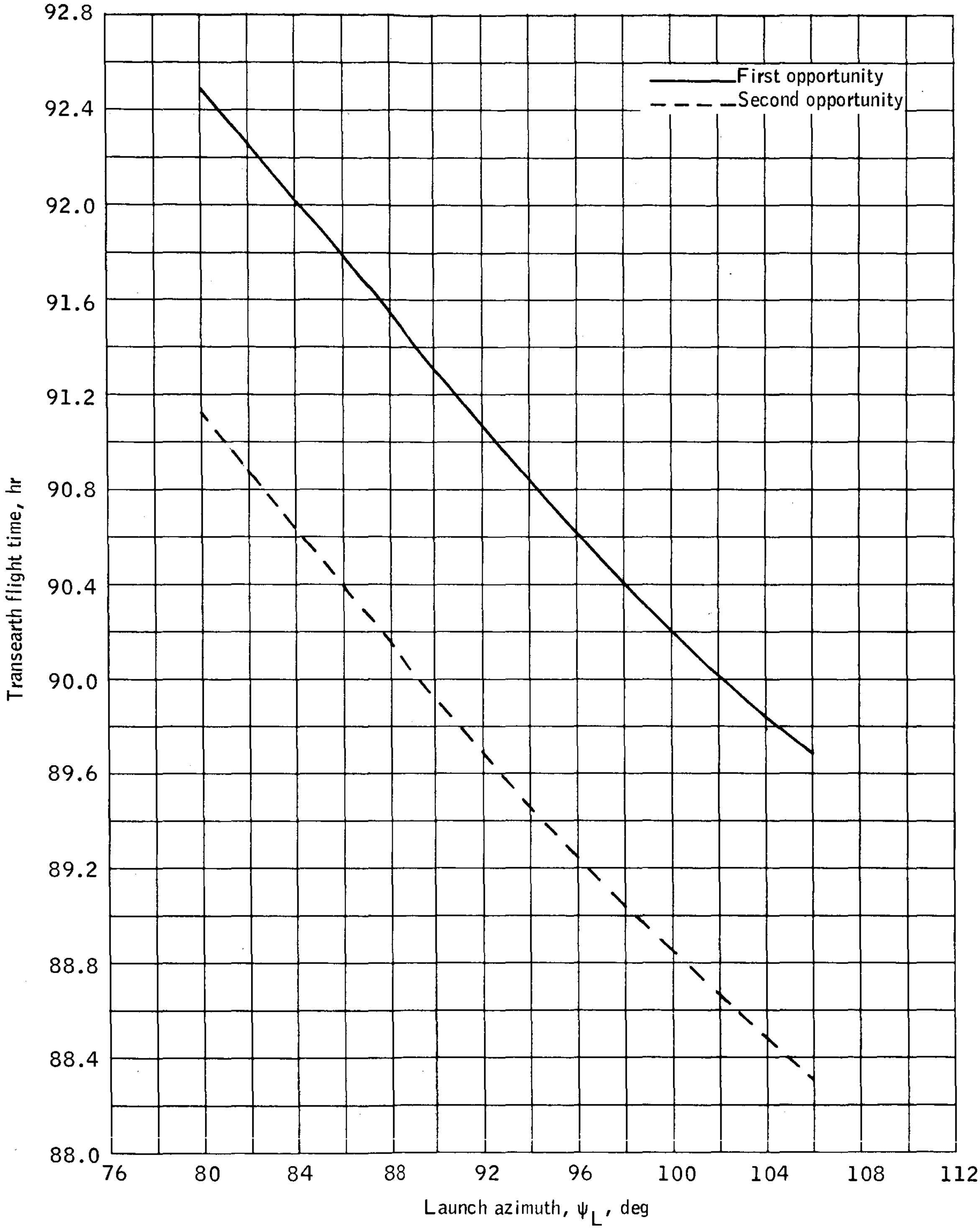

(e) Transearth flight time.

Figure 17.- Concluded.

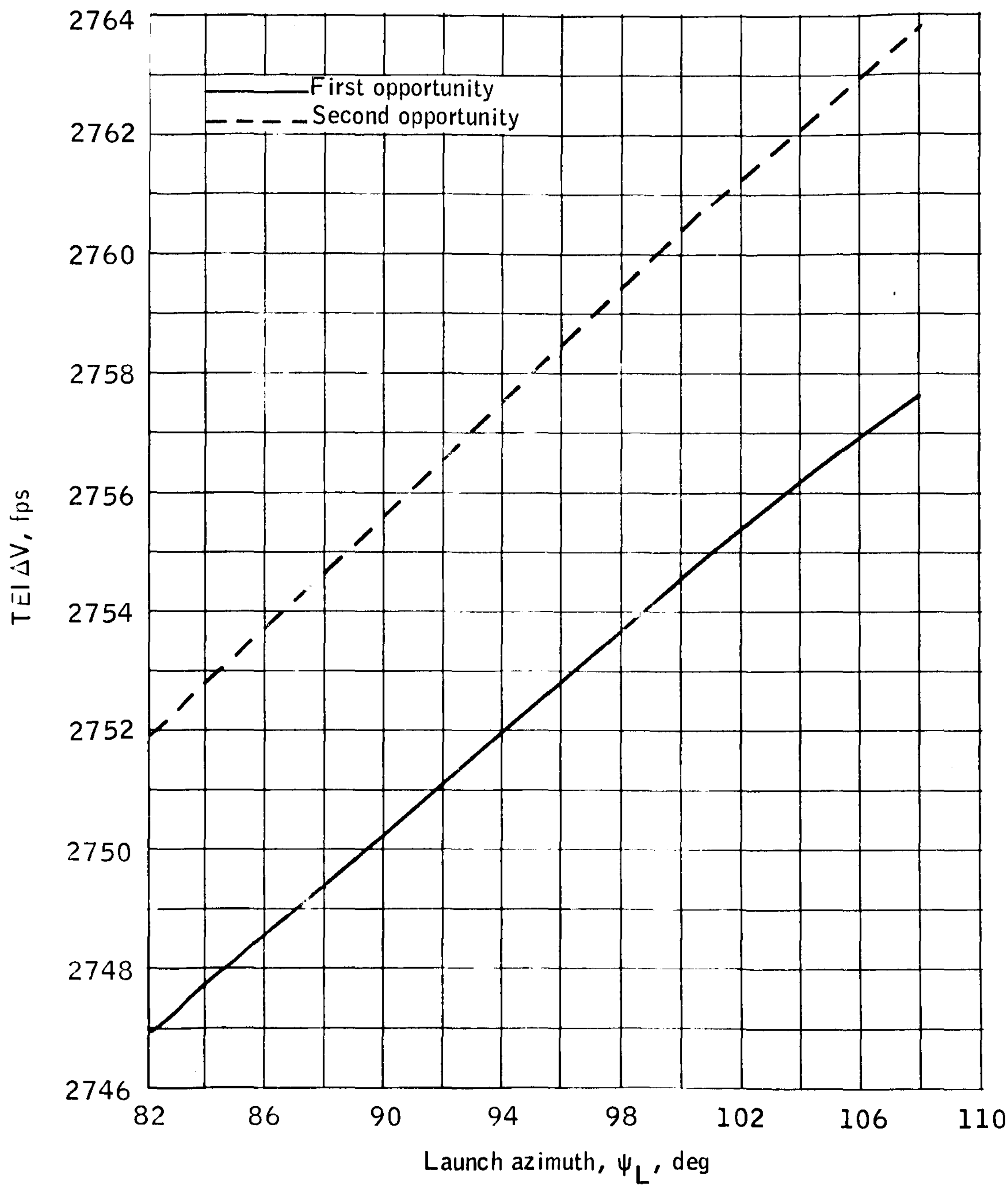

(a) TEI ΔV.

Figure 18.- Trajectory parameters as a function of launch azimuth for lift-off on July 18, 1969.

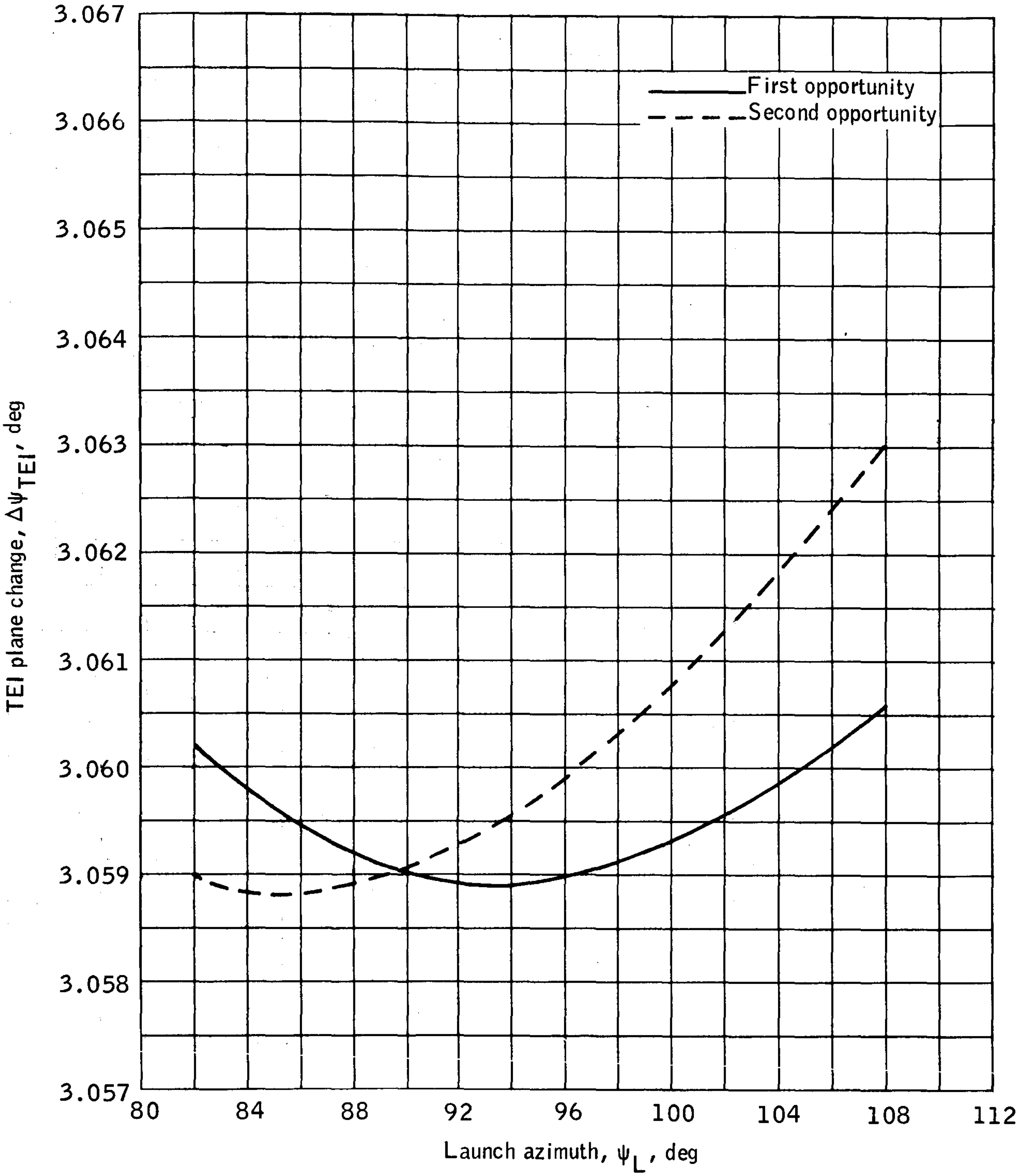

(b) TEI plane change.

Figure 18.- Continued.

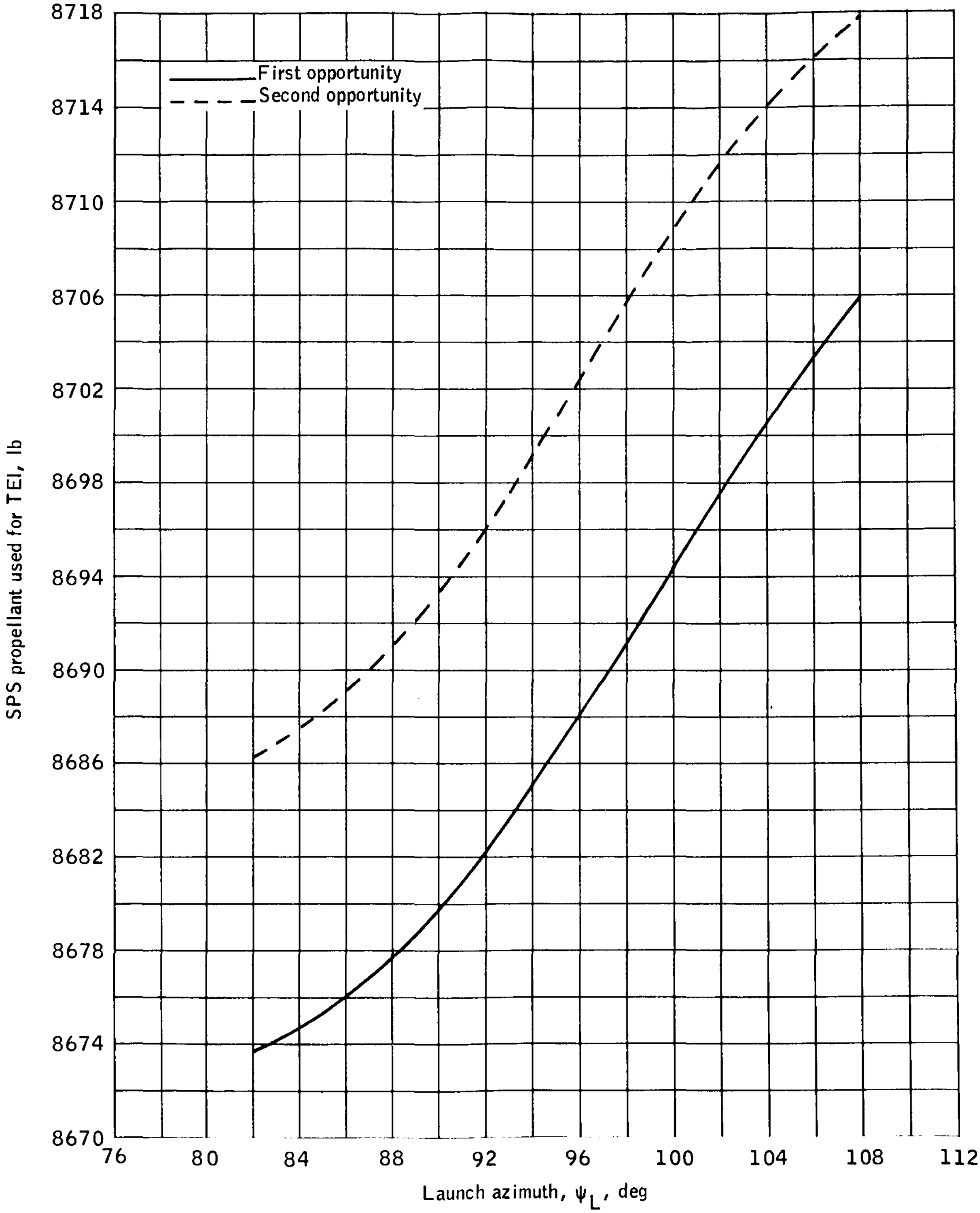

(c) SPS propellant used for TEI.

Figure 18.- Continued.

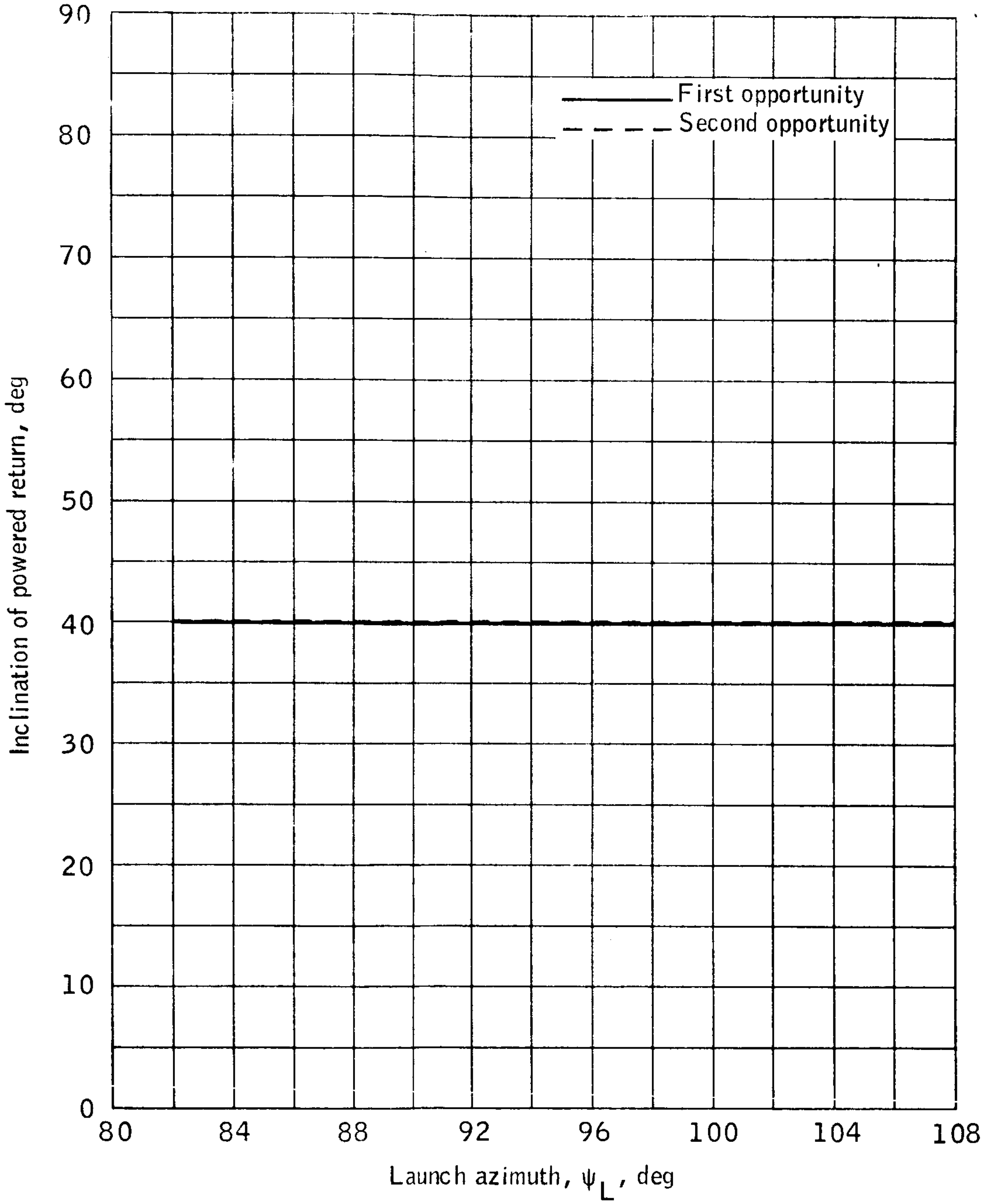

(d) Inclination of powered return.

Figure 18.- Continued.

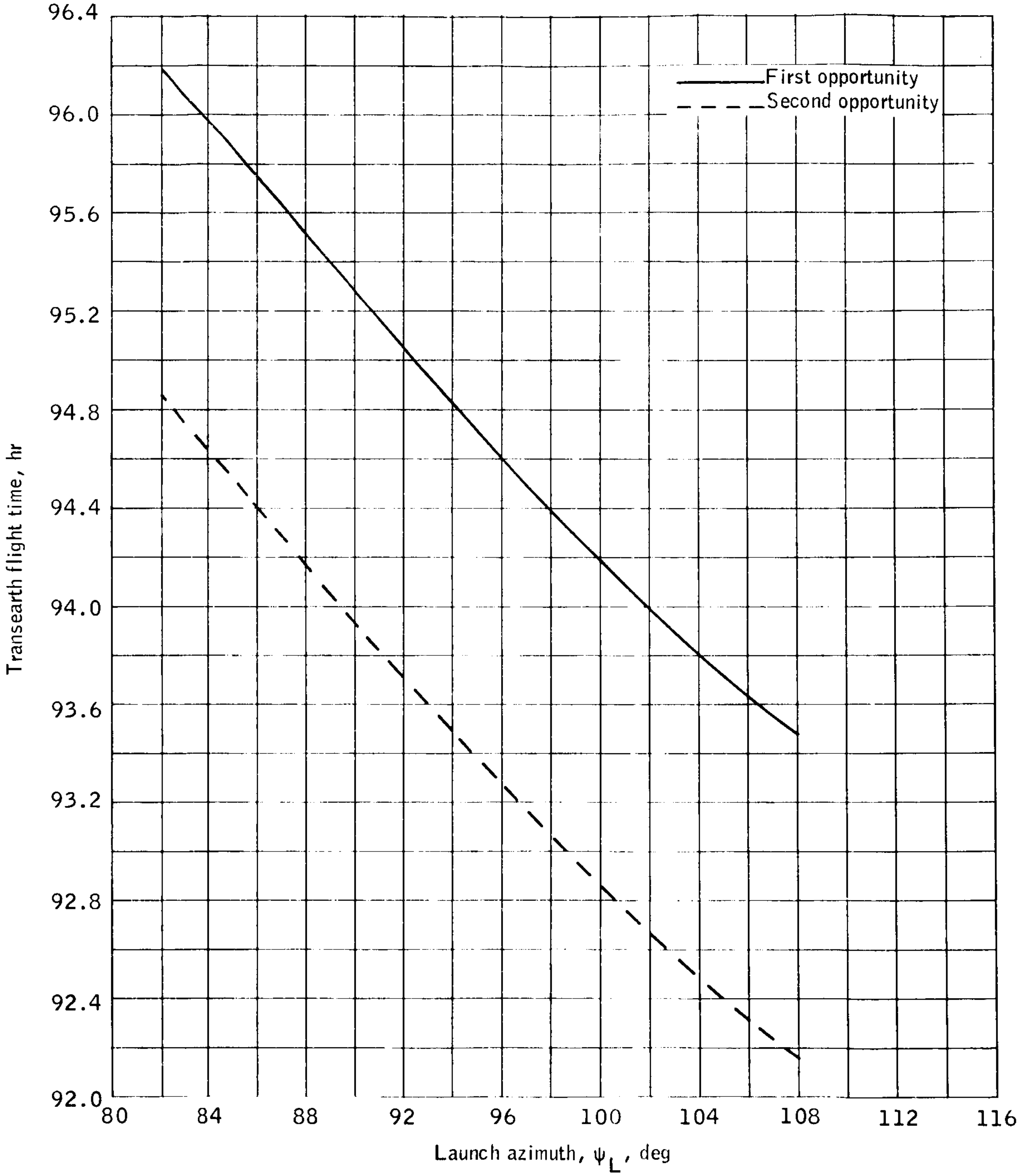

(e) Transearth flight time.

Figure 18.- Concluded.

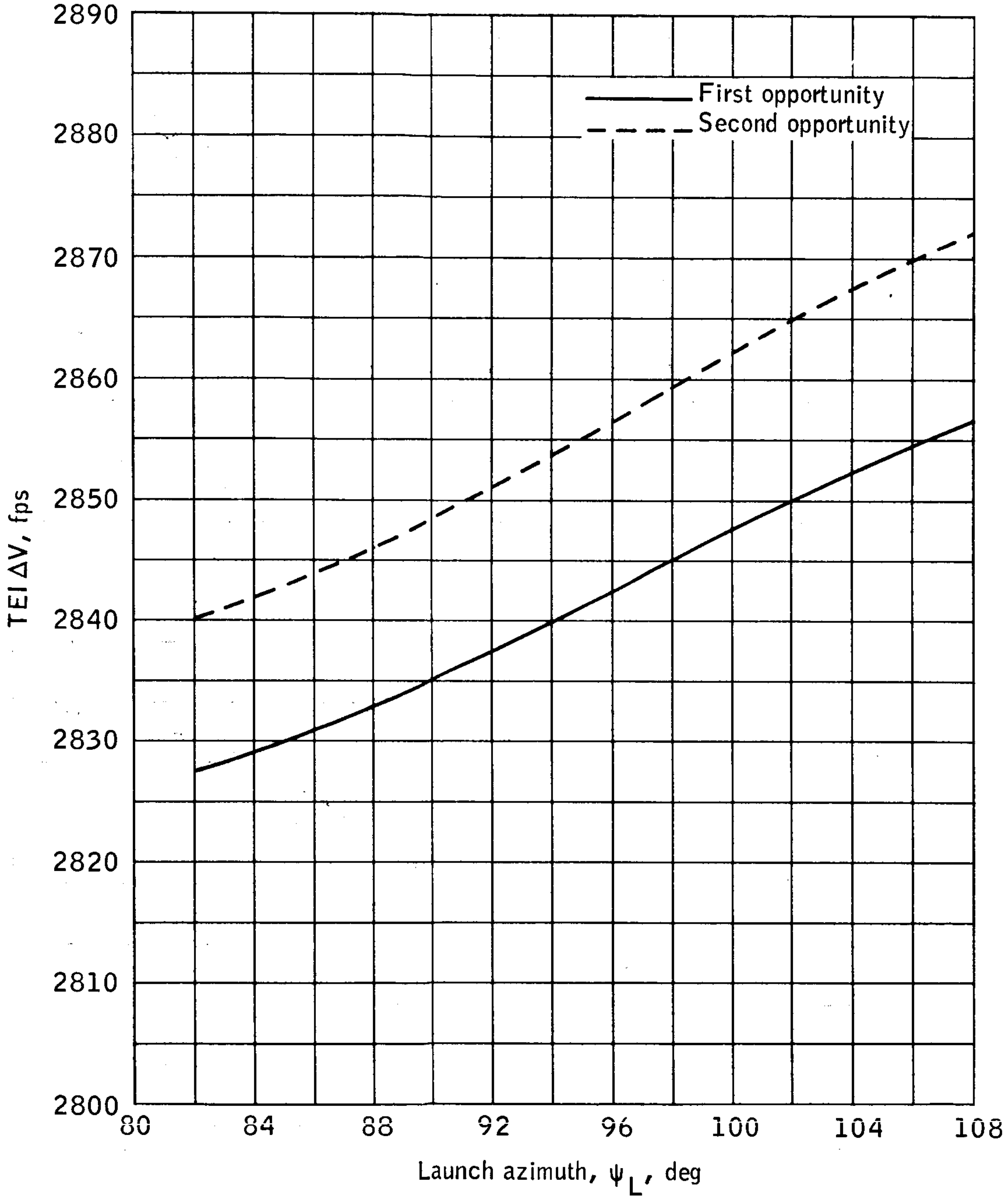

(a) TEI ΔV.

Figure 19.- Trajectory parameters as a function of launch azimuth for lift-off on July 22,1969.

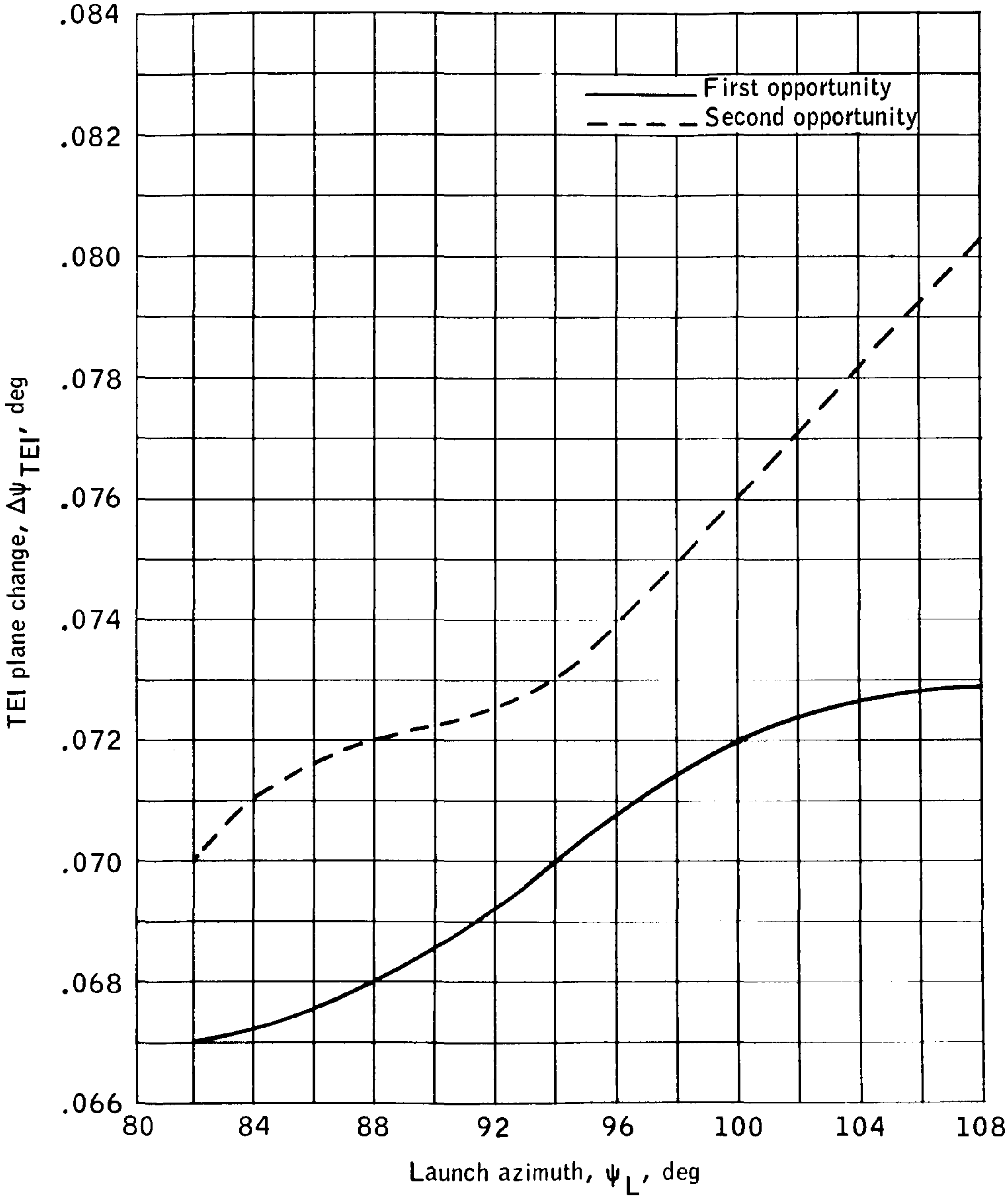

(b) TEI plane change.

Figure 19.- Continued.

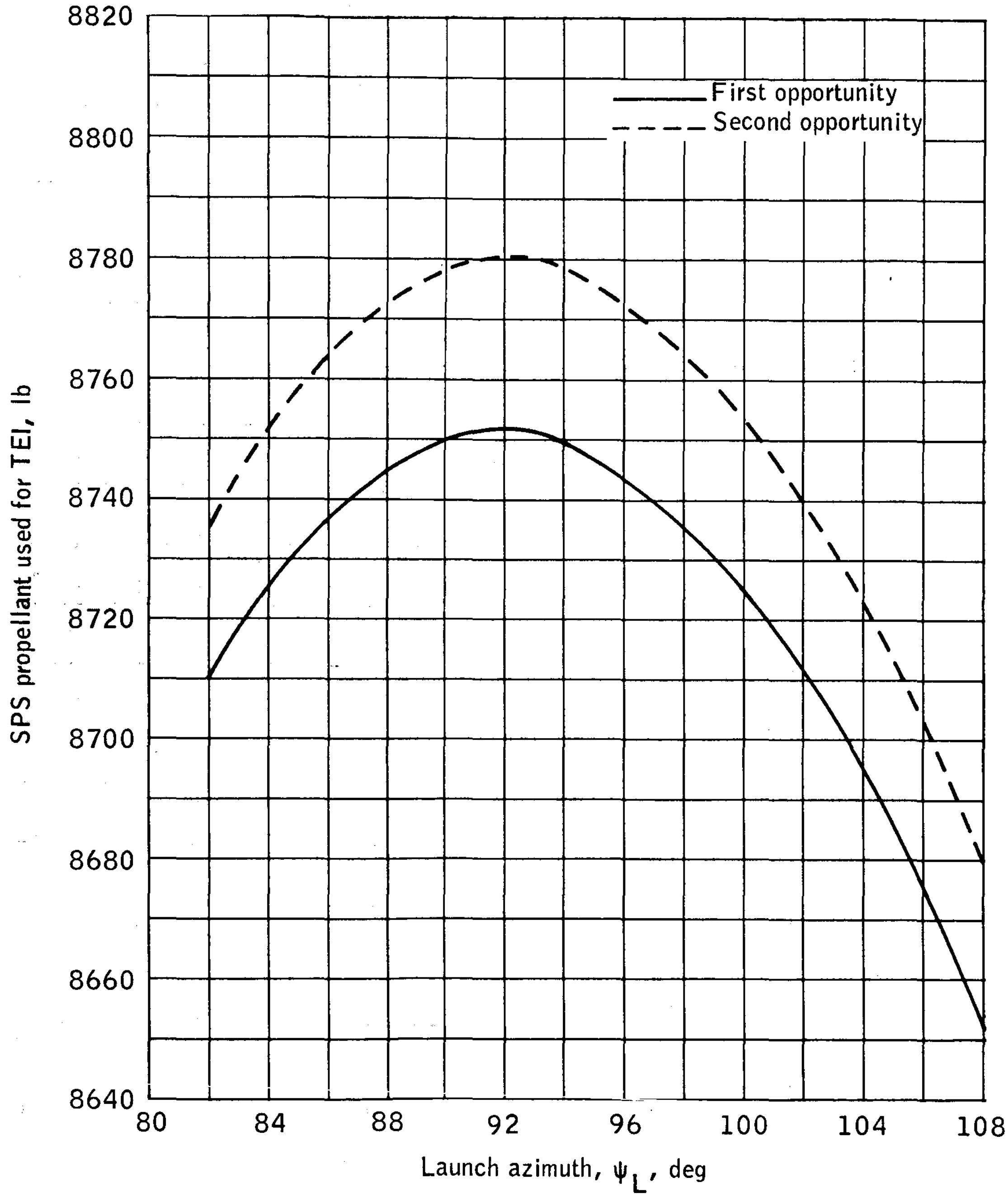

(c) SPS propellant used for TEI.

Figure 19.- Continued.

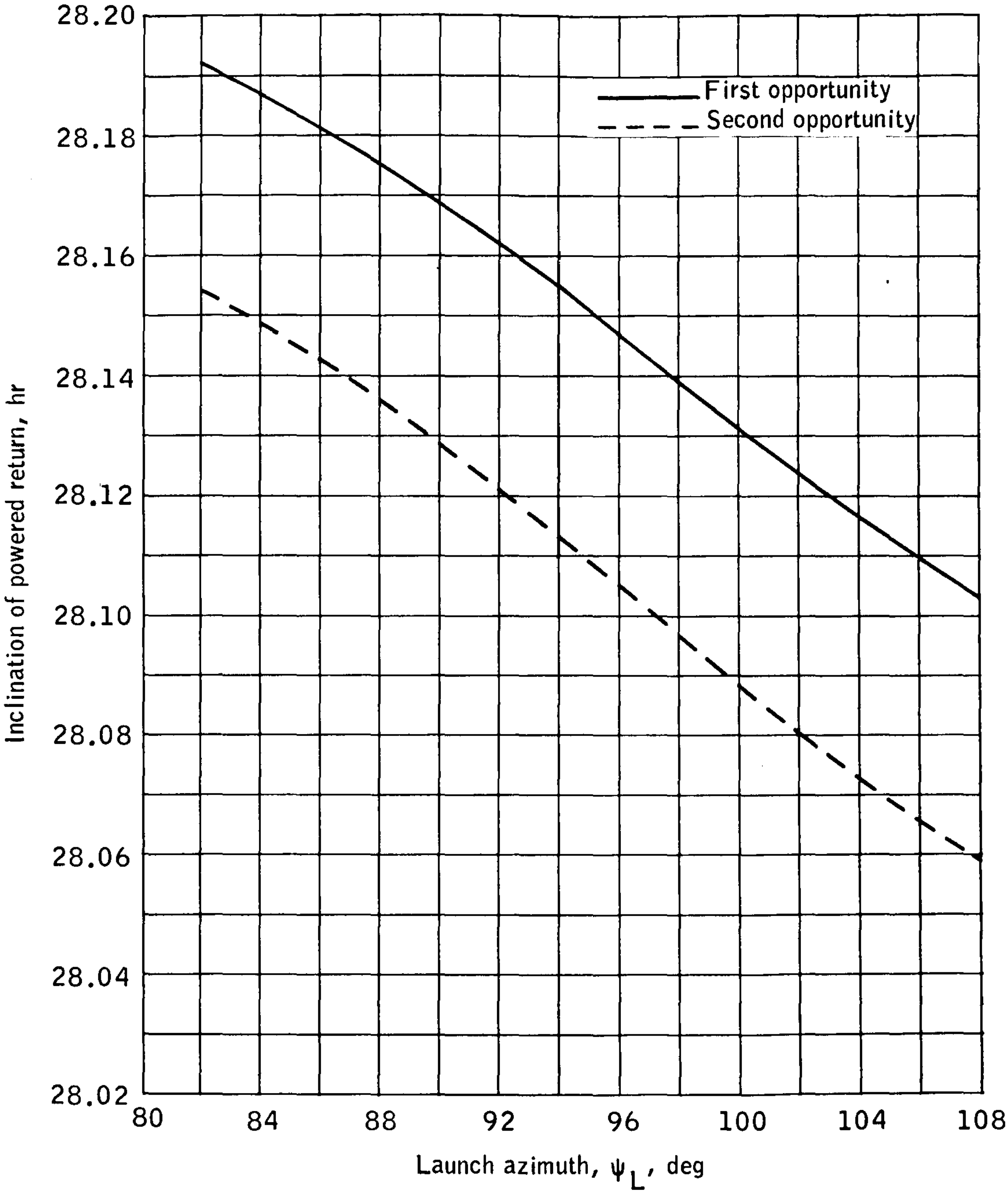

(d) Inclination of powered return.

Figure 19.- Continued.

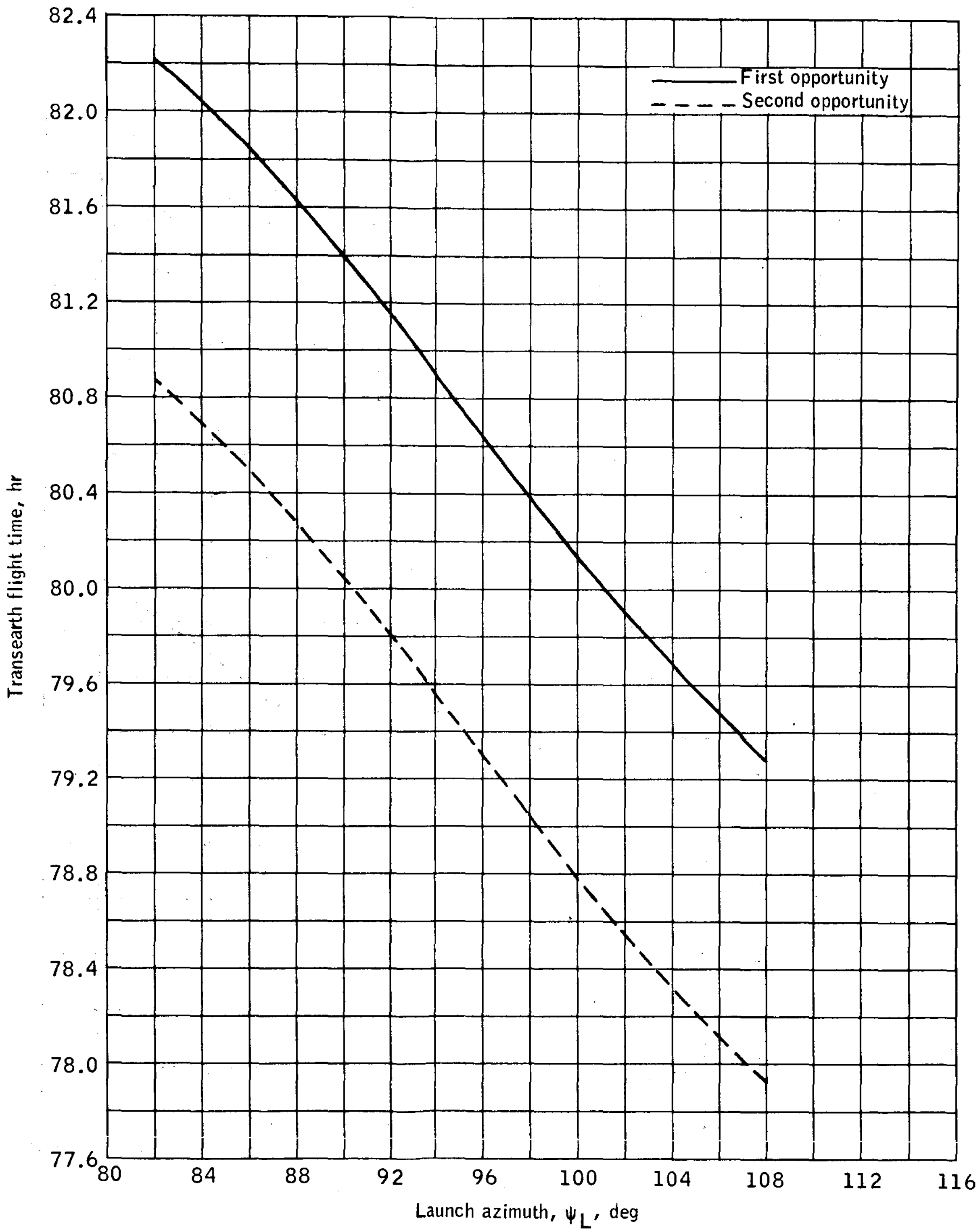

(e) Transearth flight time.

Figure 19.- Concluded.

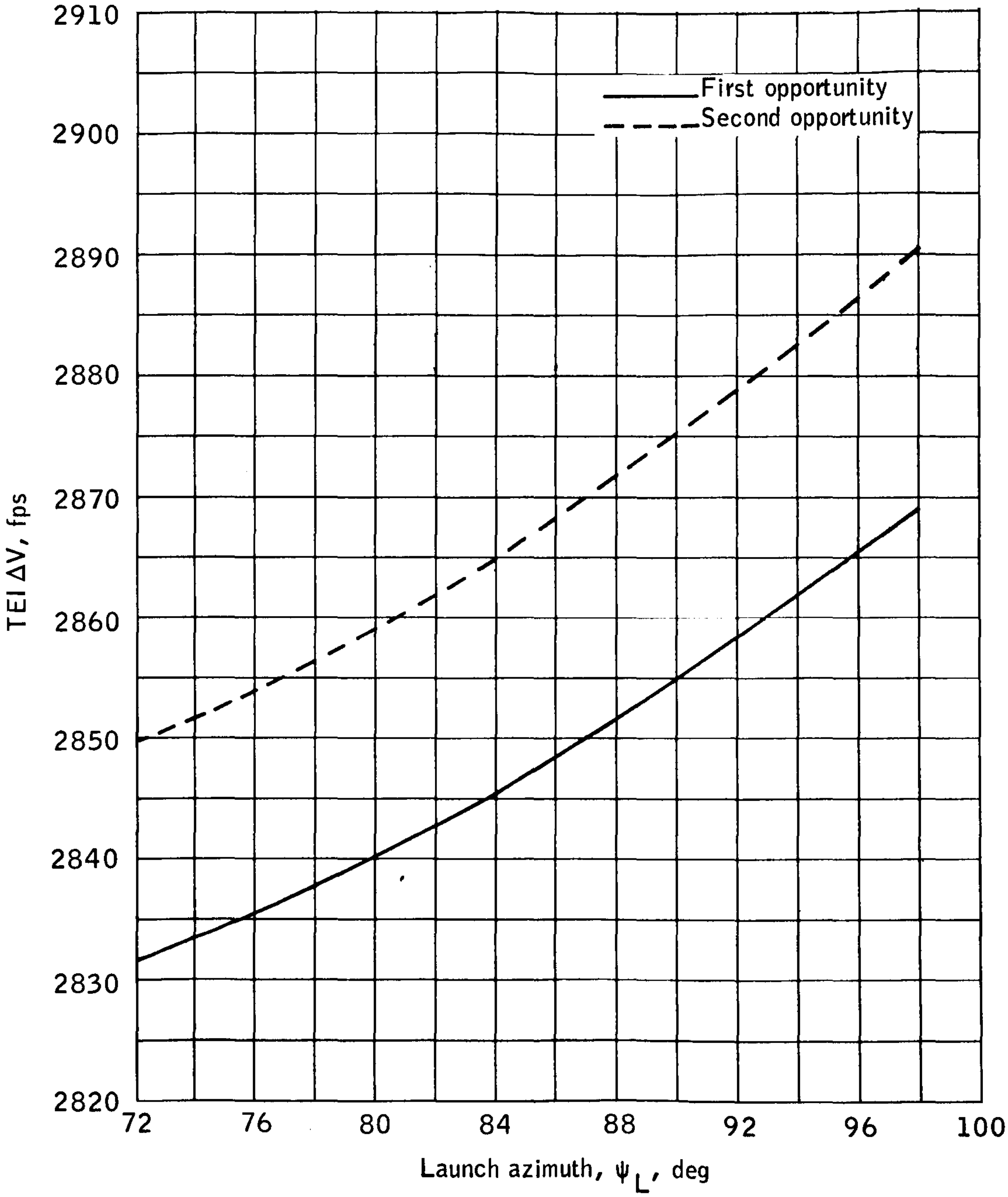

(a) TEI ΔV.

Figure 20.- Trajectory parameters as a function of launch azimuth for lift-off on August 14,1969.

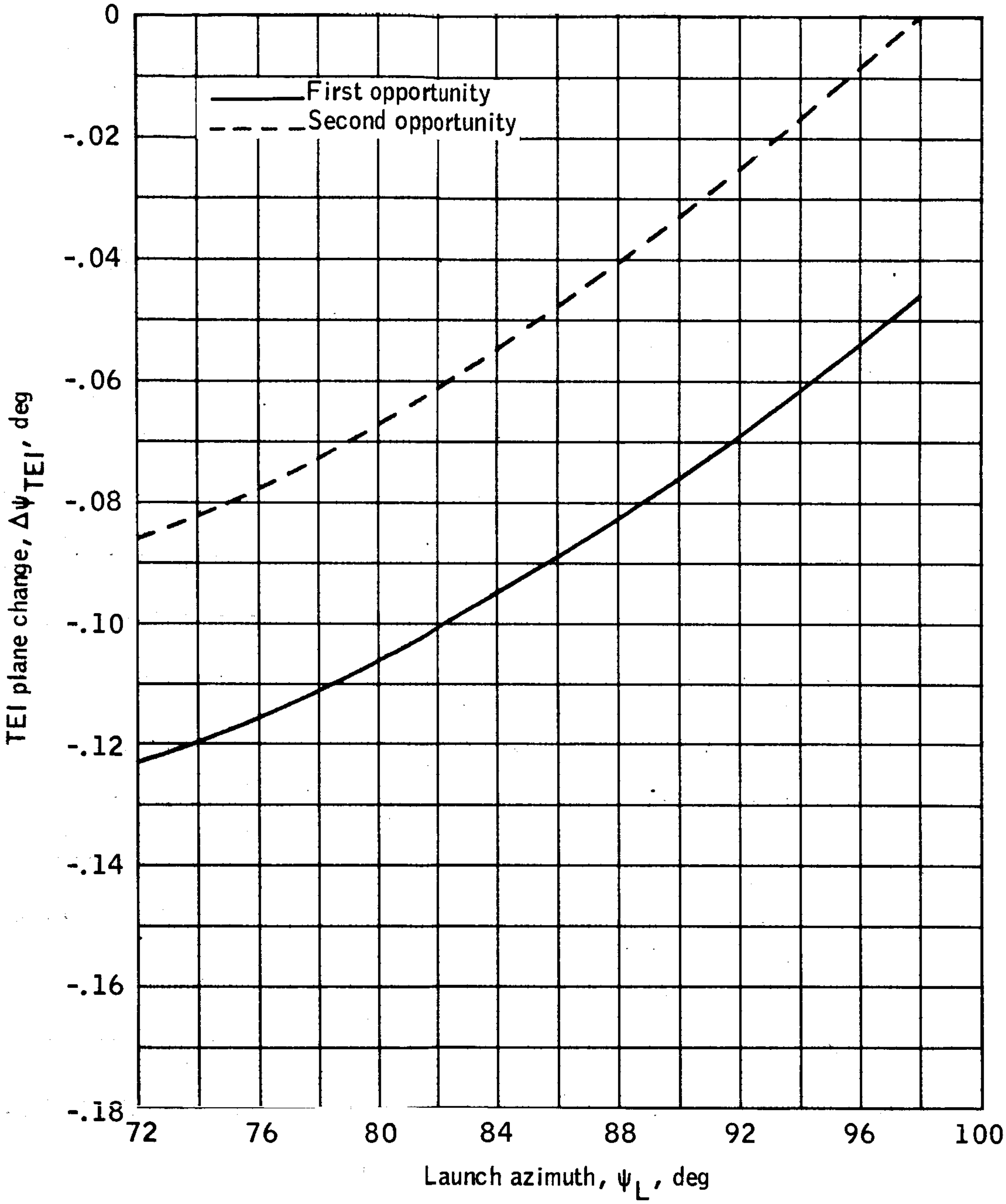

(b) TEI plane change.

Figure 20.- Continued.

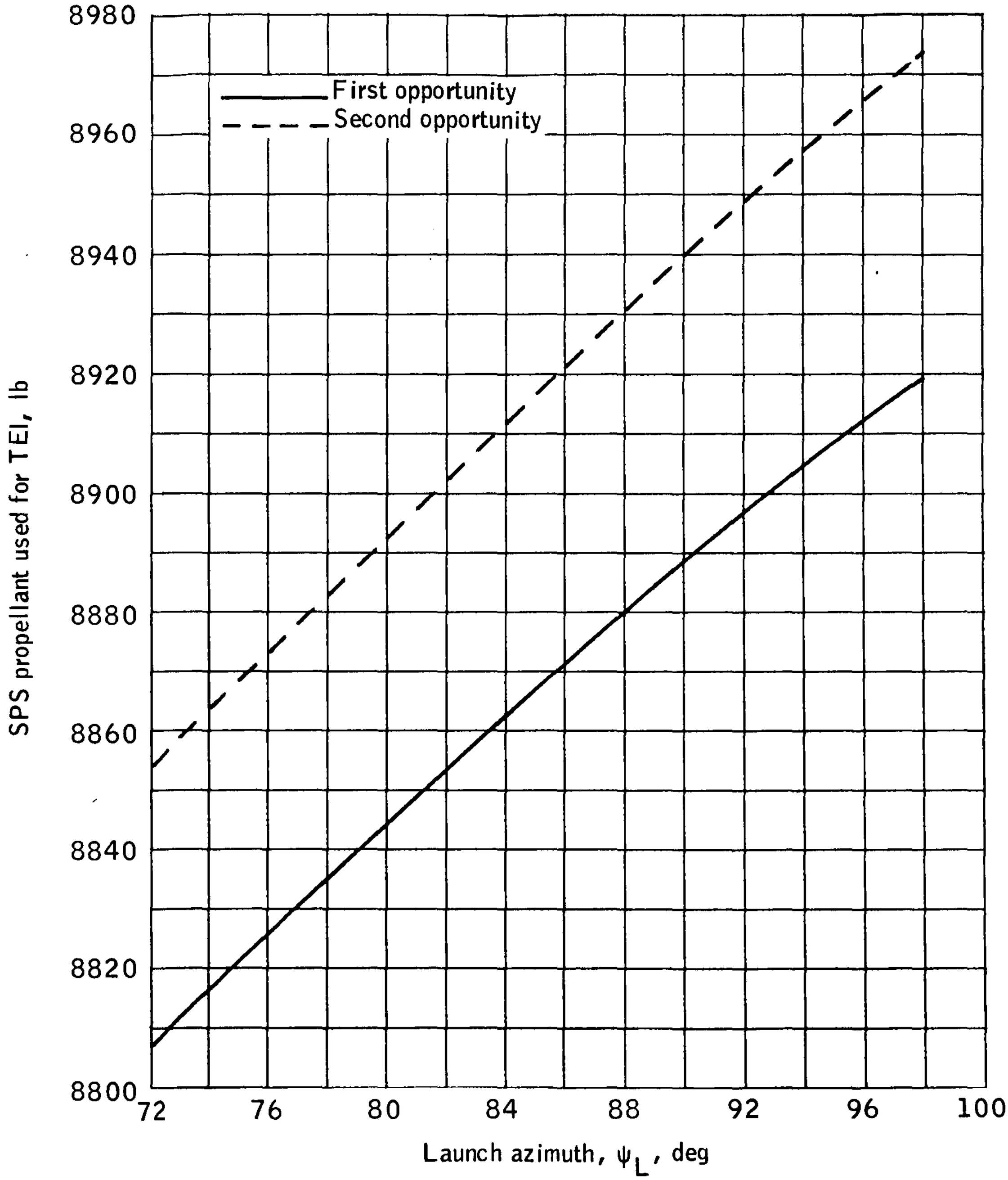

(c) SPS propellant used for TEI.

Figure 20.- Continued.

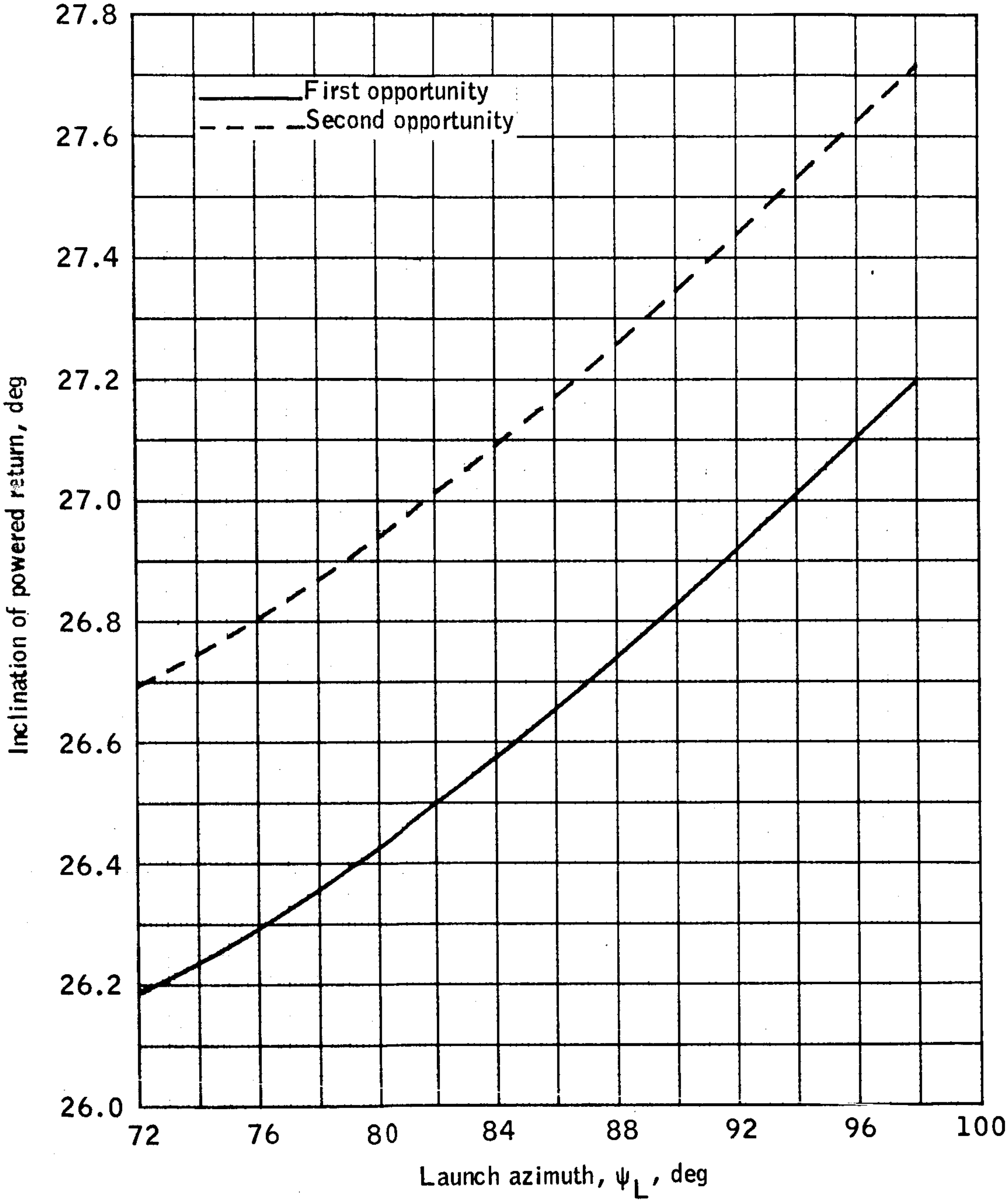

(d) Inclination of powered return.

Figure 20.- Continued.

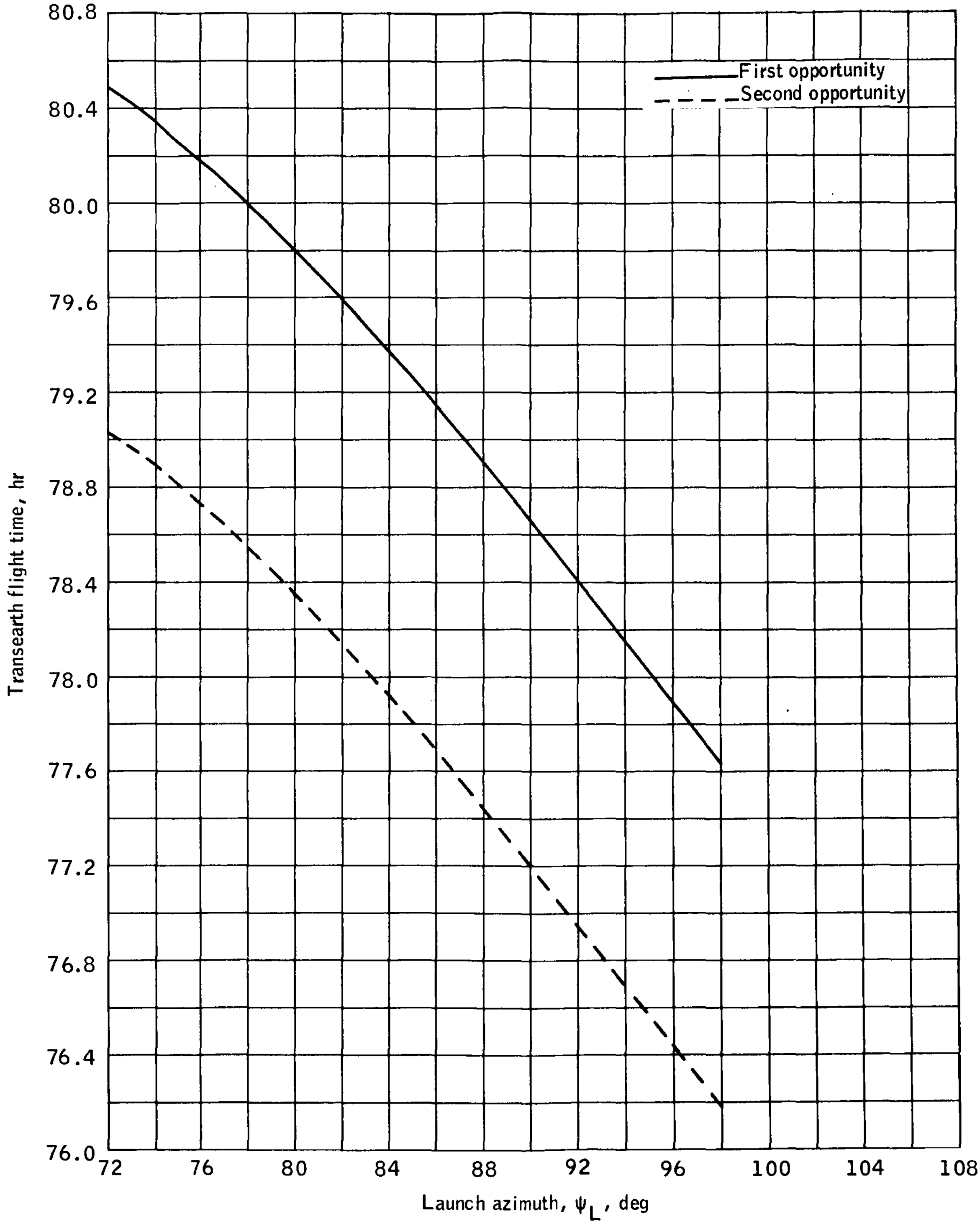

(e) Transearth flight time.

Figure 20.- Concluded.

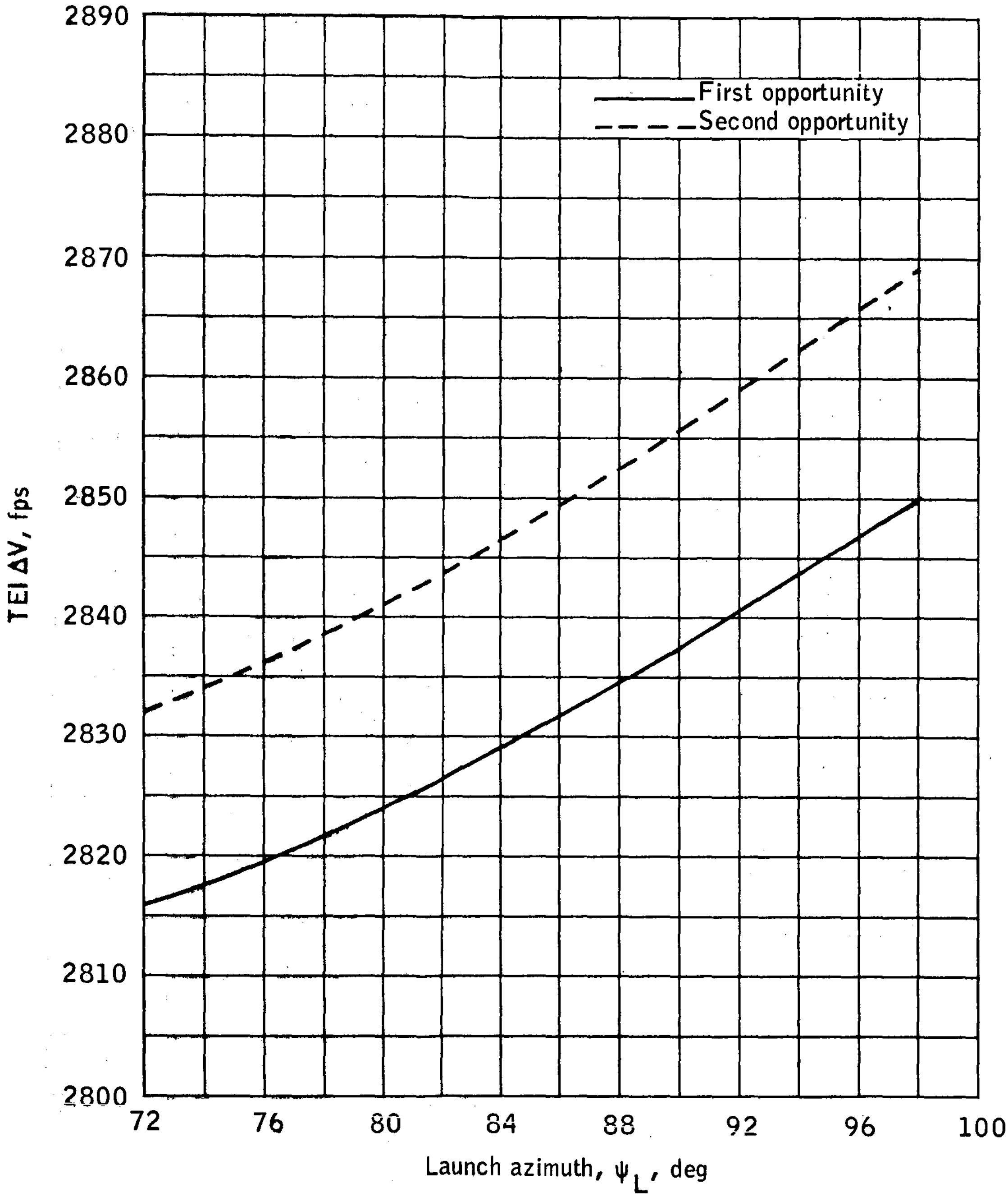

(a) TEI ΔV.

Figure 21.- Trajectory parameters as a function of launch azimuth for lift-off on August 15,1969.

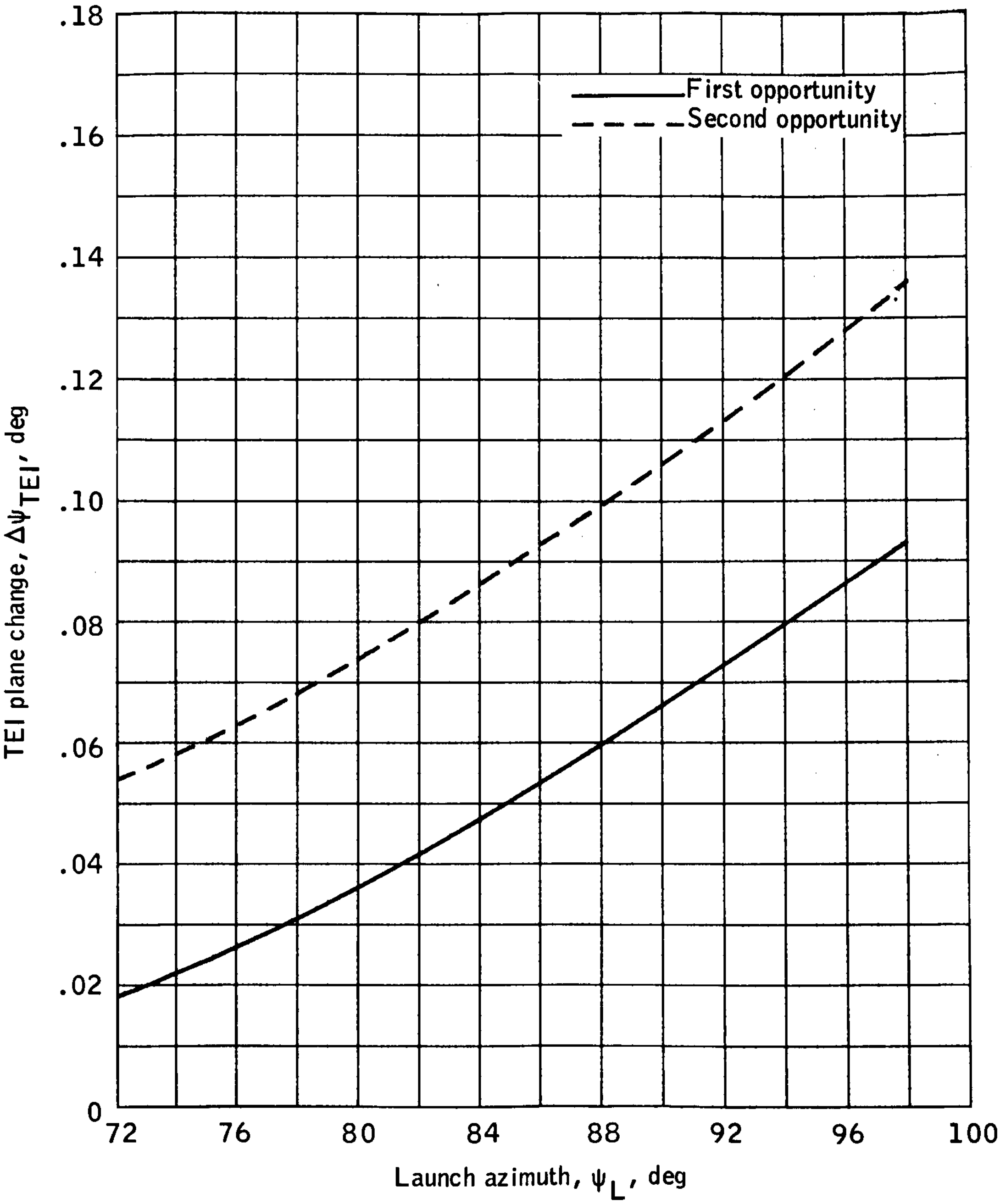

(b) TEI plane change.

Figure 21.- Continued.

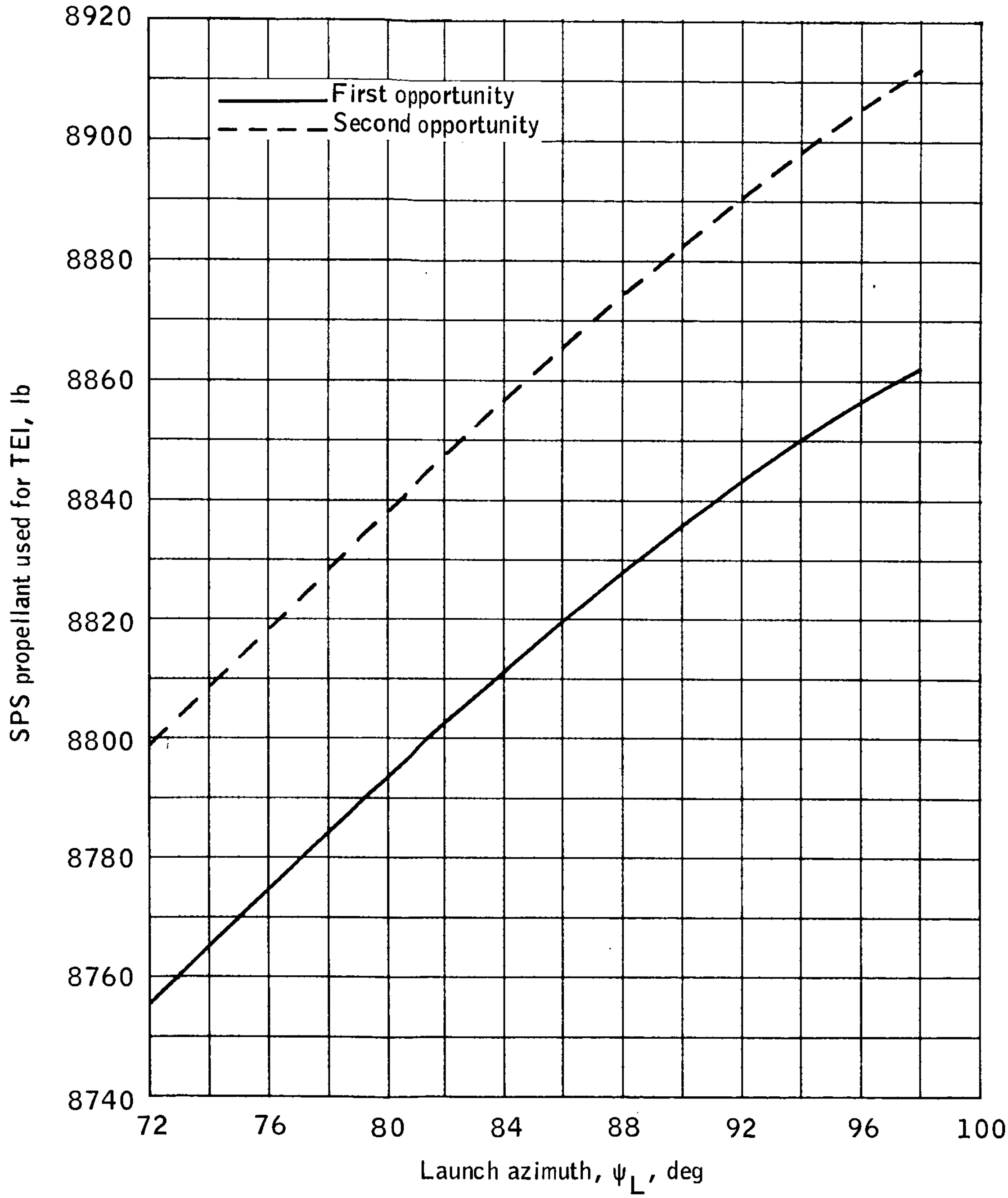

(c) SPS propellant used for TEI.

Figure 21.- Continued.

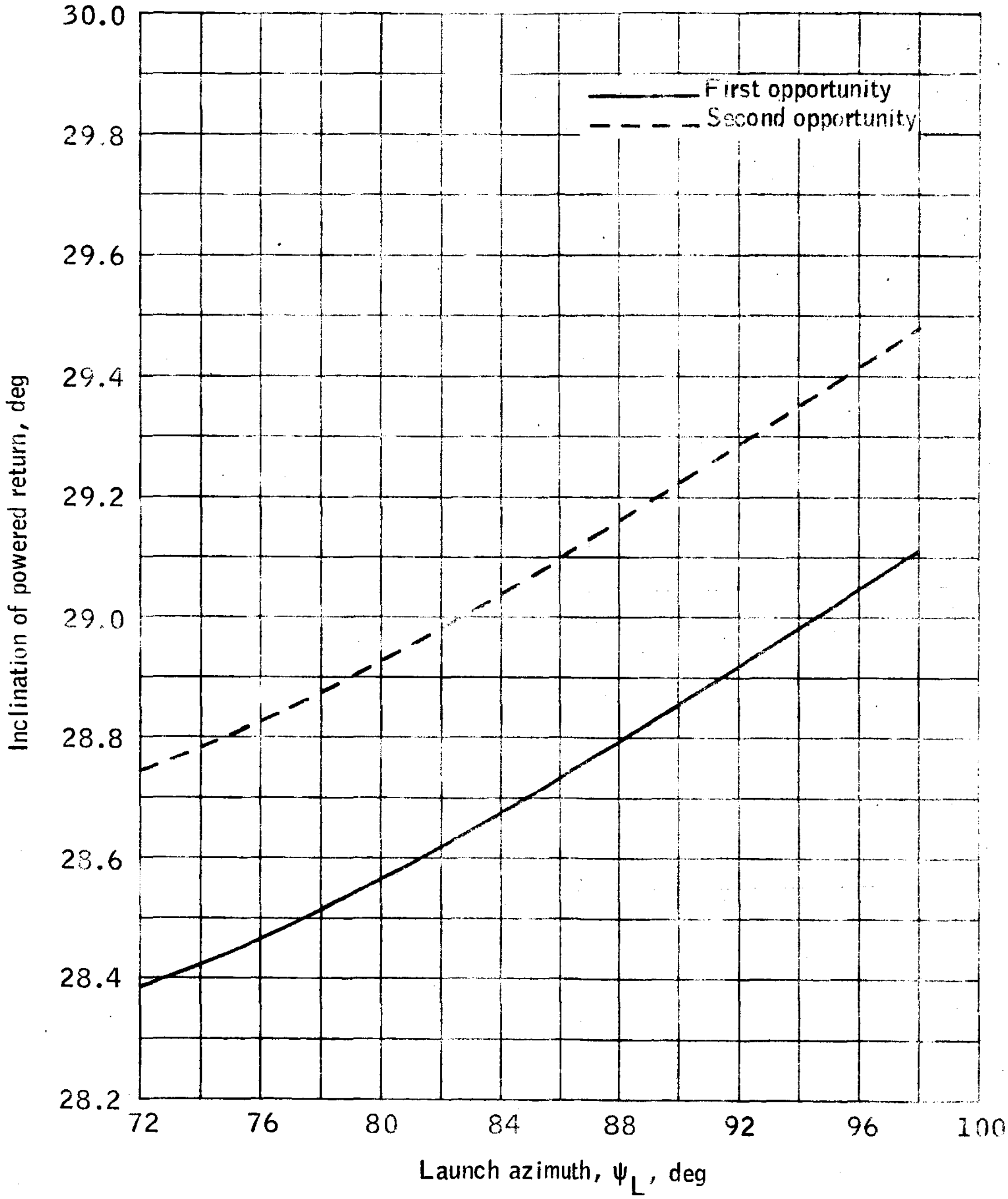

(d) Inclination of powered return.

Figure 21.- Continued.

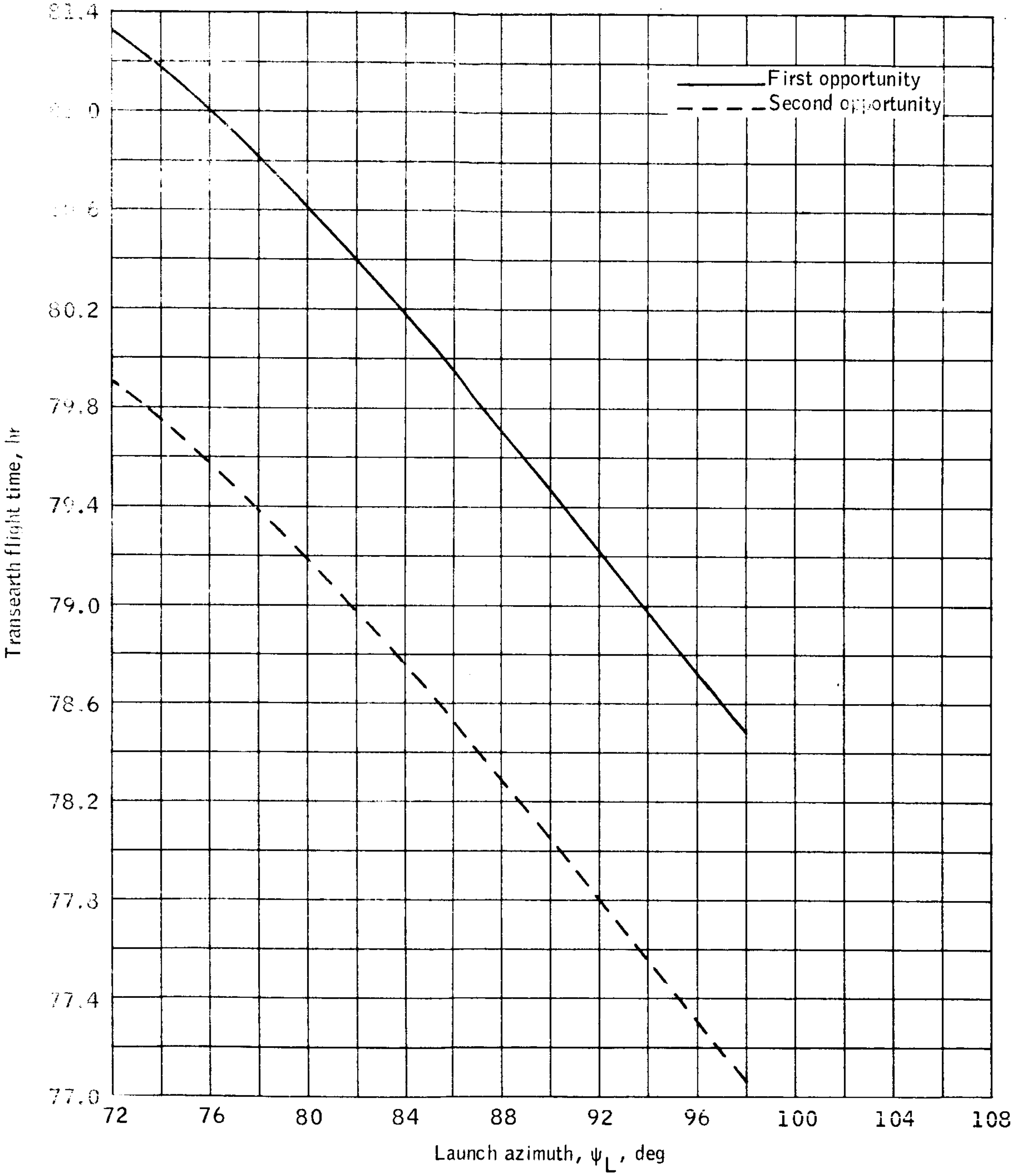

(e) Transearth flight time.

Figure 21.- Concluded.

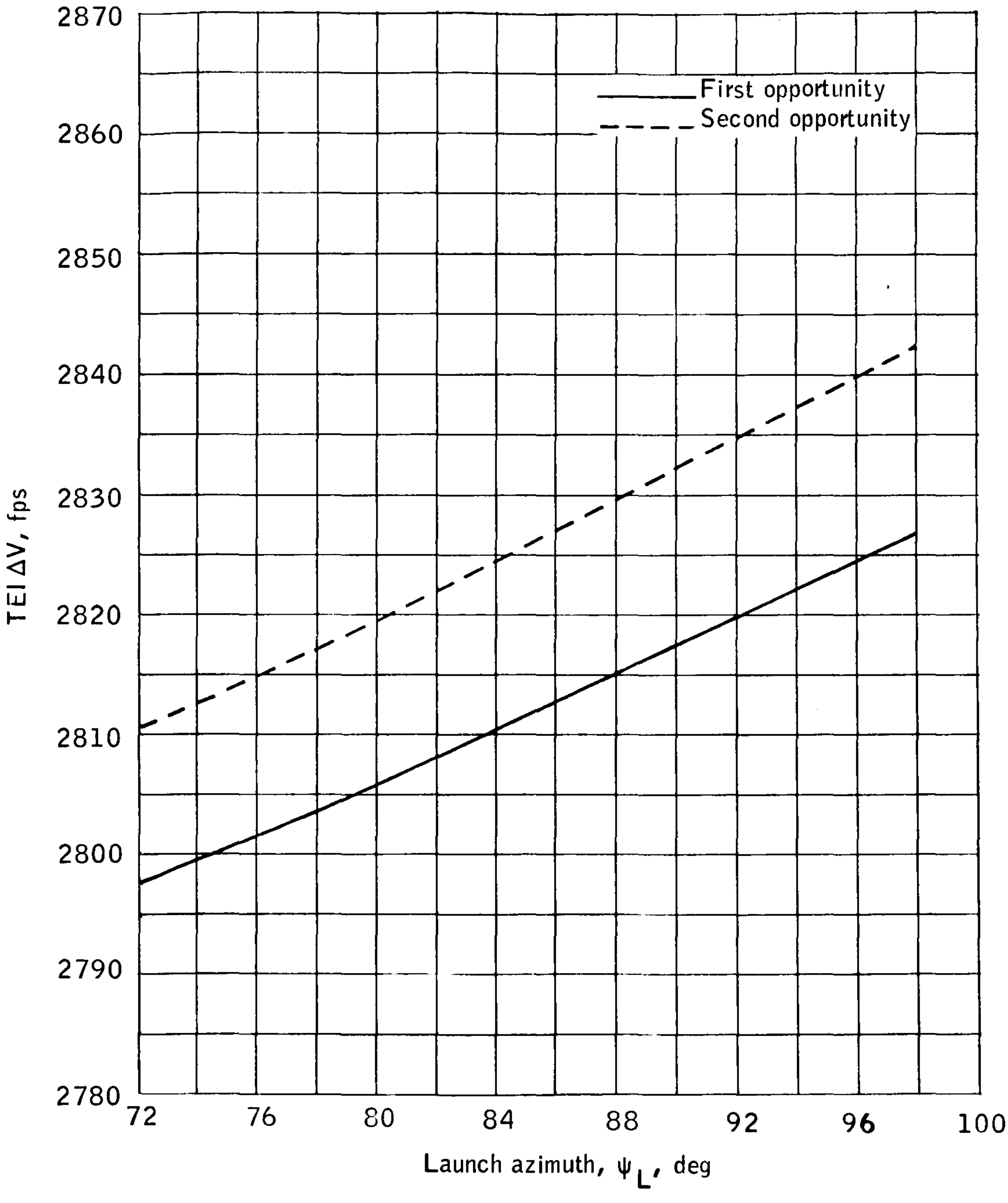

(a) TEI ΔV.

Figure 22.- Trajectory parameters as a function of launch azimuth for lift-off on August 17,1969.

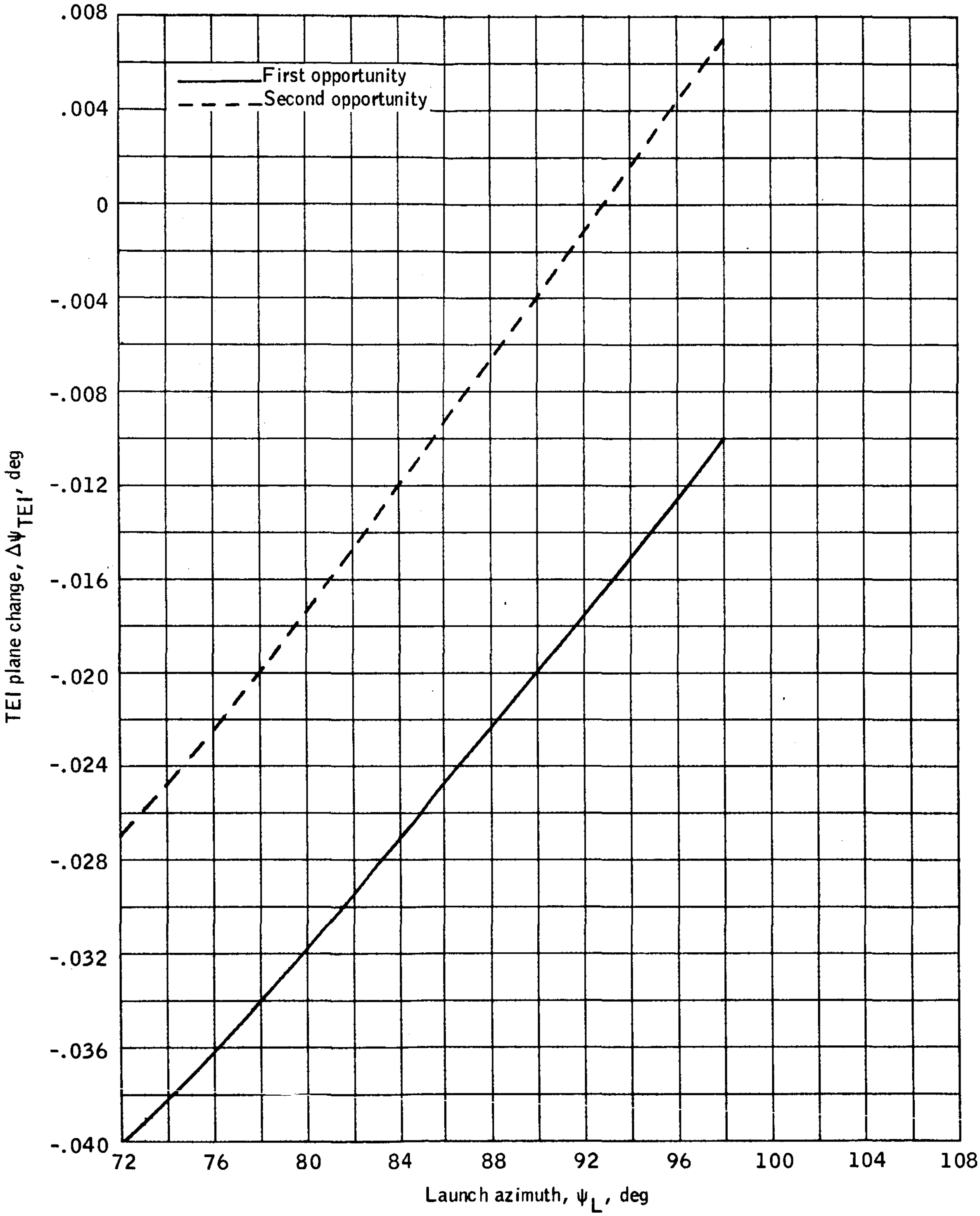

(b) TEI plane change.

Figure 22.- Continued.

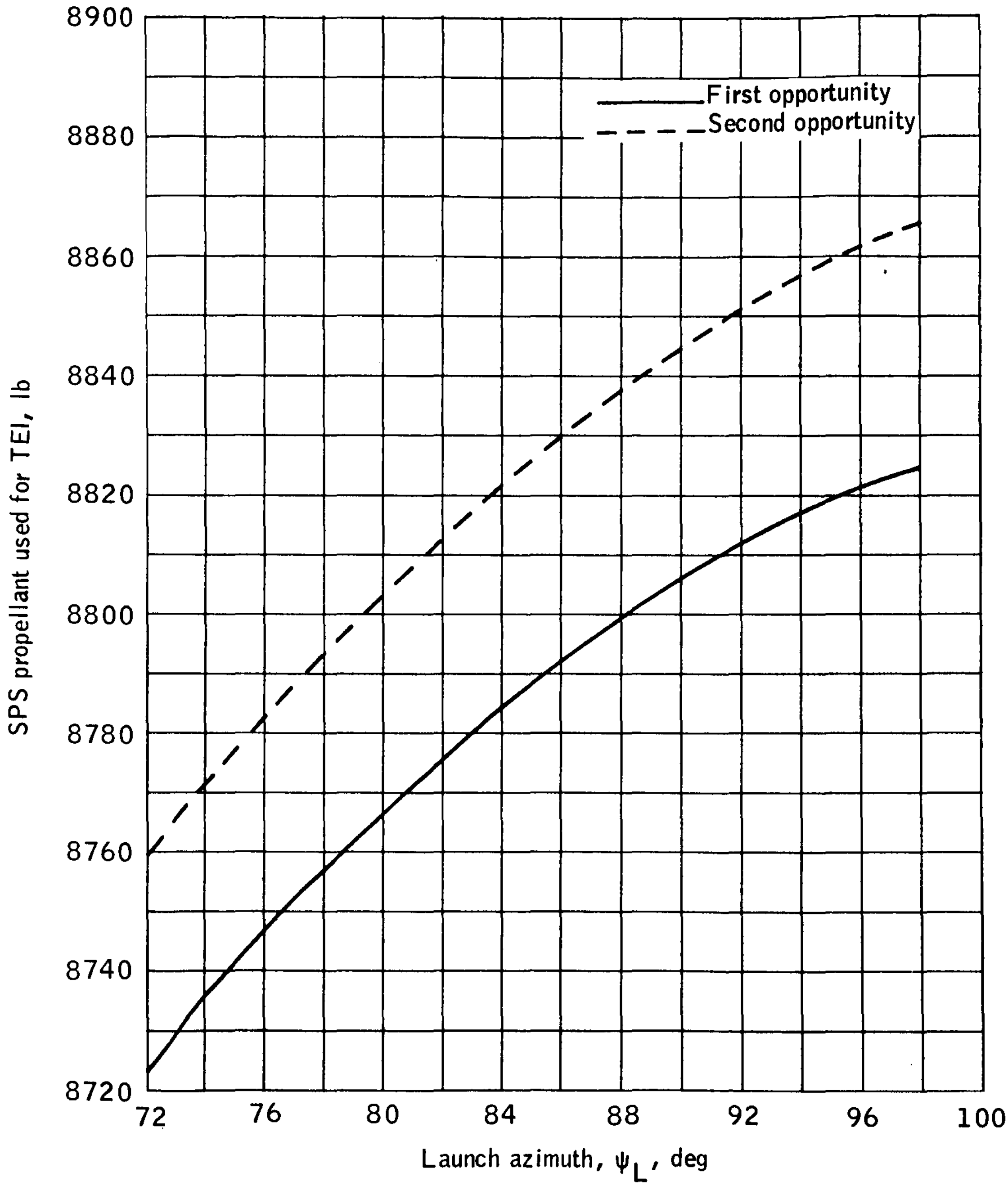

(c) SPS propellant used for TEI.

Figure 22.- Continued.

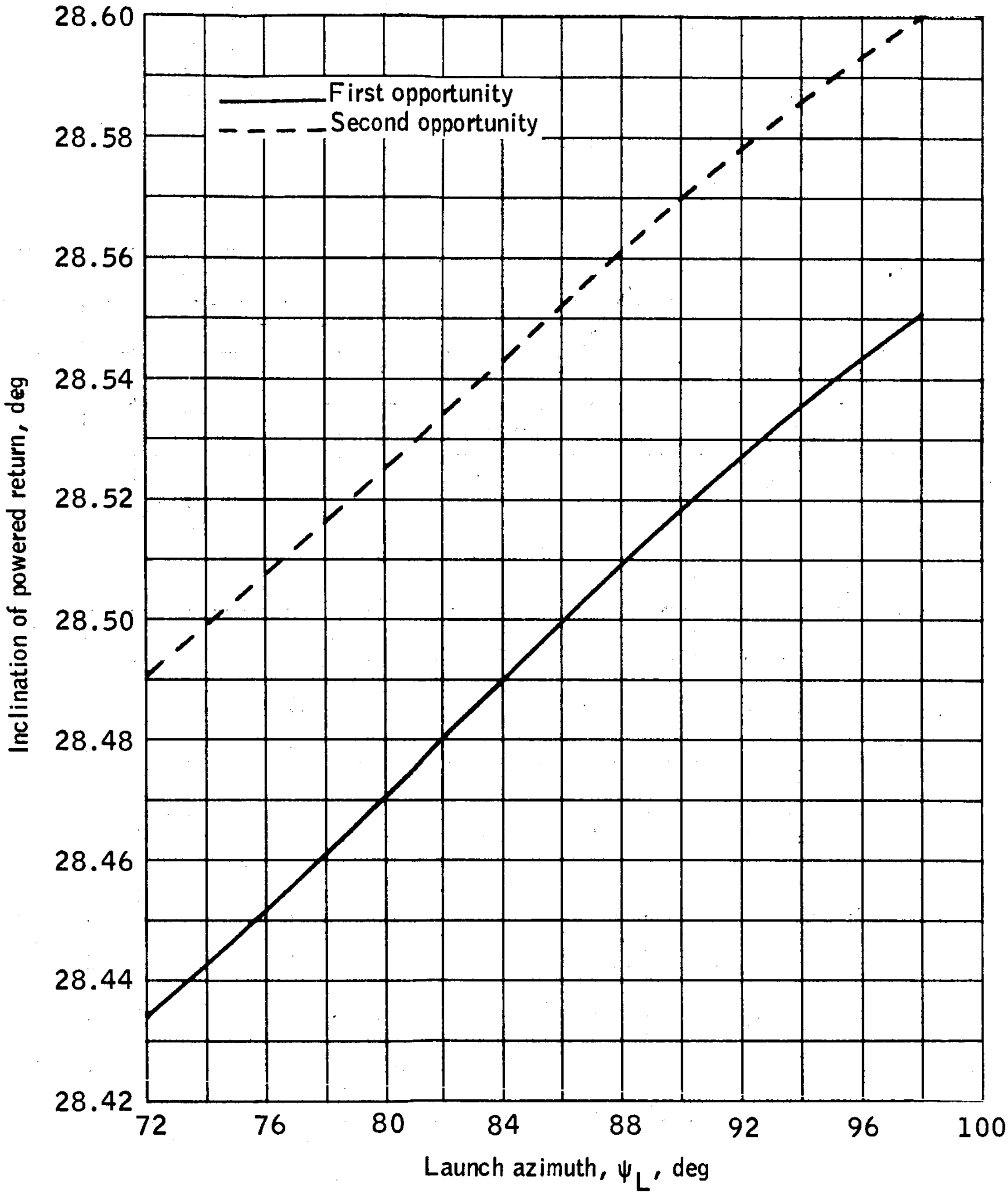

(d) Inclination of powered return.

Figure 22.- Continued.

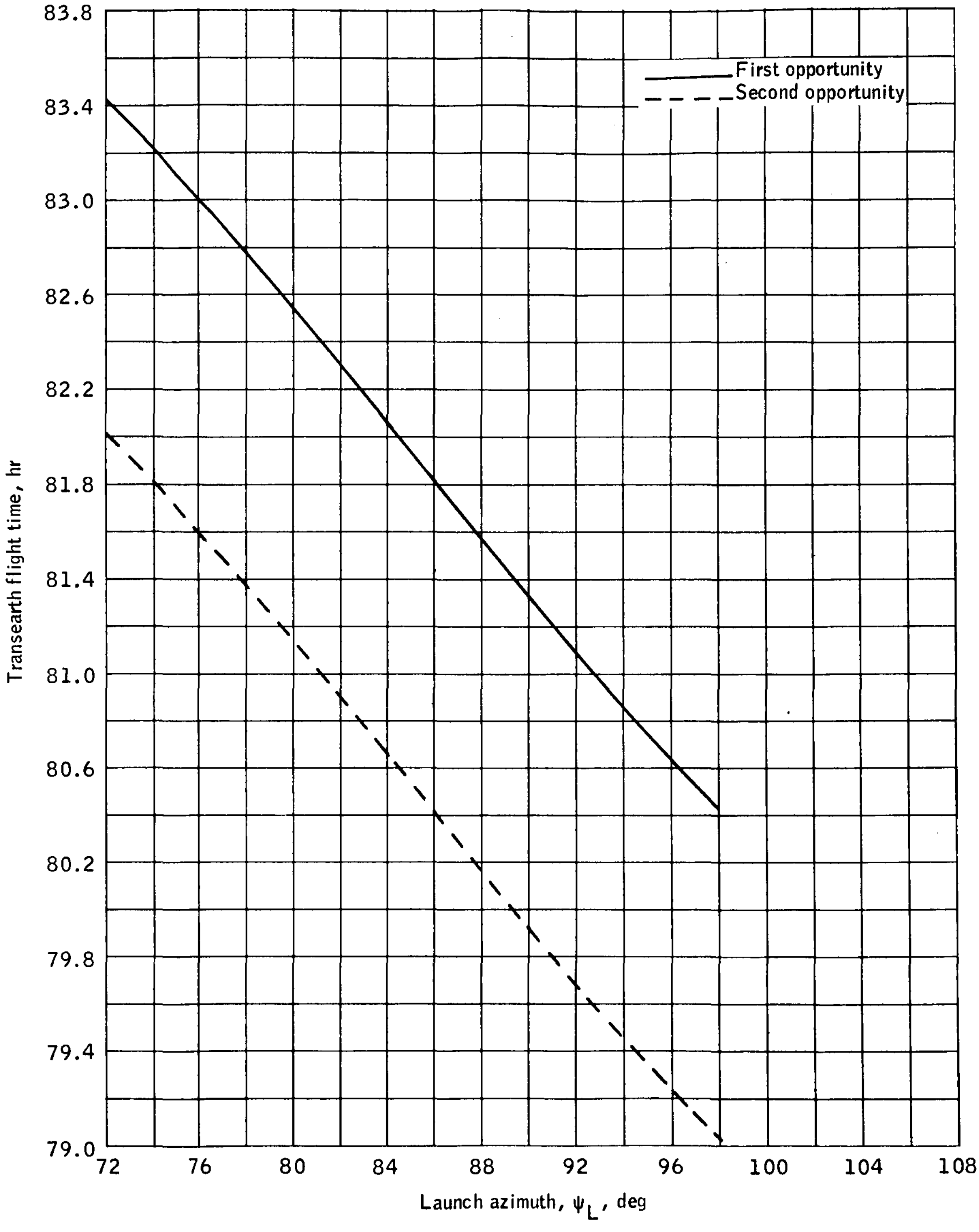

(e) Transearth flight time.

Figure 22.- Concluded.

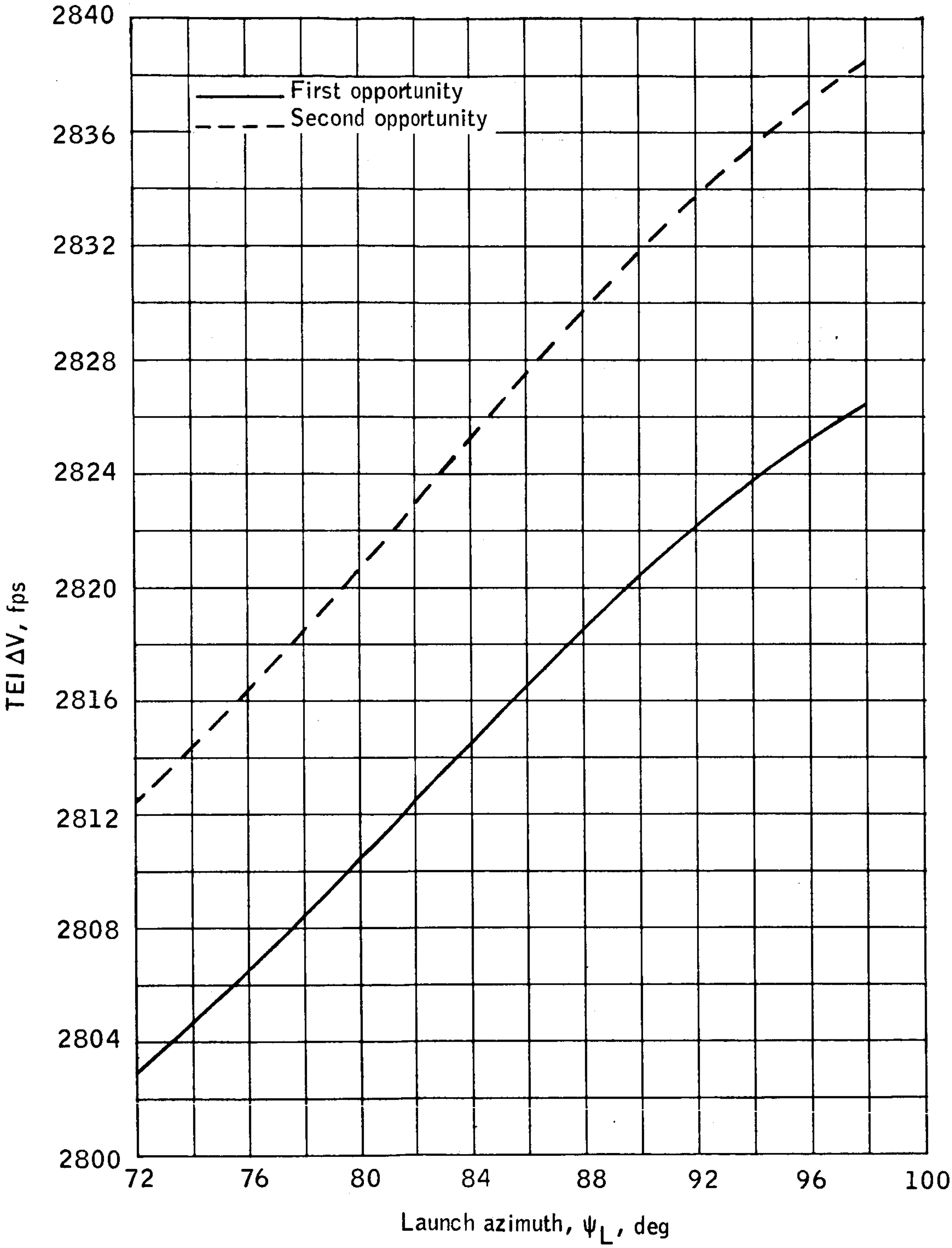

(a) TEI ΔV.

Figure 23.- Trajectory parameters as a function of launch azimuth for lift-off on August 21,1969.

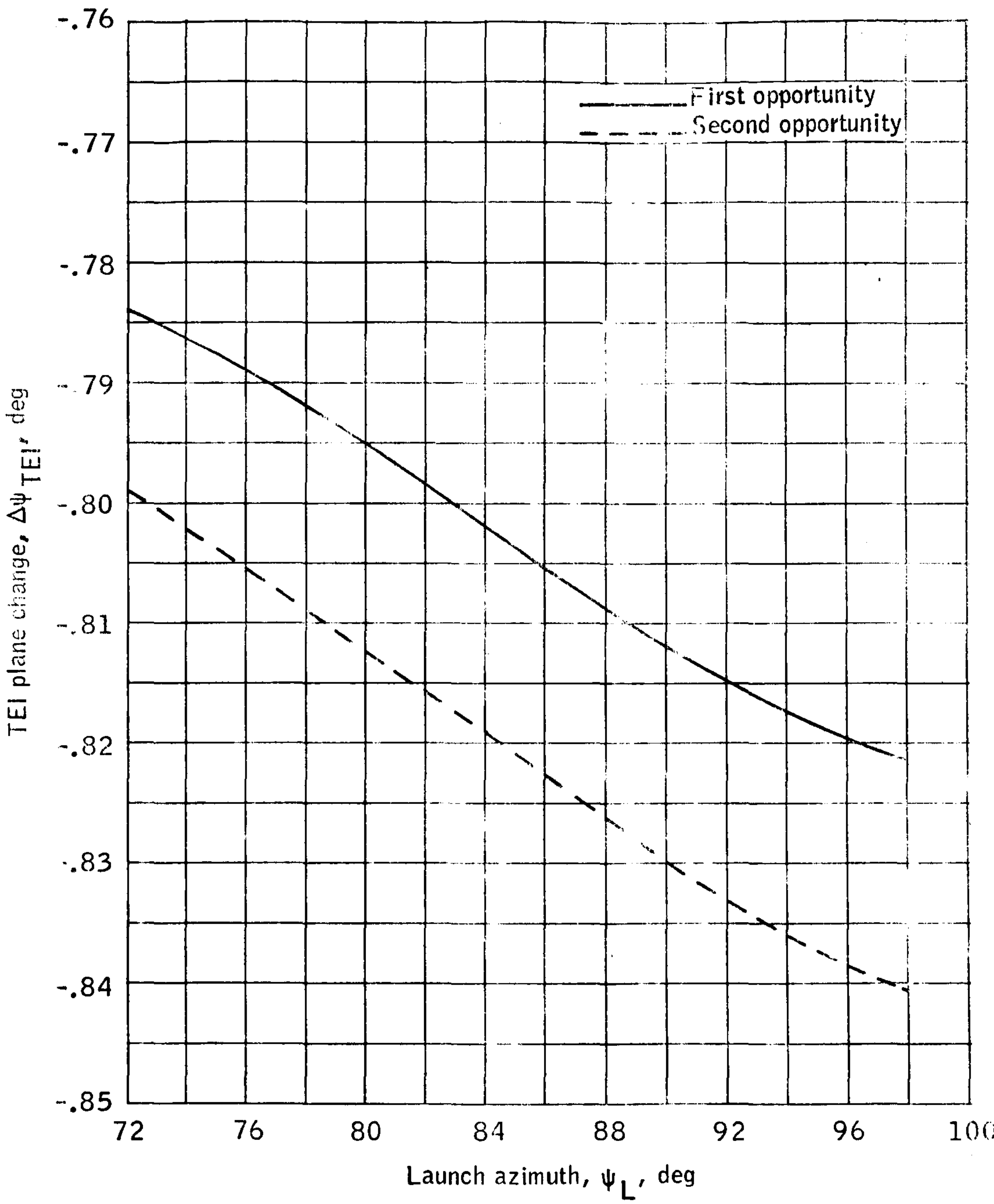

(b) TEI plane change.

Figure 23.- Continued.

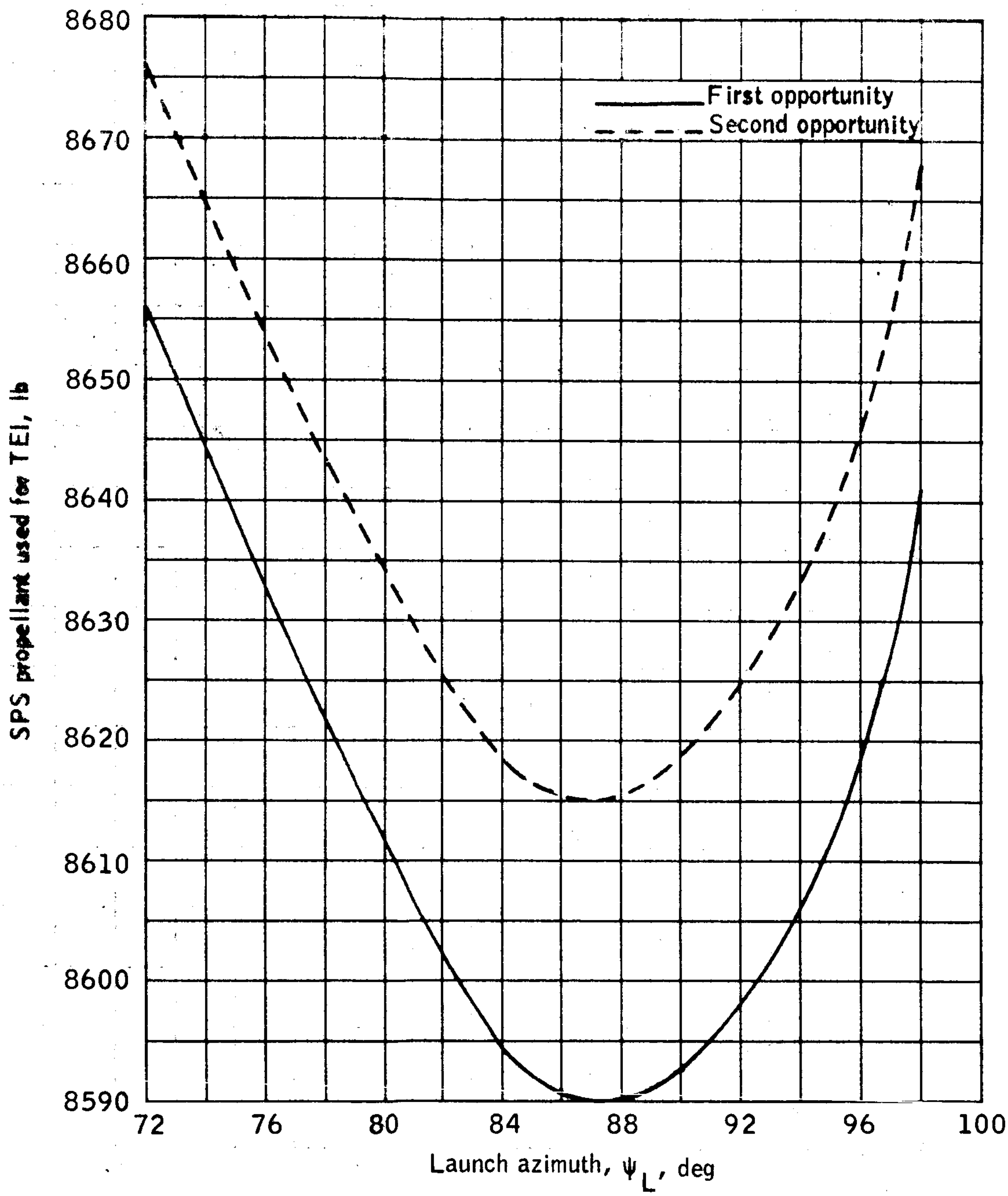

(c) SPS propellant used for TEI.

Figure 23.- Continued.

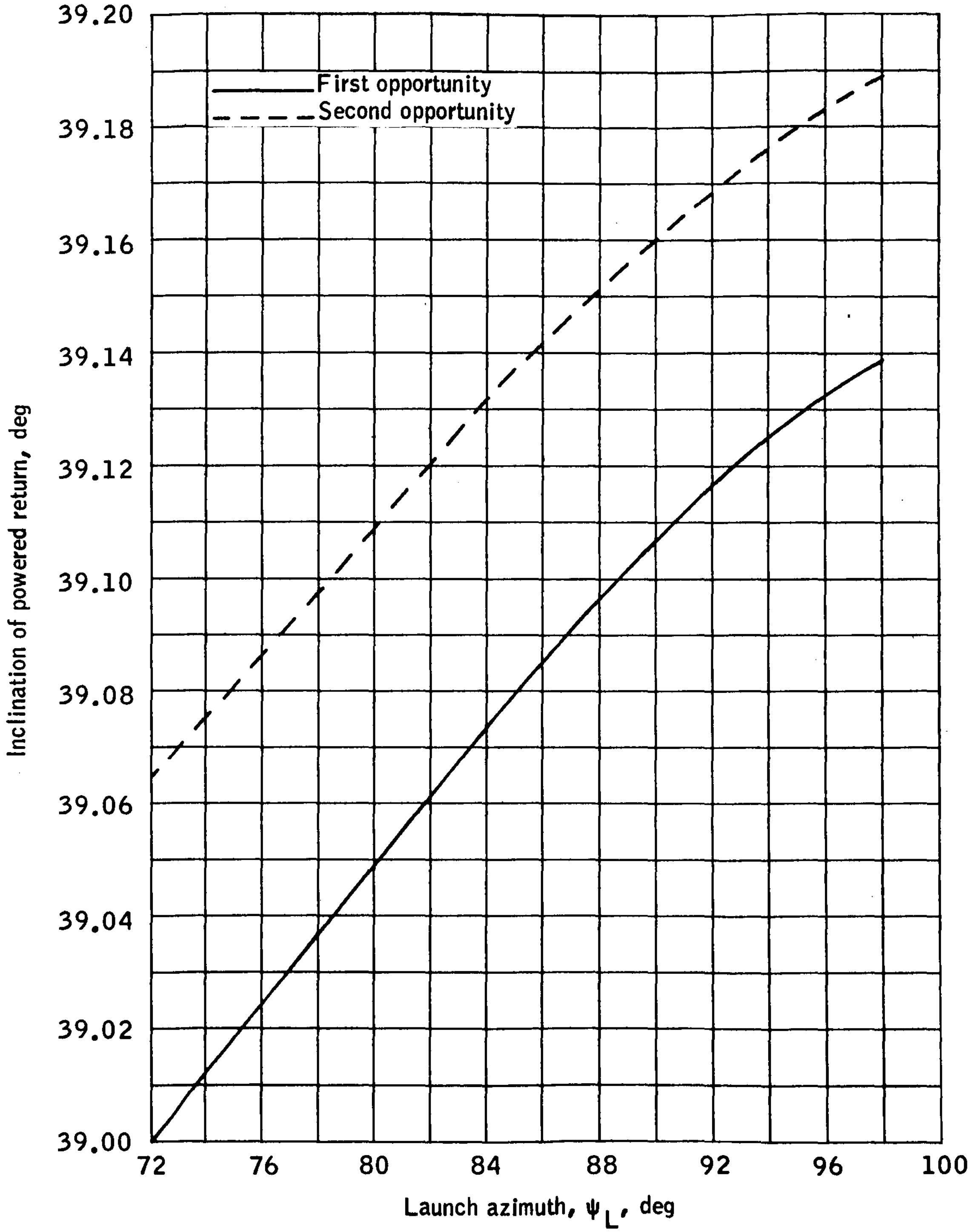

(d) Inclination of powered return.

Figure 23.- Continued.

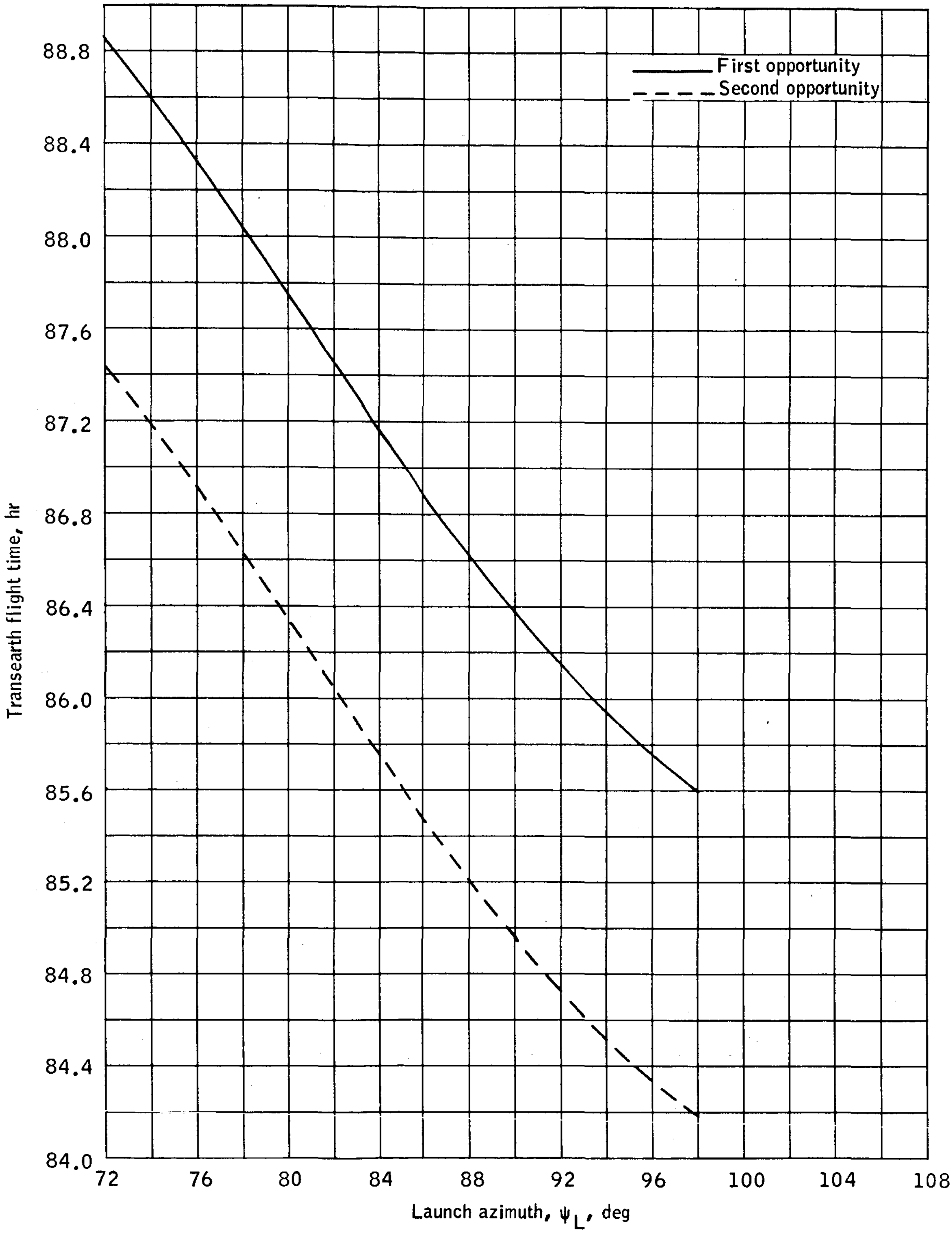

(e) Transearth flight time.

Figure 23.- Concluded.

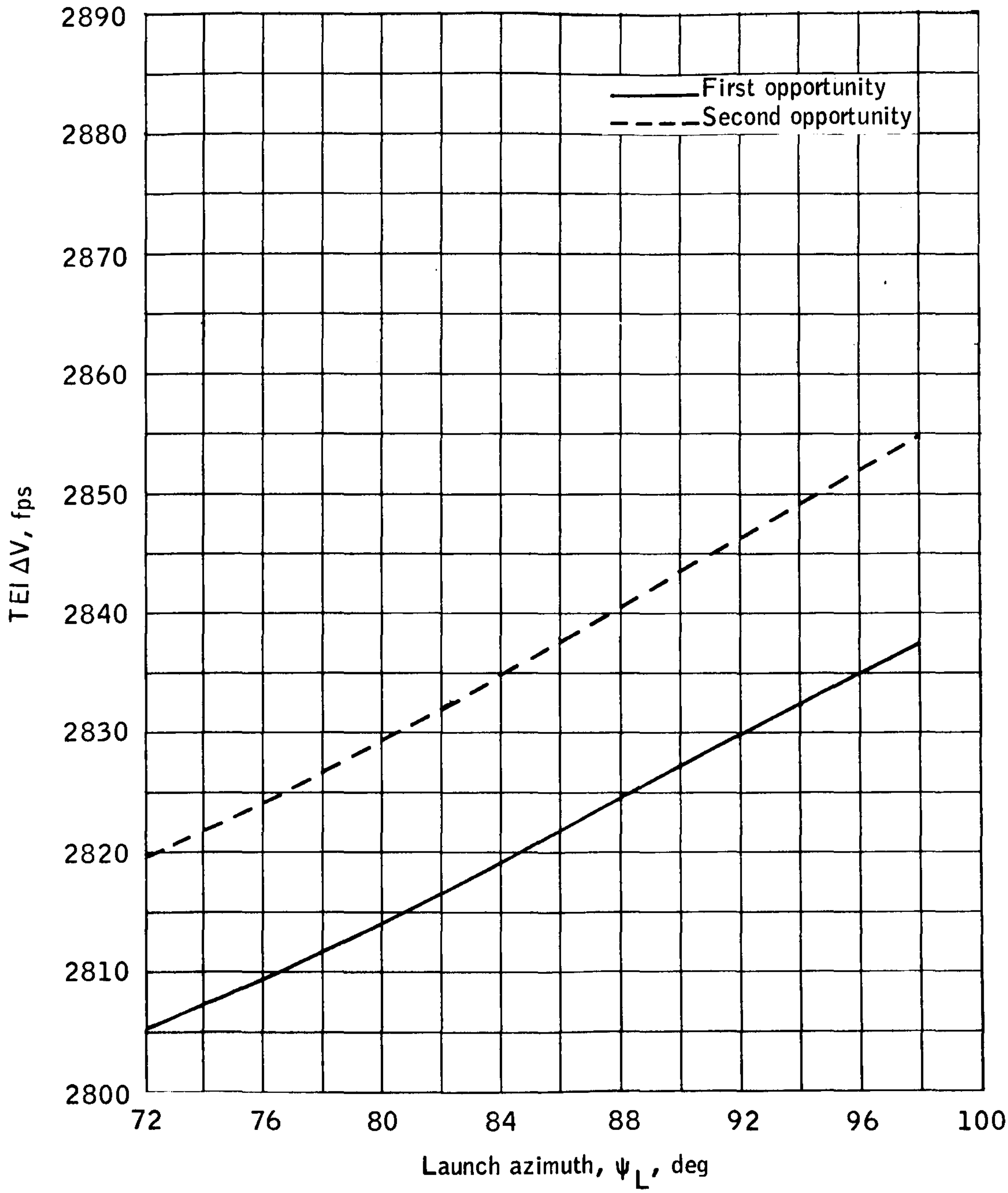

(a) TEI ΔV.

Figure 24.- Trajectory parameters as a function of launch azimuth for lift-off on September 13,1969.

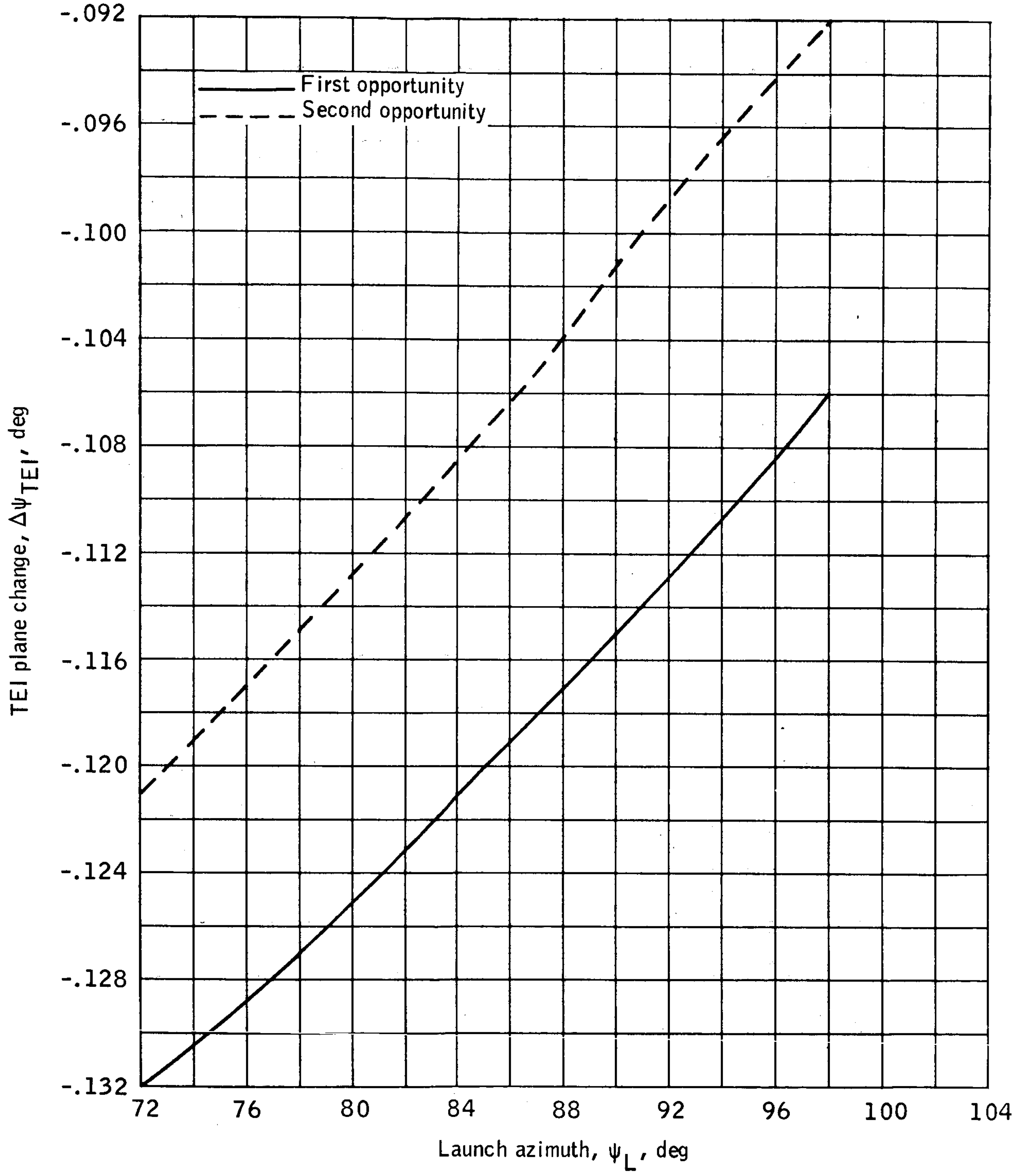

(b) TEI plane change.

Figure 24.- Continued.

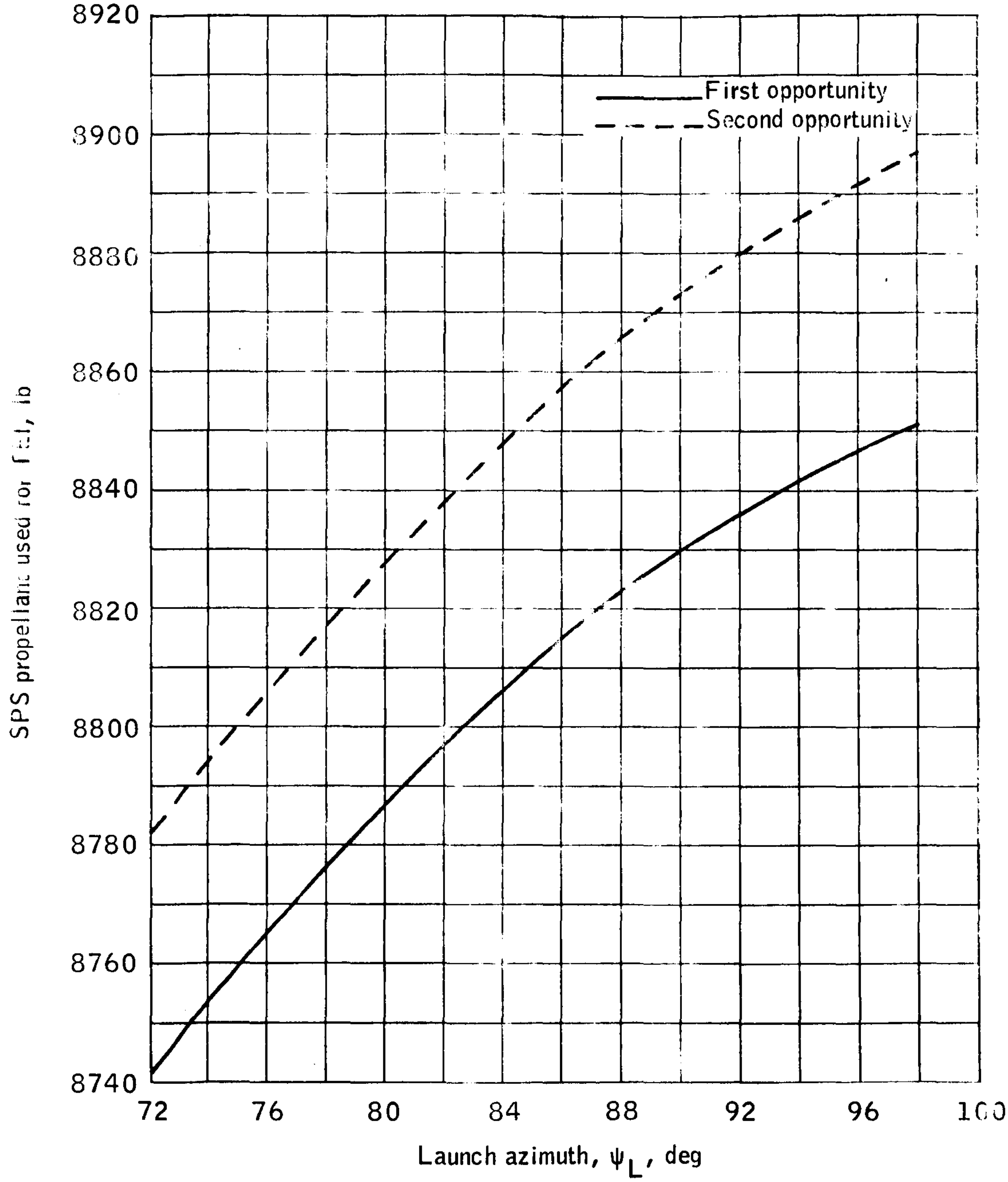

(c) SPS propellant used for TEI.

Figure 24.- Continued.

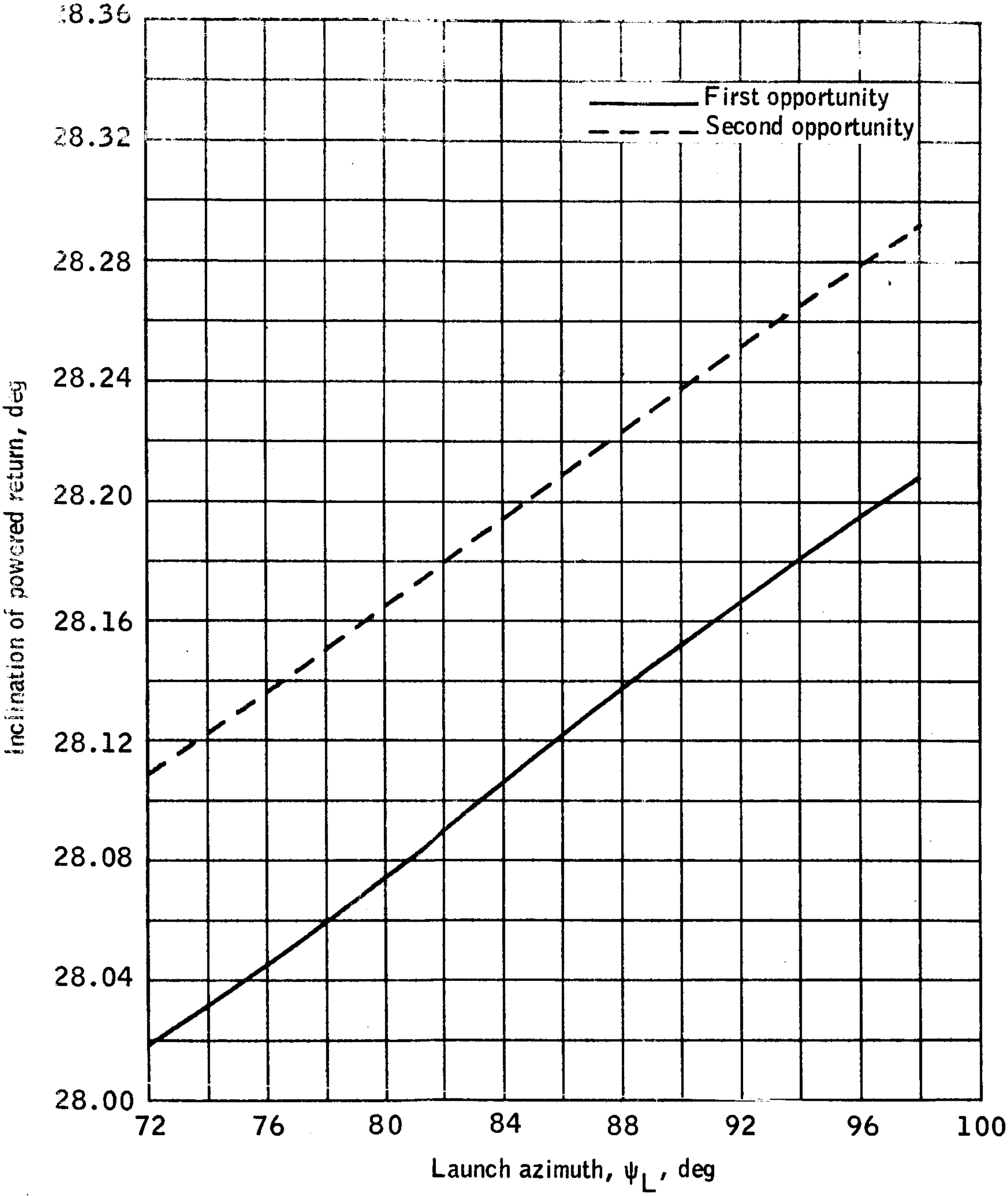

(d) Inclination of powered return.

Figure 24.- Continued.

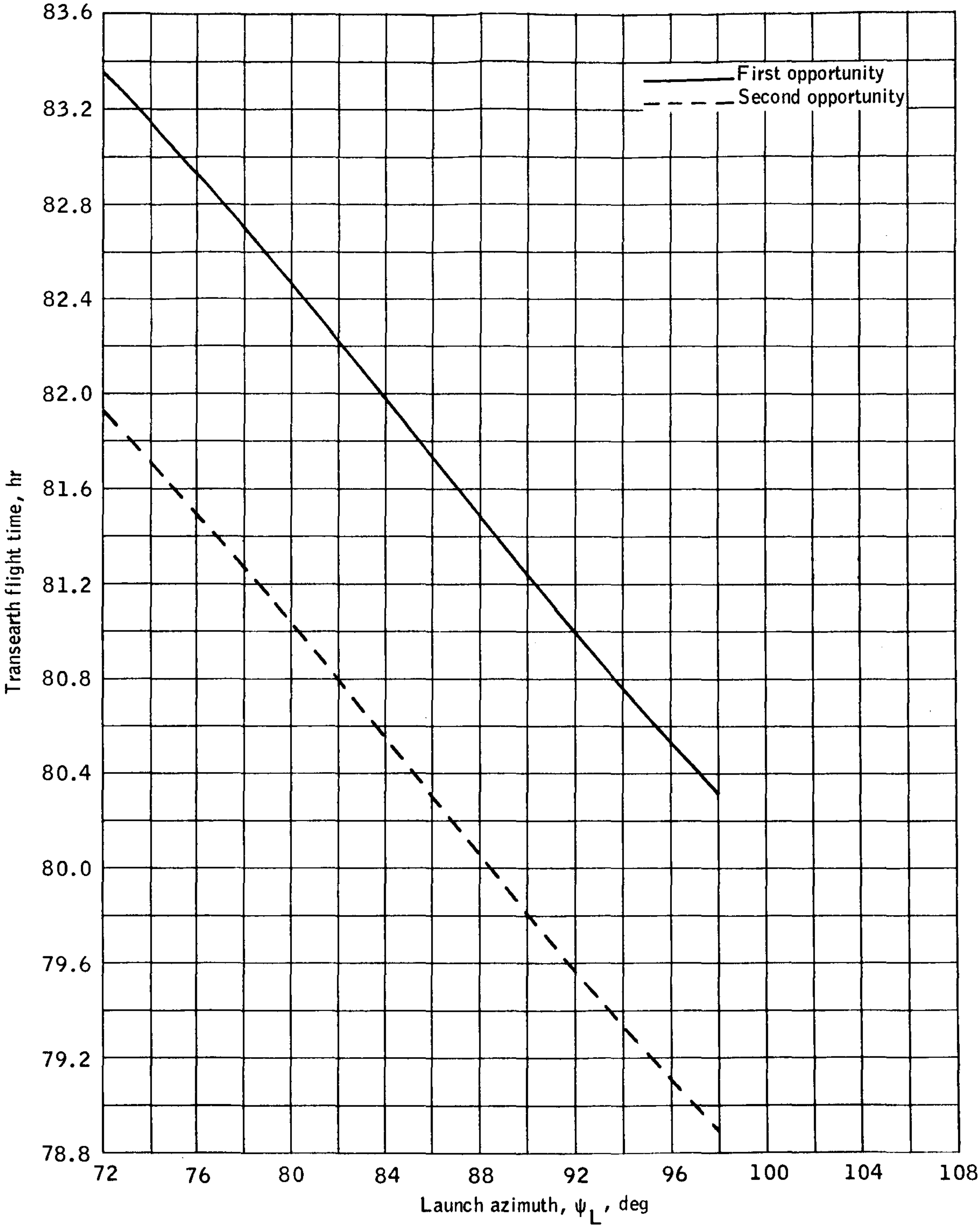

(e) Transearth flight time.

Figure 24.- Concluded.

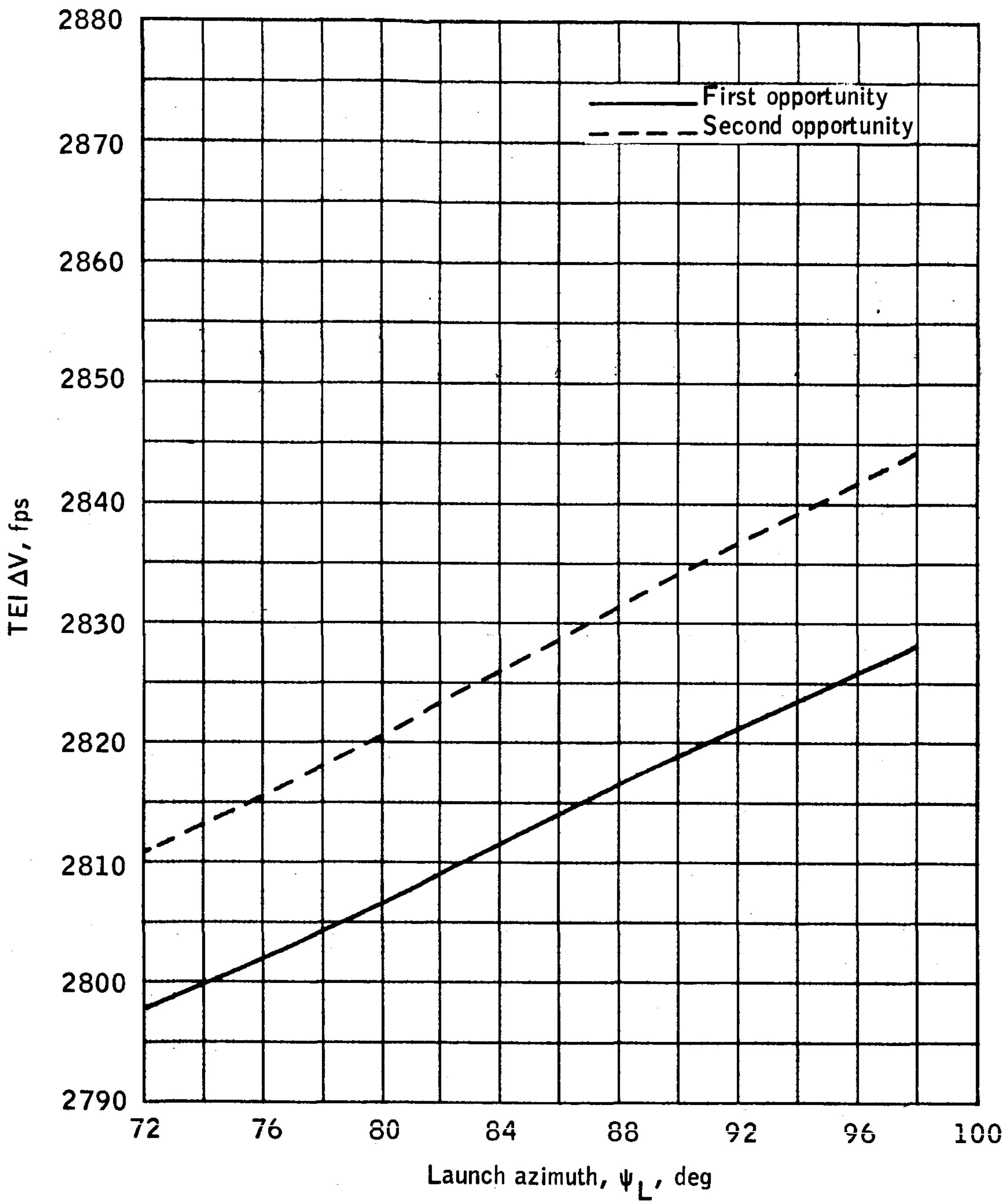

(a) TEI ΔV.

Figure 25.- Trajectory parameters as a function of launch azimuth for lift-off on September 14,1969.

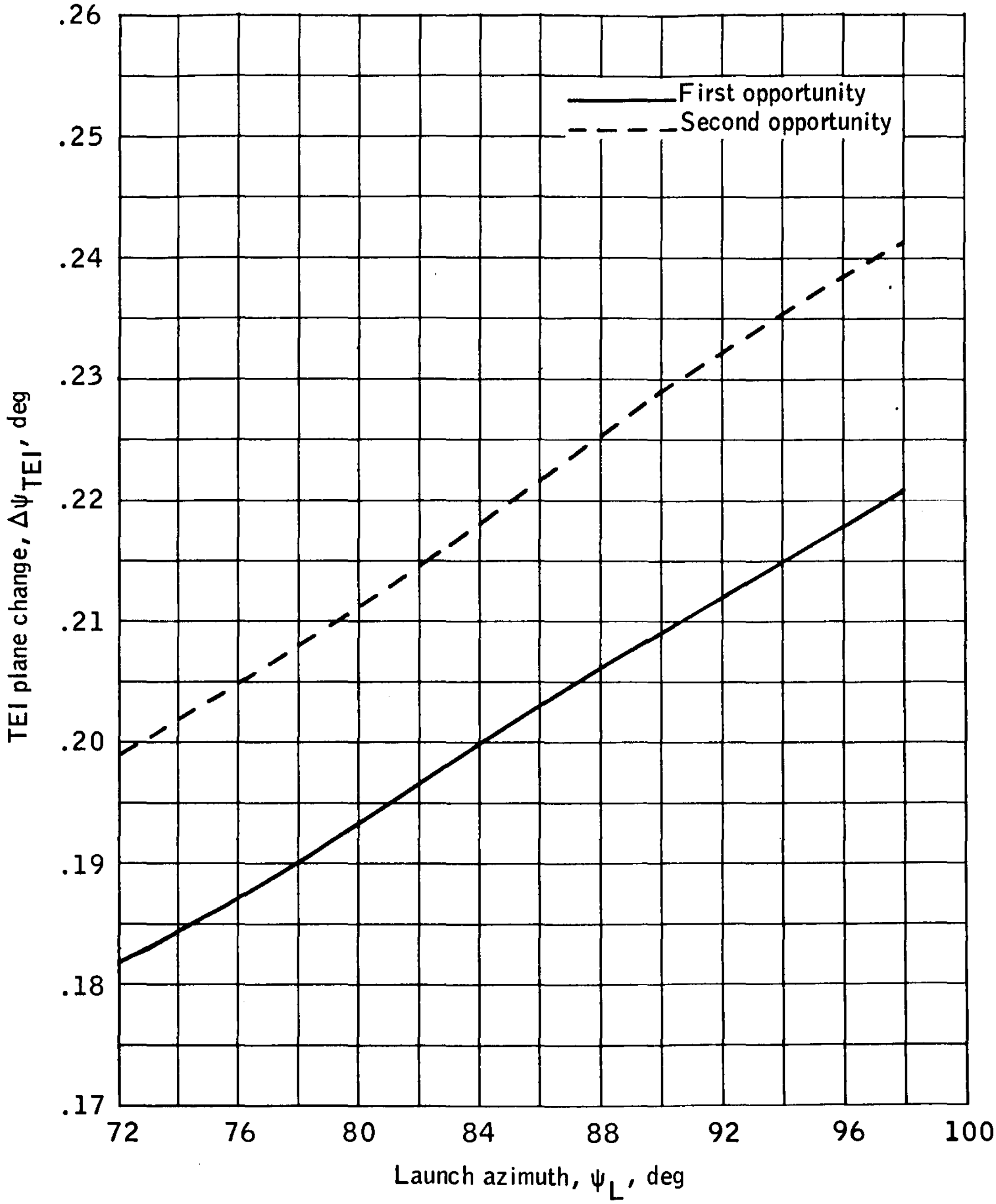

(b) TEI plane change.

Figure 25.- Continued.

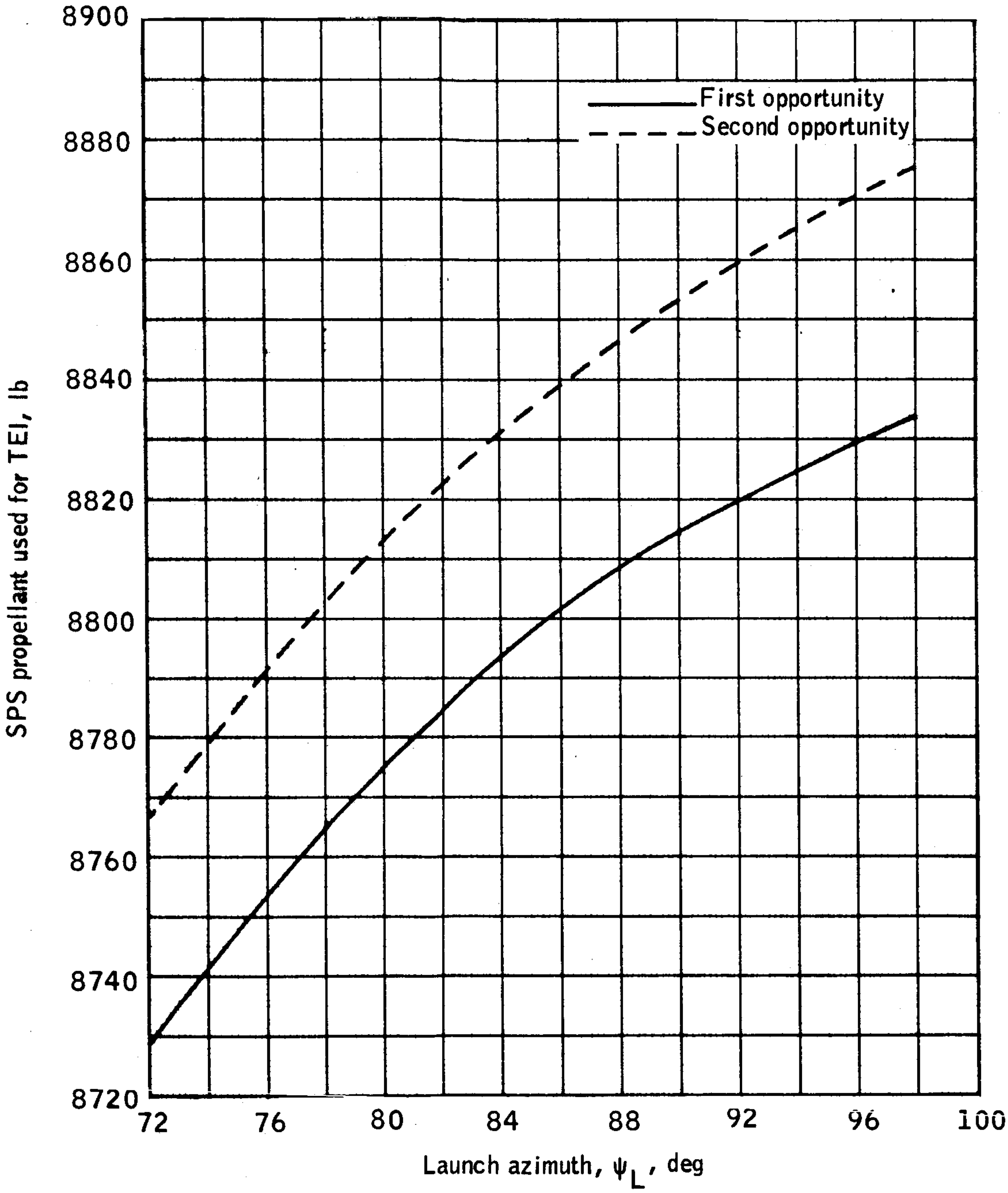

(c) SPS propellant used for TEI.

Figure 25.- Continued.

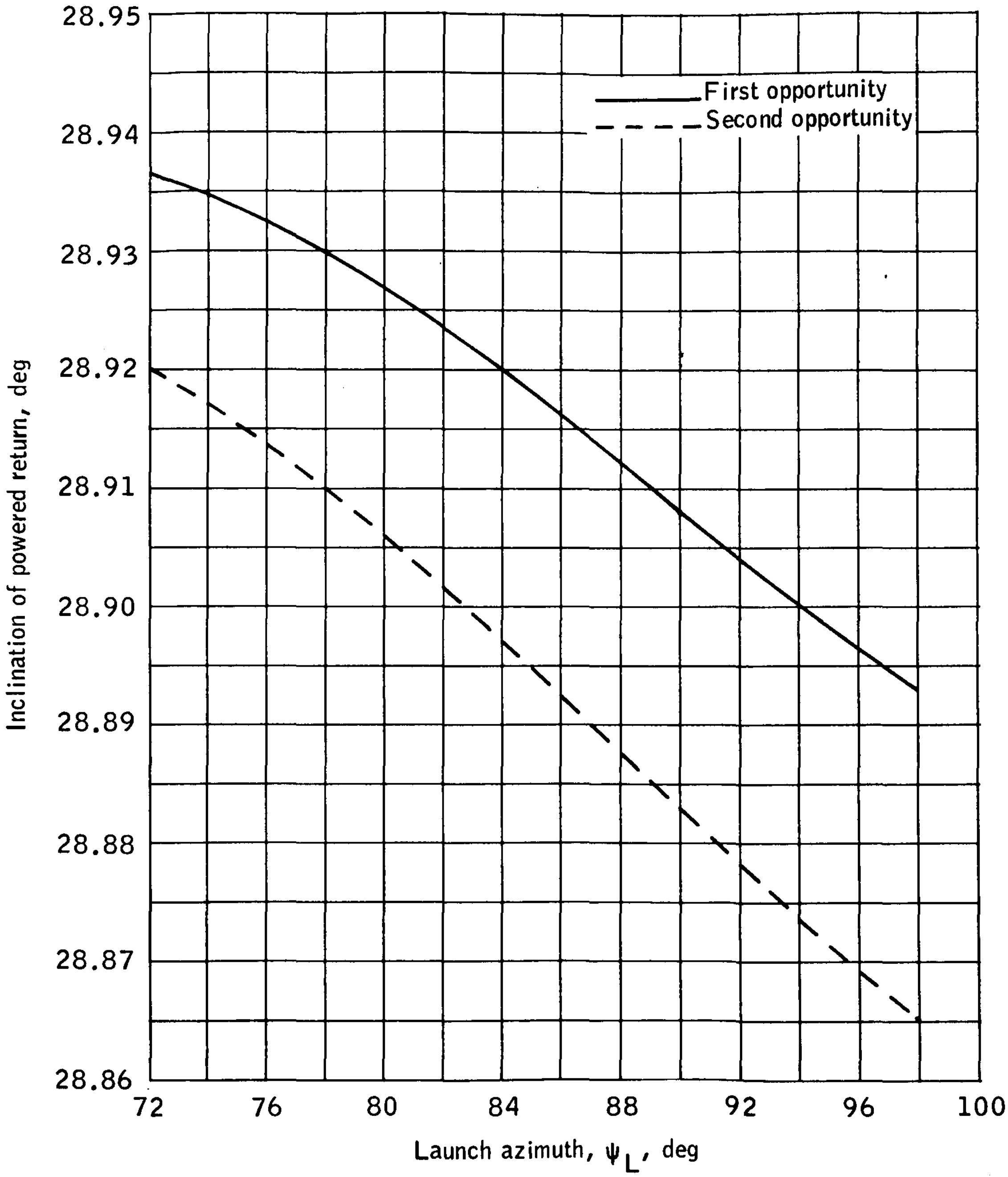

(d) Inclination of powered return.

Figure 25.- Continued.

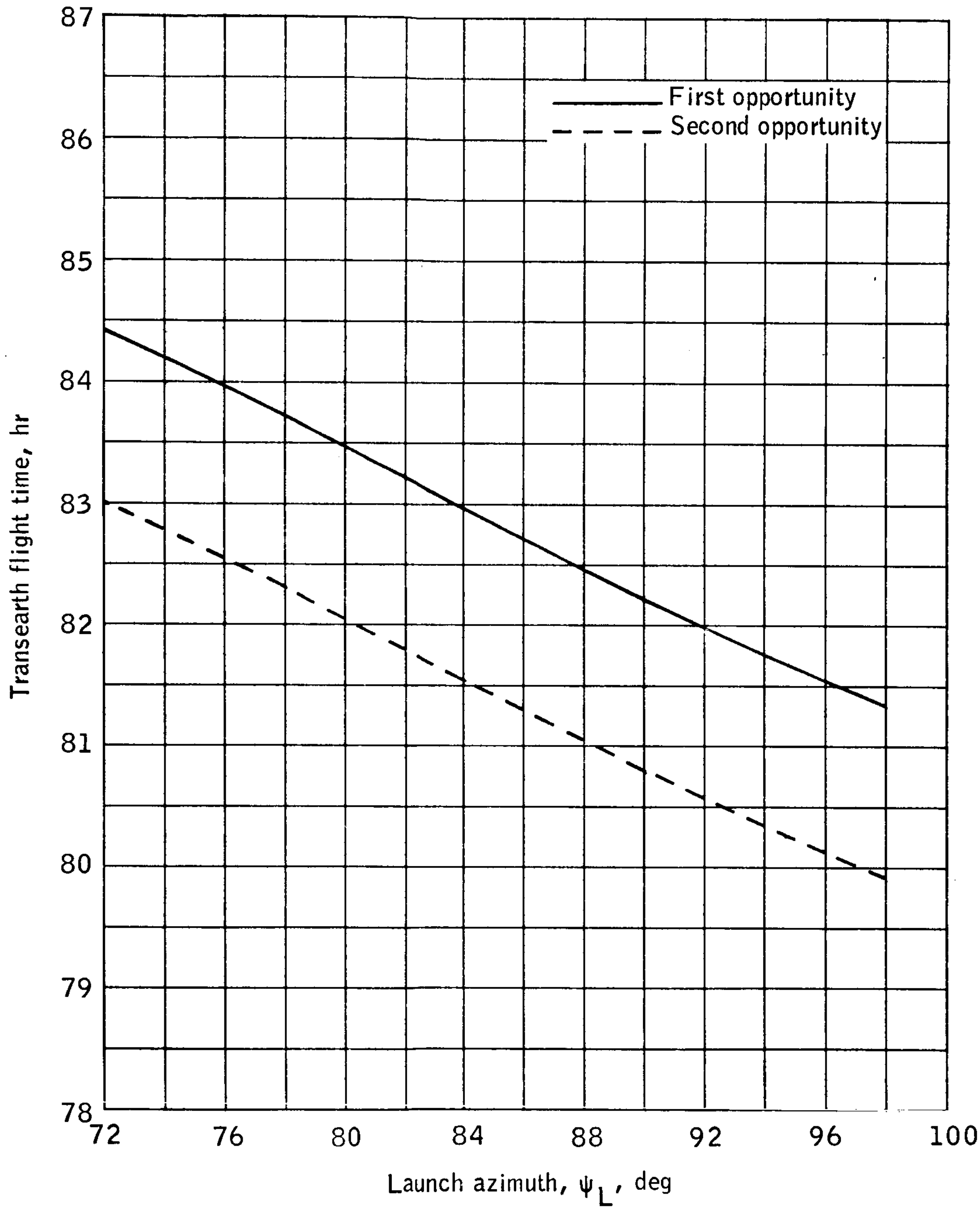

(e) Transearth flight time.

Figure 25.- Concluded.

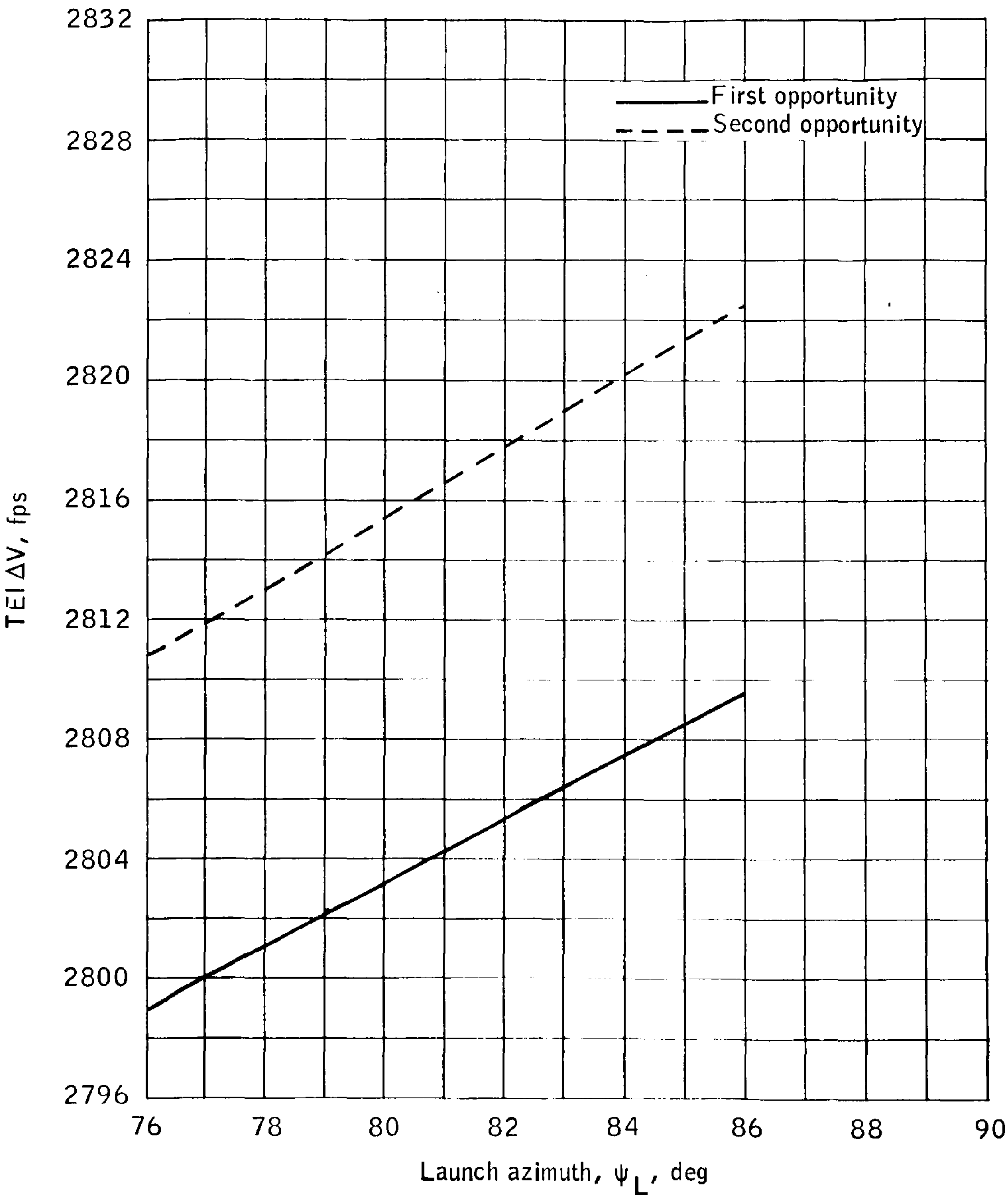

(a) TEI ΔV.

Figure 26.- Trajectory parameters as a function of launch azimuth for lift-off on September 16, 1969.

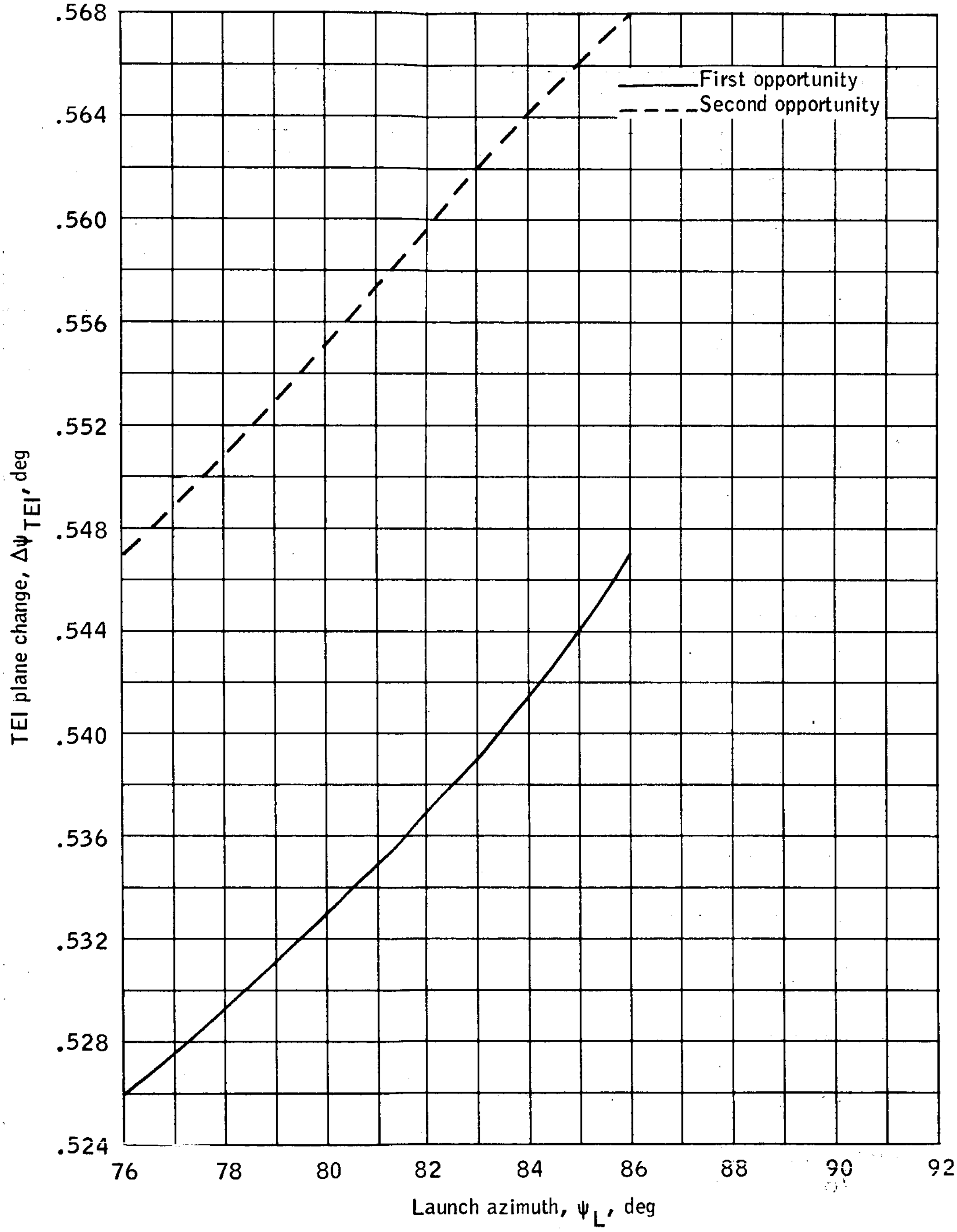

(b) TEI plane change.

Figure 26.- Continued.

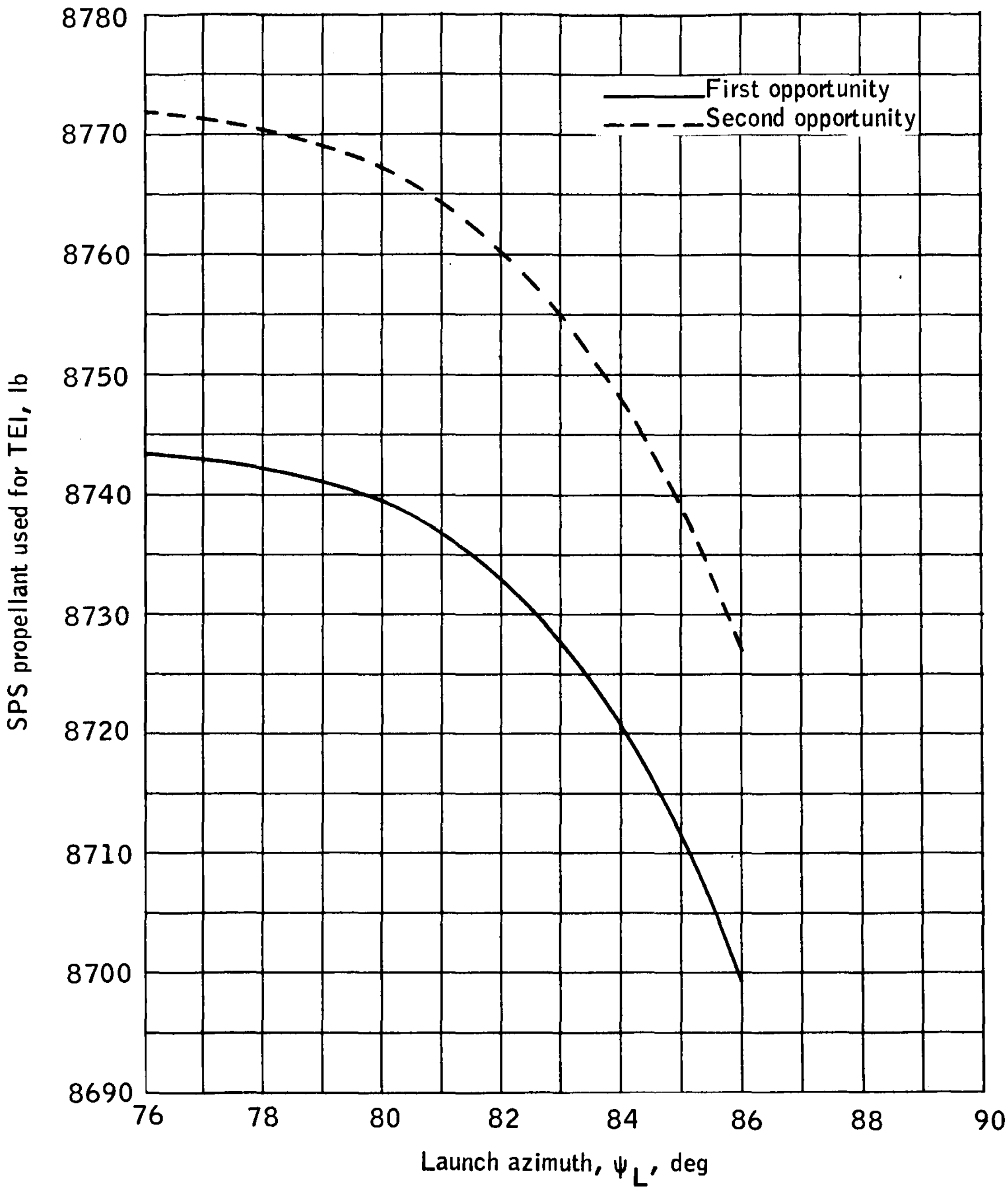

(c) SPS propellant used for TEI.

Figure 26.- Continued.

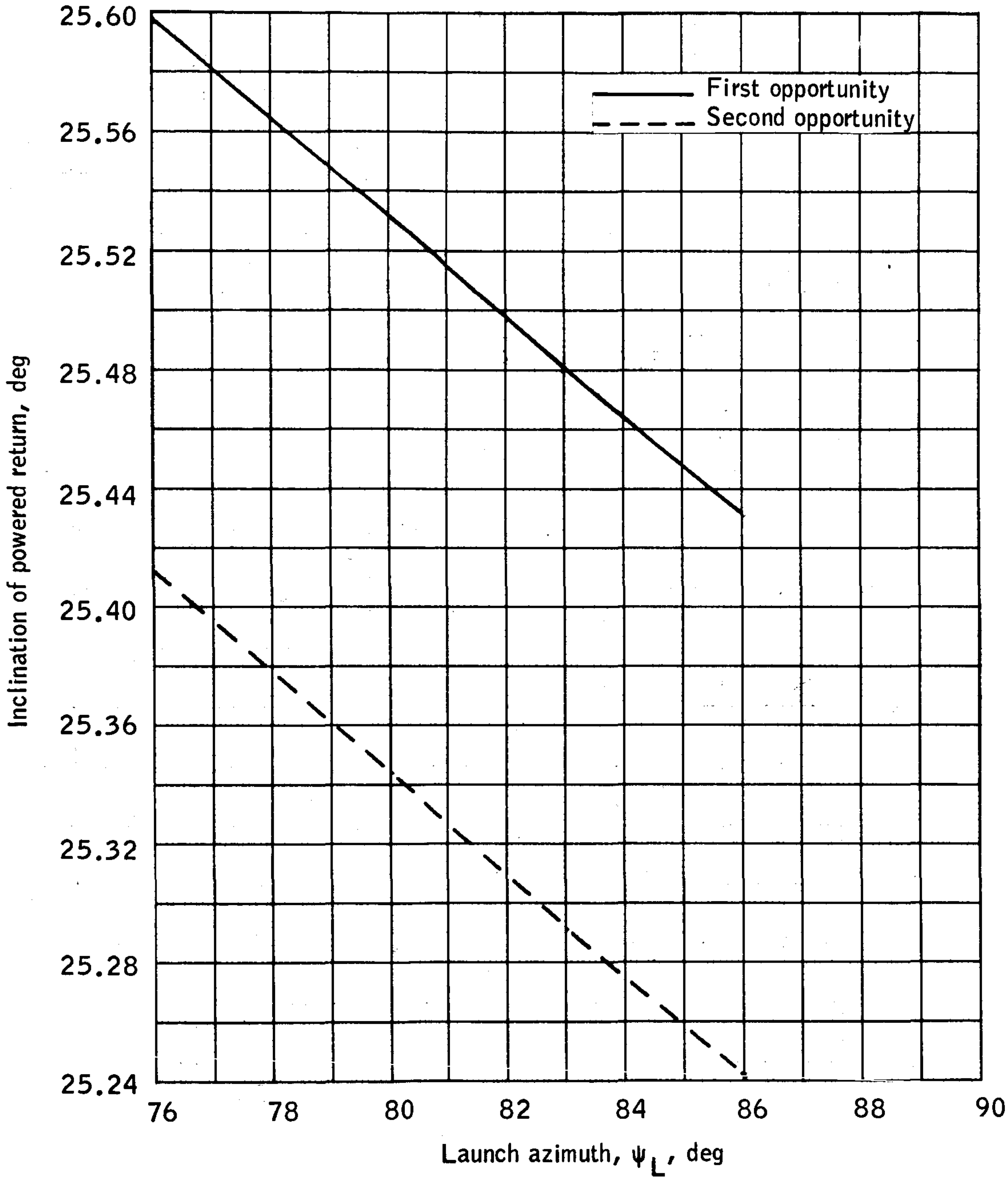

(d) Inclination of powered return.

Figure 26.- Continued.

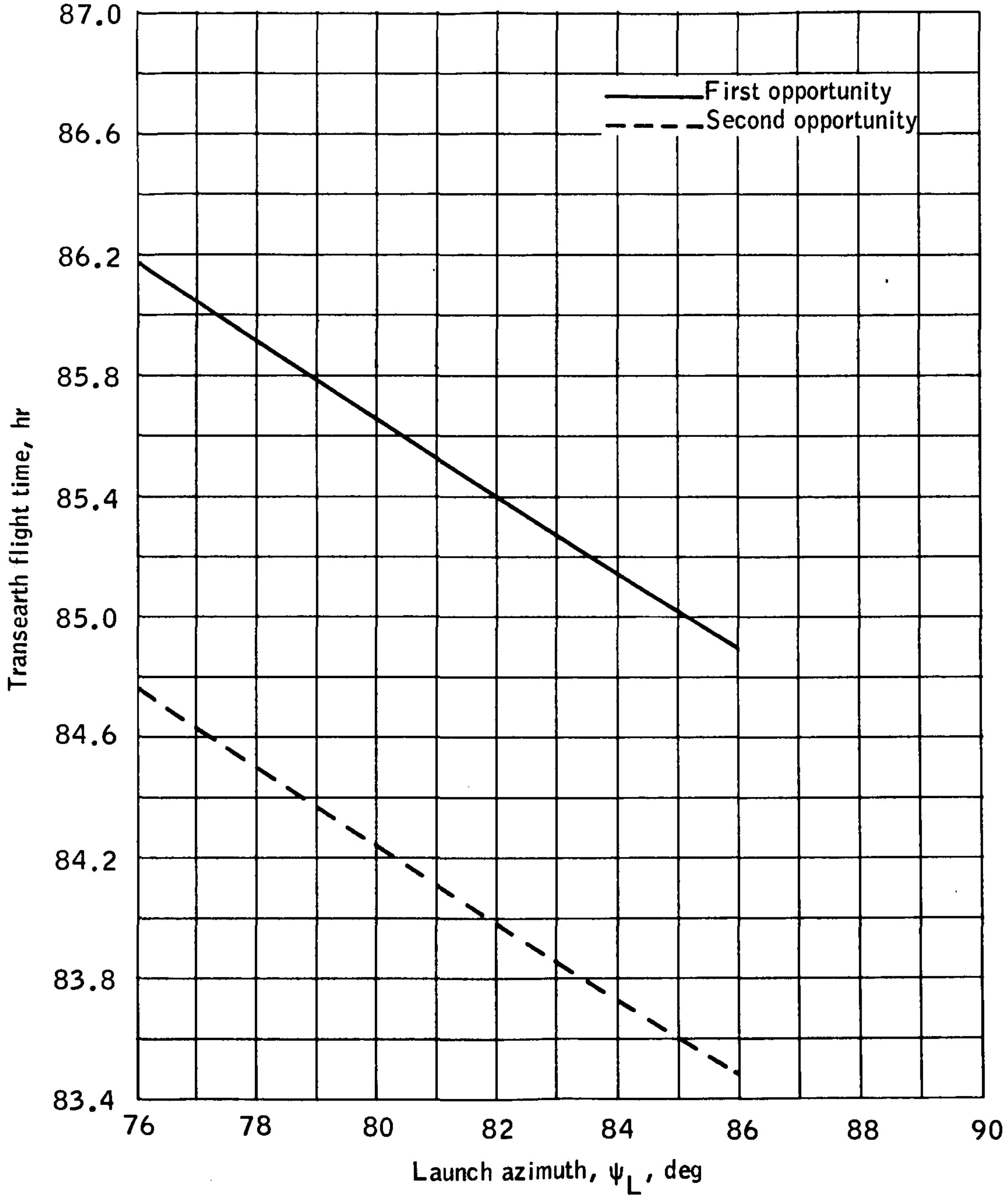

(e) Transearth flight time.

Figure 26.- Concluded.

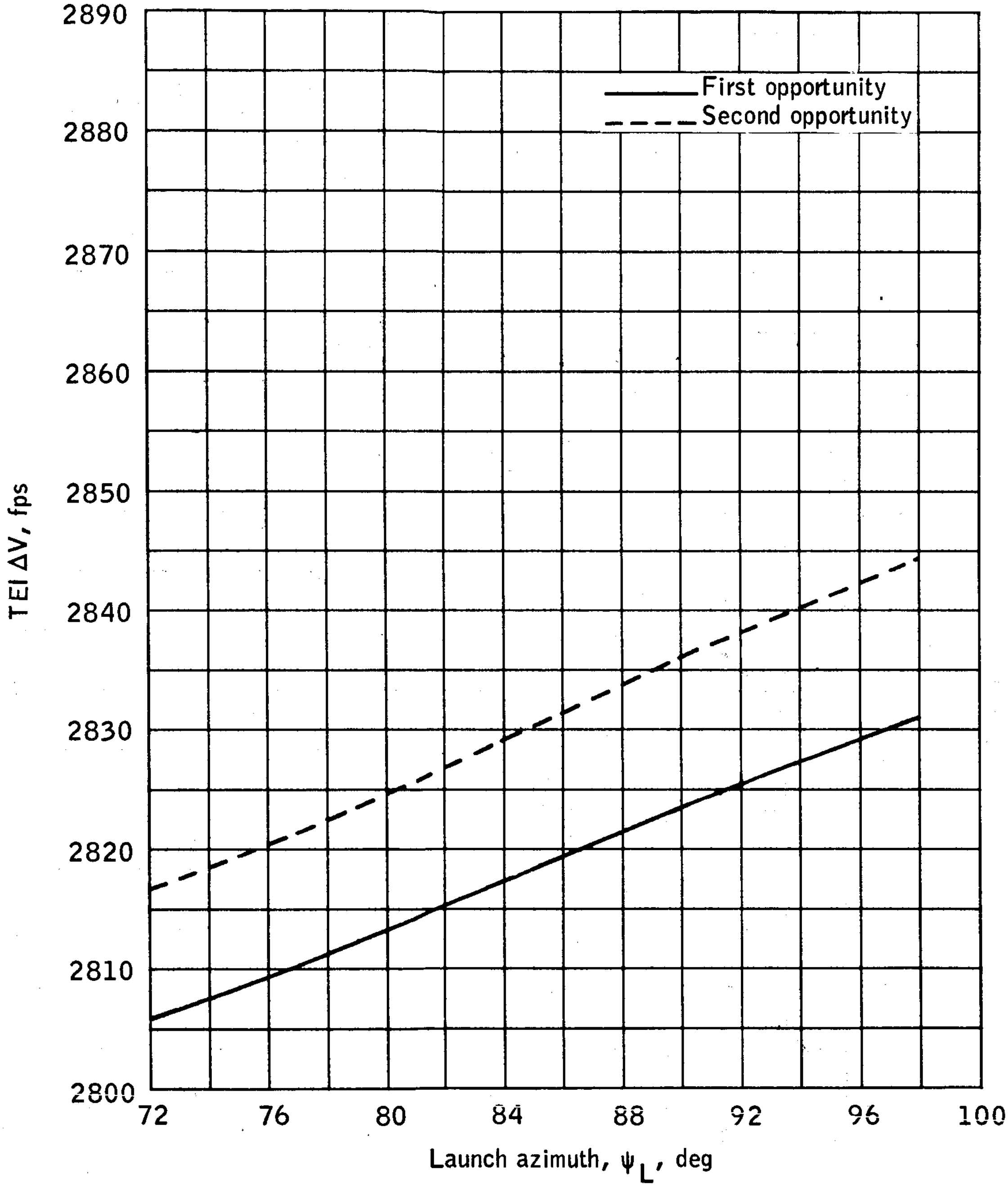

(a) TEI ΔV.

Figure 27.- Trajectory parameters as a function of launch azimuth for lift-off on September 19,1969.

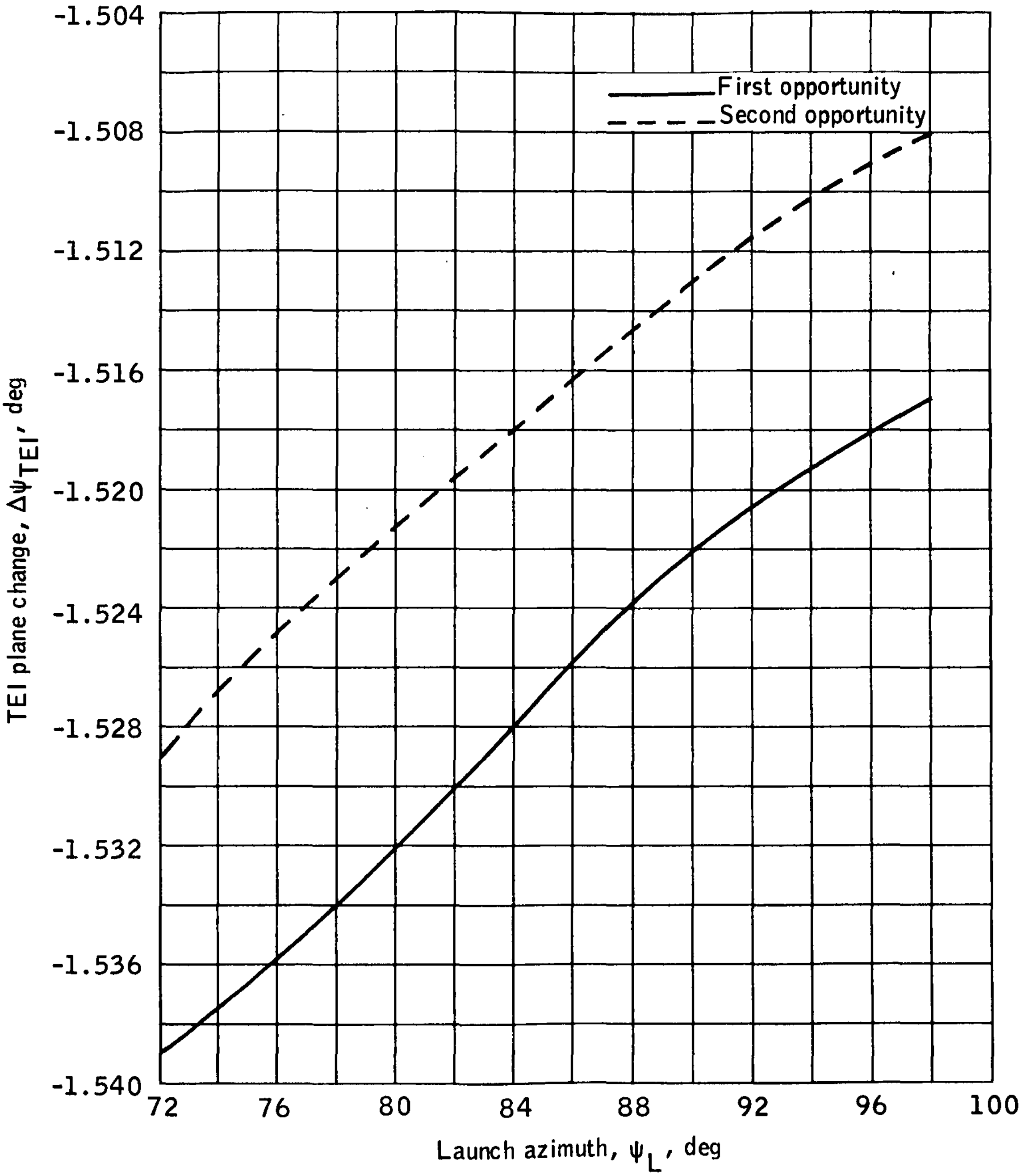

(b) TEI plane change.

Figure 27.- Continued.

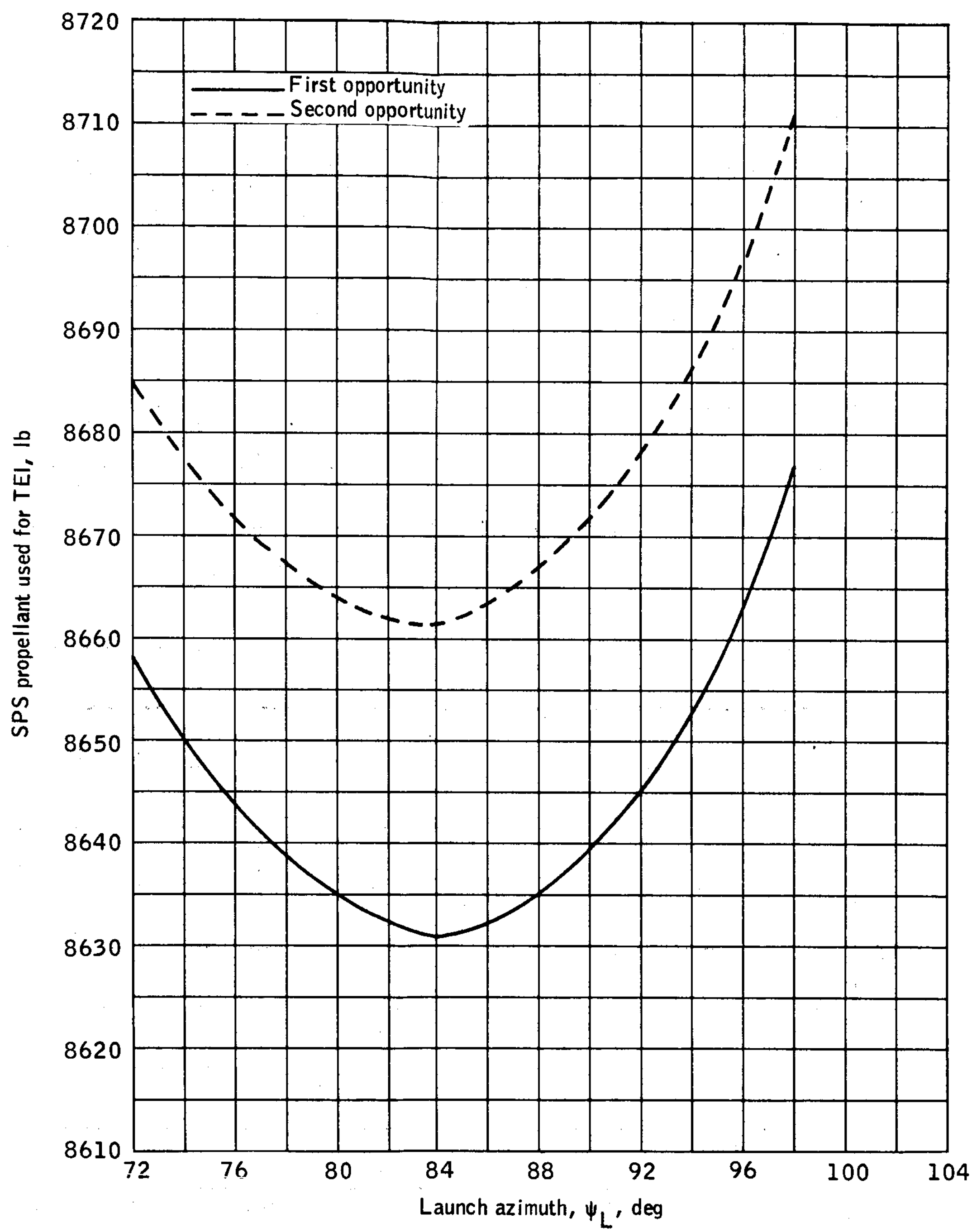

(c) SPS propellant used for TEI.

Figure 27.- Continued.

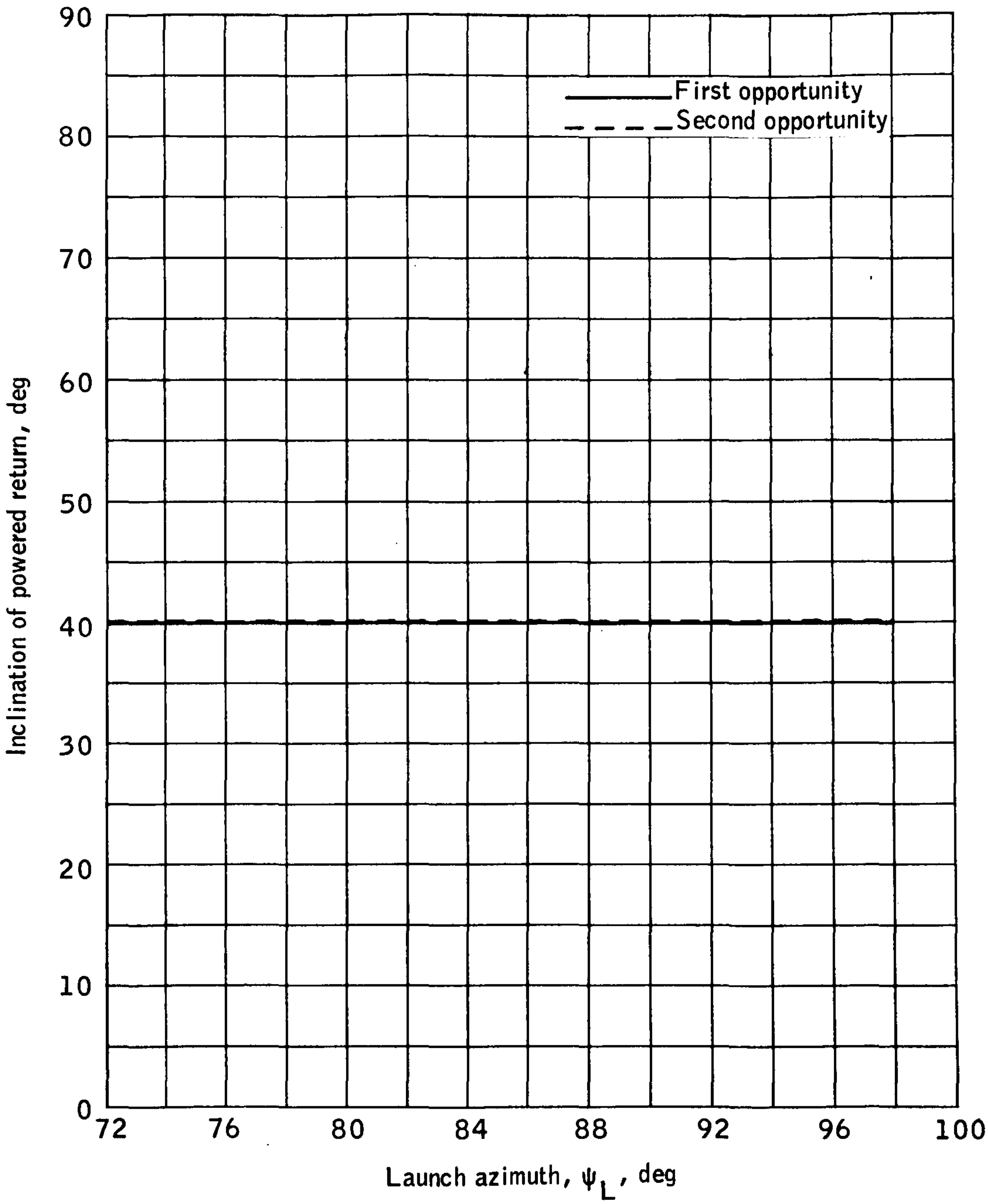

(d) Inclination of powered return.

Figure 27.- Continued.

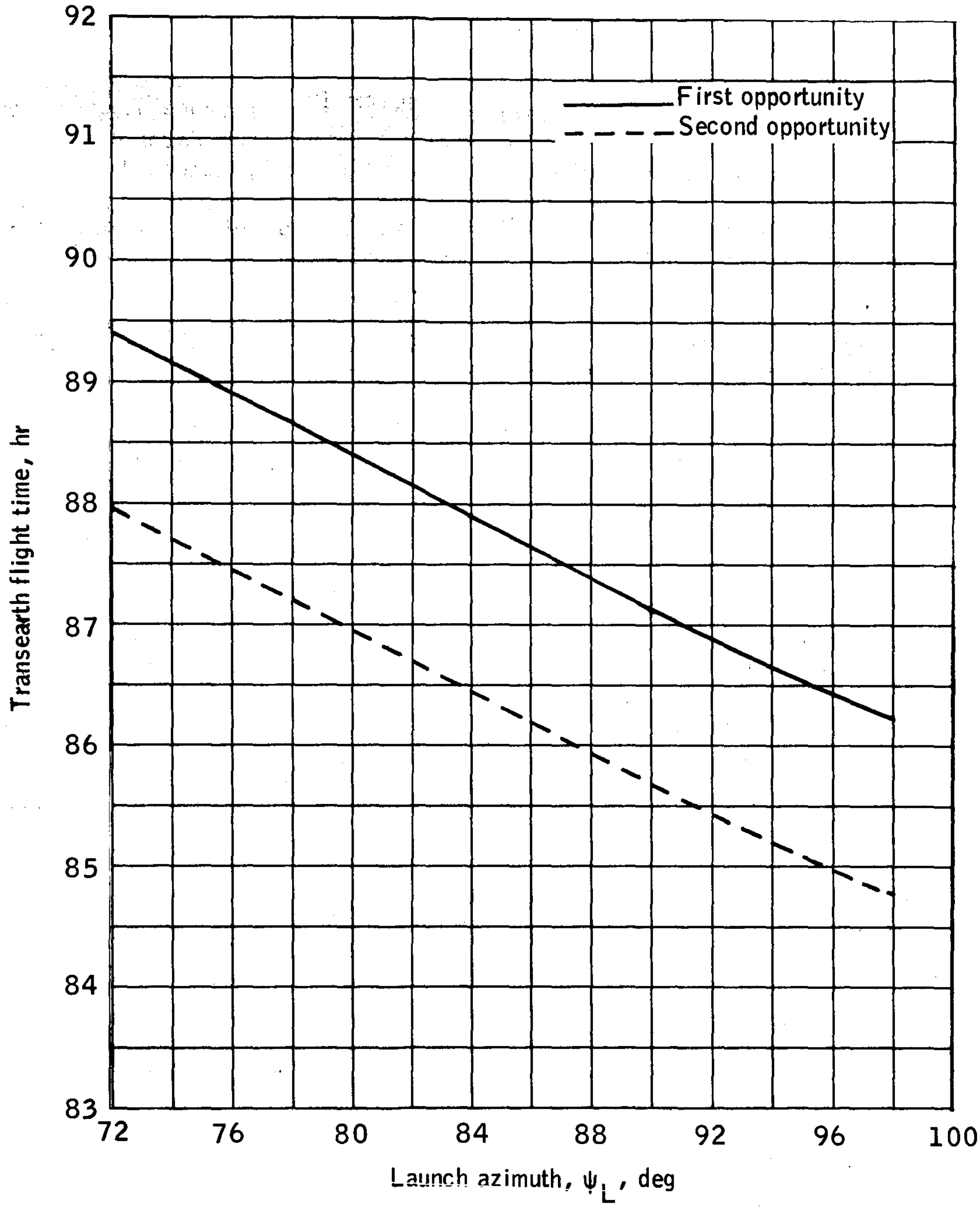

(e) Transearth flight time.

Figure 27.- Concluded.

REFERENCES

1. LMAB; and OMAB: Apollo Mission F Spacecraft Reference Trajectory, Volume II - Reference Mission Profile Trajectory Parameters (Launched August 14, 1969). MSC IN 68-FM-197, August 16, 1968.

2. LMAB: Update 1 to the Lunar Orbit Mission Trajectory Ground Rules. MSC Memorandum 68-FM55-172, May 3, 1968.

3. LMAB: Apollo Mission G Spacecraft Reference Trajectory. Volume I - Reference Mission Profile (Launched August 14, 1969). MSC IN 68-FM-196, August 9, 1968.

4. LMAB: Apollo Mission G Spacecraft Reference Trajectory, Volume II - Reference Mission Profile Trajectory Parameters (Launched August 14, 1969). MSC IN 68-FM-197, August 16, 1968.

5. NASA: Mission Requirements G-Type Mission Lunar Landing. SP08-R-008, May 23, 1968.

6. Berry, R. L.: Update 1 to the Lunar Landing Mission Trajectory Ground Rules. MSC Memorandum 68-FM55-173, May 13, 1968.

7. Joint Reference Constraints for Mission G. Flight Mechanics Panel Document No. 68-FMP-5, July 16, 1968.

8. LMAB: Lunar Orbit Timeline to be Used in the Mission G Reference Trajectory. MSC Memorandum 68-FM55-117, March 25, 1968.

9. Peterson, D. G.: Weight Data for Mission G. MSC Memorandum 68-FM74-327, July 22, 1968.

10. CSM/LM Spacecraft Operational Data Book, Volume III - Mass Properties. SNA-8-D-027, March 1968.

11. CSM/LM Spacecraft Operational Data Book, Volume I - CSM Data Book. SNA-8-D-027, May 1968.

12. Universal Mission Modular Data Book. GAEC Document LED-500-19, October 15, 1967.

13. Jiongo, E. M.: Preflight Tracking Data for the Launch Phase of a Lunar Mission. MSC IN 68-FM-38, February 14, 1968.

14. Apollo Navigation Working Group: Apollo Missions and Navigation Systems Characteristics. ANWG TR No. AN-1.2, January 17, 1967.

15. Frank, M. P.: Lunar Landing Sites Currently Being Used for Mission Planning. MSC Memorandum 67-FM51-333, September 7, 1967.

16. Maynard, O. E.: Apollo Site Selection Board Meeting. MSC Memorandum PR 12/M352, January 16, 1968.

17. York, Will; and Savely, Robert T.: Directory of Standard Geodetic and Geophysical Constraints for Gemini and Apollo. NASA General Working Paper No. 10, 020B, April 6, 1966.

18. OMAB: Revised LM-active Phase of Mission F. MSC Memorandum 68-FM64-246, July 29, 1968.

19. OMAB: CSM-active Rendezvous of Mission F. MSC Memorandum 68-FM64-289, September 6, 1968.